Study on Relay-Assisted Inter-Vehicle Communication Techniques for Advanced Intelligent Transport Systems

Le Tien Trien

Department of Communication Engineering and Informatics
Graduate School of Informatics and Engineering
THE UNIVERSITY OF ELECTRO-COMMUNICATIONS

A Dissertation Submitted in Partial Fulfilment
of the Requirements for the Degree of
Doctor of Philosophy

March 2018

Study on Relay-Assisted Inter-Vehicle Communication Techniques for Advanced Intelligent Transport Systems

SUPERVISORY COMMITTEE:

Professor	Yasushi Yamao
Professor	Yoshio Karasawa
Professor	Sadao Obana
Professor	Takeo Fujii
Associate Professor	Koji Ishibashi

概要

近年，先進的な ITS (Intelligent Transport Systems: 高度道路交通システム) のための通信技術への期待が高まっている．これには，車両がその位置や速度などの情報を交換する車車間通信，路側機が車両へ信号状態や道路規制などの情報を提供する路車間通信，車両と歩行者の間で情報の交換を行う歩車間通信などがある．これらにブロードキャスト通信を活用することで，各車両では潜在的な交通事故を予測して運転手に警告し，さらには制動を行うことにより事故を未然に回避できる．さらにこの情報を利用して車両を自動制御することで，交通流を意識した協調型自動走行を実現することが可能になるものと期待されている．

車車間通信を用いて安全運転支援およびより高度な自動走行システムを実現するためには，高信頼，かつ低遅延の無線通信技術が要求される．しかしながら道路上の移動通信では，多重波伝搬によるフェージングや建物によるシャドウイング，さらに自律分散通信システム特有の問題である隠れ端末問題による干渉などの影響で，通信の信頼度が低下する．特に事故発生確率の高い交差点ではその影響が顕著である．

本論文では車車間通信の品質を改善することを目的として，交差点等に中継局 (Relay Station; RS) を設置し，車車間通信パケットを転送中継する中継アシスト車車間通信に関する諸技術が提案されている．中継局は交差点付近の信号機などに併設され，高いアンテナ高を有することと，他の車載局に対して見通し内(Line-of-Sight; LOS) 伝搬環境にあるため，中継アシストシステムはシャドウイングやフェージングの問題の軽減に有効であることが既に示されている．しかしながら，トラヒックが増加するにつれて中継局での輻輳問題が発生し，中継効果が低下するという課題があった．そこで本論文では中継によるエアトラ

ヒックの増加を抑える方法として，中継送信時に複数のパケットペイロードをまとめて１つのパケットに再構成して送信するペイロード合成中継法を提案する．本提案法により中継局での輻輳問題が解決でき，中継効果が向上することを解析結果から明らかにした．

交差点における中継アシスト車車間通信のもう 1 つの課題として，中継局受信時に隠れ端末問題の影響で受信成功率が低下することがある．この課題に対しては中継局受信時にセクタアンテナを用いることが有効であることが示されているが，本研究ではペイロード合成中継法にセクタ化受信を組合せたセクタ化受信ペイロード合成中継法を提案し，その効果を理論解析およびシミュレーションにより示した．セクタ化受信によって中継局での受信成功率を改善すると中継すべきパケット数が増加するが，提案法ではペイロード合成によって中継パケットの送信効率を高めることができるので，結果として中継効果を高めて平均パケット伝送成功率を大幅に向上できることを明らかにした．

さらに，複数交差点からなる市街地環境におけるセクタ化受信ペイロード合成中継法の効果を，大規模ネットワークシミュレーションを用いてブロードキャスト配信成功率として総合的に評価した．他の車両および離れた中継局など干渉源が複数存在する市街地環境においても，提案法を用いることによって隠れ端末問題の影響が有効に回避できること，隣接する中継局間で互いに棲分け中継をすることで非常に高い中継効果が得られることを明らかにした．

以上のように提案法は中継アシスト車車間通信の特性を大幅に改善できるが，通信トラヒックがさらに高い環境に対処するため，中継パケットのエアトラヒックをさらに圧縮できる方法として，複数ノード環境に適したネットワークコーディング法を用いたペイロード合成中継法を提案する．本提案法では，車車間ペイロードのソーティングと合成対象パケットの選択アルゴリズムによって複数ノード環境でのネットワークコーディングの弱点を抑えつつ，輻輳問題に有効に対処できることを示した．結果として本提案法をセクタ化受信と組合せることで，幅広い通信トラヒック条件においてブロードキャスト配信成功率が大きく向上することを明らかにした．

Summary

Wireless vehicular communications for advanced Intelligent Transport Systems (ITS) have the potential to support safety driving, enhance the efficiency of transportation and play an important role in the future automated driving system. The vehicle-to-vehicle (V2V), vehicle-to-infrastructure (V2I) and vehicle-to-pedestrian (V2P) communications in the advanced ITS enable safety support applications that can predict potential traffic accidents, warn drivers and, in some cases, directly control vehicles to prevent collisions. Such applications require highly reliable broadcast communications. However, the reliability of wireless communication in vehicular environments suffers from fast fading due to multipath propagation, shadowing, and distance-dependent path loss. In addition, hidden terminal (HT) problem is a great concern in CSMA/CA based wireless networks due to its distributed access nature. The packet delivery rate (PDR) of V2V communications rapidly decreases especially under non-line-of-sight (NLOS) environments such as intersections.

A vehicle-roadside-vehicle relay-assisted V2V communication scheme has been proposed to improve the reliability of V2V communications. In the scheme, packets sent from a vehicle can be directly received by other vehicles or relayed by a relay station (RS) to the other vehicles. Then path diversity effect can be obtained that improves PDR of V2V communications. However, when the V2V traffic becomes higher, the number of packets that RS has to retransmit becomes larger. This leads to a large number of packets waiting in the transmit queue of RS and packet congestion happens. If the normal relay scheme is employed, the packets may be dropped due to the limited queue size. Then the gain obtained by relay-assist may be decreased.

A packet payload combining relay (PCRL) scheme is proposed to deal with the congestion issue. In the scheme, multiple V2V packet payloads are combined into a single packet and the resultant packet is rebroadcasted once the channel becomes idle.

Analytical and simulated results show that the proposed PCRL scheme can remarkably alleviate the congestion issue and improve the relaying performance.

The PCRL scheme, however, still suffers from HT problem. In the intersection environments where LOS propagation between VSs is often unavailable, the packet collision frequently happens due to HTs when RS receives V2V packets. If RS cannot receive V2V packets, the advantage of relay-assist becomes smaller. Therefore an improved PCRL scheme with sectorized receiving RS (SR-V2VC/PCRL) is proposed to mitigate the effect of HT problem as well as alleviating the congestion issue. An analytical model is then developed to analyze the performance of SR-V2VC/PCRL scheme considering a single intersection scenario. Numerical results show that the reliability of V2V communications is significantly improved by the proposed scheme.

Furthermore, performance of the SR-V2VC/PCRL scheme is discussed for an urban environment with multiple intersections. In such environment, RSs at intersections should cooperate with each other to obtain the largest diversity gain. After theoretically analyzing the performance of the sectorized receiving scheme under multiple interference sources, large-scale simulations are conducted to evaluate the performance of SR-V2VC/PCRL scheme. It is shown that the SR-V2VC/PCRL remarkably improves the reliability of V2V communications. SR-V2VC/PCRL scheme even performs better when employing higher data rate modulation for V2V and relay transmissions.

The aforementioned proposals can remarkably improve the reliability of V2V communications. In order to improve the performance of relay-assisted scheme when traffic load becomes even higher, a network coding (NC) based PCRL scheme (PCRL-NC) with a payload sorting and selection algorithm is proposed to adapt multiple node environment in an intersection. It is shown that the scheme can benefit from NC in alleviating the congestion issue while effectively mitigating the disadvantage of NC. As a result, the introduction of PCRL-NC to the proposed SR-V2VC/PCRL scheme can remarkably improve the reliability of V2V communications under various traffic environments.

Acknowledgment

I am using this opportunity to express my gratitude to everyone who supported me throughout the course. Foremost, I would like to express my sincere gratitude to my supervisor Professor Yasushi Yamao for the continuous support of my study and research, for his patience, immense knowledge. I have studied from him how to find and solve a research problem, and what we need to put our effort to. The experiences and knowledges I have after spending 6 years in Yamao lab will help me a lot for sure when I become an industrial researcher from April 2018. I also would like to thank my fellow lab-mates in Yamao, Fujii, Ishibashi and Adachi Labs for the stimulating discussions, for all the fun we have had in the last six years.

I would like to thank the Japanese Ministry of Education, Culture, Sports, Science and Technology (MEXT) for the financial support for 11 years since April 2007. Without the scholarship, I could not finish my PhD course.

I would like to thanks all my Vietnamese friends in UEC for encouraging me and supporting me so much. Sharing of child rearing and research is such a hard work, and I could not handle without the help from them. I also want to share my excitement with my best friends in Japan (Hai Anh, Hang, Hoan, Huy, Tien) for always being with me.

Last but not least, I would like to thank my family: my parents, Le Trong and Phan Thi Xuan, for giving birth to me and supporting me spiritually throughout my life, my sisters and my brother for their words of encouragement and supports. I would like to thank my wife, Le Thi Hang, for her special love and sacrifice. Especially, she gave me the most precious thing in my whole life: Kumon-kun. We live our life full of love and full of fun from the moment he said hello to the world.

Contents

List of Figures

List of Tables

Acronyms

16QAM	16-Quadrature Amplitude Modulation
3GPP LTE	3rd Generation Partnership Project Long-Term Evolution
64QAM	64-Quadrature Amplitude Modulation
AAA	American Automobile Association
A-ITS	Advanced Intelligent Transport Systems
ARQ	Automatic Repeat reQuest
ASV	Advanced Safety Vehicle
BPDR	Broadcast Packet Delivery Rate
BPSK	Binary Phase Shift Keying
BS	Base Station
BSS	Basic Service Set
CBR	Channel Busy Ratio
CCA	Clear Channel Assessment
CINR	Carrier-to-Interference-and-Noise power Ratio
CS	Carrier Sense
CSL	Carrier Sense Level
CSMA	Carrier Sense Multiple Access
CSMA/CA	Carrier Sense Multiple Access with Collision Avoidance
CW	Contention Window
DCF	Distributed Coordination Function
DIFS	Distributed Inter Frame Space
DOOR	Dynamic Optimization On Range
DOT	Department of Transportation (U.S.)
DSRC	Dedicated Short-Range Communications
D-V2VC	Direct V2V communications
ETC	Electronic Toll Collection
FBR	Front-to-Back Ratio
FFT	Fast Fourier Transform
FSR	Front-to-Side Ratio
GPS	Global Positioning System
HT	Hidden Terminal

ICI	Inter-Carrier Interference
ISI	Inter-Symbol Interference
I-VS	Interfering Vehicle Station
LOS	Line-Of-Sight
MAC	Medium Access Control
NACK	Negative-ACKnowledgement
NAV	Network Allocation Vector
NC	Network Coding
NHTSA	US National Highway Traffic Safety Administration
NLOS	Non-Line-Of-Sight
OBU	On-Board Unit
OFDM	Orthogonal Frequency-Division Multiplexing
ORA	Omnidirectional Receive Antenna
OR-V2VC	Relay-assisted V2V communications with omnidirectional receiving RS
OR-V2VC/PCRL	Relay-assisted V2V communications with omnidirectional receiving and payload combining
PCRL	Packet Payload Combining ReLay
PCRL-NC	Network Coding based Payload Combining ReLay
PDF	Probability Density Function
PDR	Packet Delivery Rate
PGF	Probability Generating Function
PHY	Physical Layer
PLCP	Physical Layer Convergence Protocol
PRR	Packet Reception Rate
PTR	Packet Transmission Rate
QPSK	Quadrature Phase Shift Keying
RL	Normal ReLay
RS	Relay Station
RSSI	Received Signal Strength Indicator
RSU	Roadside Unit
RTS/CTS	Request-To-Send/Clear-To-Send
RTTT	Road Transport and Traffic Telematics
R-V2VC	Relay-assisted V2V Communications
R-VS	Receiving Vehicle Station
SDP	Successful Decoding Probability
SRA	Sectorized Receiving Antenna

SR-V2VC	Relay-assisted V2V communications with sectorized receiving RS
SR-V2VC/PCRL	Relay-assisted V2V communications with sectorized receiving and payload combining
SR-V2VC/PCRL-NC	Relay-assisted V2V communications with sectorized receiving and network coding based payload combining
TDG	Time Division Grouping
TDMA	Time Division Multiple Access
T-VS	Transmitting Vehicle Station
UAV	Unmanned Aerial Vehicle
V2I	Infrastructure-to-Vehicle
V2V	Vehicle-to-Vehicle
VS	Vehicle Station
VSC	Vehicular Safety Communications
WAVE	Wireless Access in Vehicular Environment
WHO	World Health Organization
WLAN	Wireless Local Area Network
XOR	eXclusive-OR

Chapter 1. Introduction

1.1 Research Background

World Health Organization (WHO) indicates that road traffic accidents annually cause more than 1.2 million deaths on the world's roads and have a huge impact on health and development. They are the leading cause of death among young people aged between 15 and 29 years, and cost governments approximately 3% of GDP [1]. A study from the American Automobile Association (AAA) concluded that car crashes cost the U.S. 300 billion dollar per year [2]. While there has been progress in road safety legislation and in making vehicles safer, the pace of change has been too slow. Urgent action is thus needed to achieve the ambitious target for road safety: halving the global number of deaths and injuries from road traffic crashes by 2020. In Japan, although the number of deaths gradually decreases in recent years, it still keeps much higher than 2,500, a target number set by Japanese government. The government is aiming to reduce annual road fatalities to that or less by 2018.

According to the Japanese national police agency, the lack of safety confirmation by driver is the most cause of traffic accidents (Fig. 1.1), which leads to delay in controlling the vehicle [3]. Advanced Safety Vehicle (ASV) has been developed for years in Japan to prevent accidents caused by driver oversight due to low visibility or inattention. ASV is a joint initiative involving industry, academia and government, and headed by the Japanese Ministry of Land, Infrastructure, Transport and Tourism [4]. By employing advanced Intelligent Transport Systems (A-ITS) that consists of varieties of technologies based on electronics, sensors, wireless communications and artificial intelligence (AI), ASV can recognize surrounding environment, provide drivers with information on potential hazards such as the approach of vehicles and pedestrians, and support drivers even when visibility is low (Fig 1.2). In some cases, ASV can directly control the vehicle to avoid collisions.

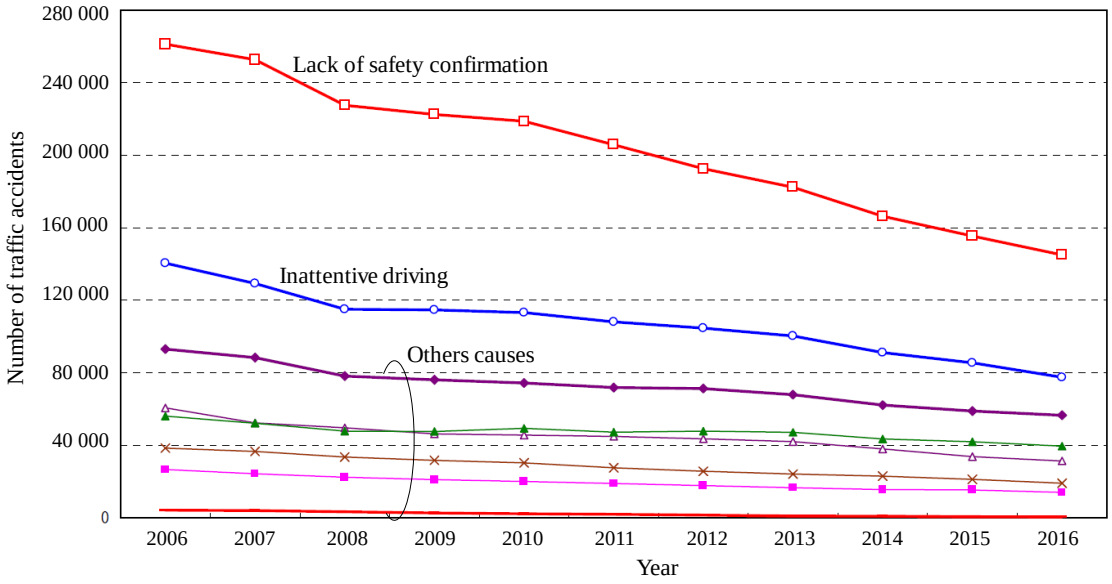

Source: Japan national police agency.

Fig. 1.1: Lack of safety confirmation is the most cause of accidents [3].

Source: http://www.mlit.go.jp/jidosha/anzen/01asv/resourse/data/asv5pamphlet.pdf

Fig. 1.2: Advanced Safety Vehicle (ASV)

To enable information exchange between vehicles and roads for preventing potential accidents, wireless communication is the essential means in A-ITS. According to the U.S. Department of Transportation (DOT), vehicular communication systems potentially address about 80 % of all-vehicle target crashes [5]. In Japan, more than 70 % of the accidents are due to rear-end collision, collision at intersection as well as left-turn and right-turn collisions [3]. These types of crashes can be potentially alleviated by employing vehicle-to-vehicle (V2V) and infrastructure-to-vehicle (V2I) communications.

Besides traffic safety improvements, vehicular networks have several other benefits that can be achieved by real-time data processing. Examples include congestion detection and avoidance, travel-time estimation, route guidance and cooperative driving. These services can save both time and fuel and therefore they have significant economic advantages. Furthermore, vehicular communications have been supposed to play an important role in the future automated driving systems [6].

Many efforts have been done in the area of vehicular communications for safety support applications. In 1999, the U.S. Federal Communication Commission allocated 75MHz of Dedicated Short-Range Communications (DSRC) spectrum at 5.9 GHz to be used exclusively for V2V and V2I communications [7]. In 2004, a task group was formed in order to develop a standard for wireless access in vehicular environment (WAVE). By 2010, the IEEE 802.11p standard was approved by IEEE as a PHY/MAC protocol for DSRC [8]. It is modified from the IEEE 802.11a standard and encompasses enhancements to the physical (PHY) and medium access control (MAC) layers to address communications in vehicular environments. The PHY layer is based on orthogonal frequency-division multiplexing (OFDM), and the MAC layer uses a carrier sense multiple access (CSMA) scheme to control access to the transmission medium. The operational functions and complexity related to DSRC are handled by the upper layers of the IEEE 1609 set of standards, which define how applications that utilize WAVE will function in a vehicular environment. More specifically, IEEE P1609.1 [9] defines management activities, while IEEE P1609.2 [10] defines security protocols, and IEEE P1609.3 [11] defines networking protocols. The IEEE 1609.4 [12] covers definitions and recommendations for multi-channel operation. In Japan, instead of the 5.8 GHz band, which is currently used for ETC (Electronic Toll Collection) system, the

band of 760 MHz was allocated for V2V and V2I communications [13]. In 2012, ARIB STD-T109 was established as a standard for V2V and V2I communications [14]. It uses the same physical layer with IEEE 802.11p, but employs a modified MAC layer that mixes CSMA/CA (Carrier Sense Multiple Access with Collision Avoidance) with time slotted access to share the single channel by V2V and V2I communications.

Another candidate technology for vehicular communications is long-term evolution (LTE)-Advanced standardized by 3rd generation partnership project (3GPP). In the infrastructure-based LTE approach, each vehicle station (VS) in a cell transmits its beacon message in the uplink channel to the base station (BS). Then the BS retransmits the beacon in the downlink channel to other intended recipients [15].

1.2 Motivations and Contributions

1.2.1 Motivations

This dissertation focuses on V2V communication that employs the IEEE 802.11p standard, which is ready and validated for deployment after around 10 years of researches, tests and field trials. In December 2016, the US National Highway Traffic Safety Administration (NHTSA) proposed to mandate IEEE 802.11p based DSRC for all new light vehicles [16].

In IEEE 802.11p based V2V communications for safety support applications, the reliability of communications is the most important performance requirement. In ARIB STD-T109 [14], it is specified that cumulative packet reception rate should satisfy 95 % while a vehicle moves 10 m (or 5 m when GPS accuracy level becomes better in the near future). If vehicle speed is 60 km/h, there are only triple chances of the reception during the move of 5 m. Then reliability of each reception should keep more than 63.2 %. More reliable communication will be required for the future automated driving systems. For example, the cumulative packet reception rate should satisfy 99 % while a vehicle moves 5 m. However, the reliability of wireless communications is severely affected by distance dependent path loss, shadowing, and fast fading caused by multipath propagation. It is known that the packet delivery rate (PDR) from transmitting VS (T-VS) to receiving VS (R-VS) of direct V2V communications (D-V2VC) rapidly

deteriorates under non-line-of-sight (NLOS) environments such as intersections [17]. Furthermore, a hidden terminal (HT) problem is a great concern in CSMA/CA based wireless network due to its distributed access nature [18]-[19]. In V2V communications, buildings around corners not only reduce the communication range but also cause HT problem. Thus, it is difficult for the D-V2VC to achieve reliable communications near intersections.

This dissertation focuses on improving the reliability of V2V communications for ITS safety support applications considering intersection scenarios. The reason to focus on intersections is most of the accidents happen around intersections in urban area as shown in Fig. 1.3. There are several approaches proposed in the literatures to improve the reliability of V2V communications. In [20], a simple retransmission scheme is proposed to combat HT problem and improve the reliability of V2V communications. In the scheme, a receiver that identifies a collision process sends a NACK signal back to the senders to require retransmissions. In [21], another retransmission scheme using network coding is proposed. The scheme combines multiple V2V packets that were transmitted by different vehicles into a single retransmission by using the concept of network coding. In [22], a message rate adaptation, which adjusts the transmit rate and/or transmit power for the beacon messages is proposed. The scheme can control the channel load below a certain threshold, and thus effectively to mitigate congestion in V2V communications. In [23] and [24], system parameters such as transmit power and

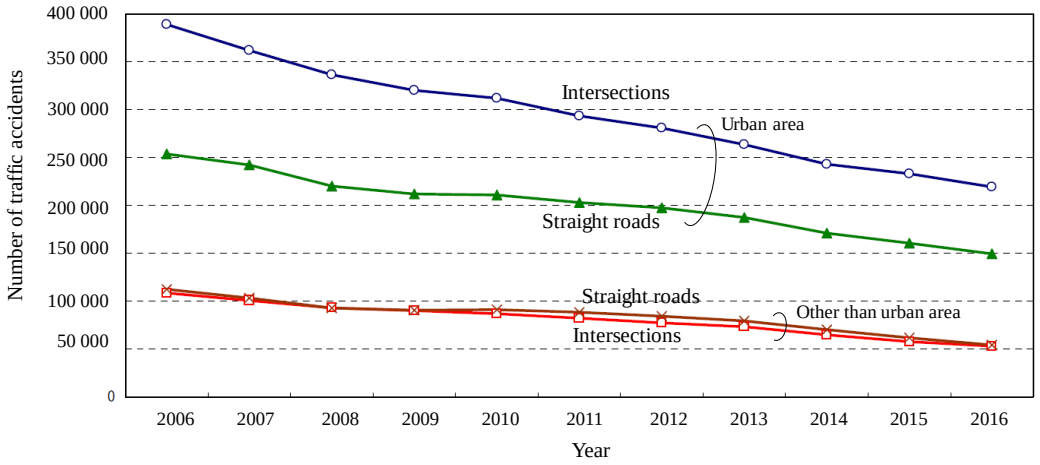

Source: Japan national police agency.

Fig. 1.3: Traffic accidents happen most often in urban area, especially around intersection [3]**.**

carrier sensitivity are adaptively adjusted according to the environments. Although all the works intend to improve the reliability of V2V communications, their effectiveness in intersection scenarios are not clear. At intersections, corners are often occupied by buildings, which may block line-of-sight (LOS) paths and severe shadowing loss hinders communications between vehicles. Under this circumstance, successful delivery of safety related messages by the direct V2V communications is challenging.

In order to overcome the shadowing problem in NLOS situations such as intersections, the utilization of parked vehicles as relay nodes has been proposed in [25]. The effect of obstacles can be mitigated through the packet retransmission by the parked car around the intersections. However, it is not guaranteed that a parked vehicle exists around the intersection. Furthermore, even if there is any parked car, it cannot be utilized if its engine is turned off. In [26], unmanned aerial vehicles (UAVs) are introduced to relay packets between vehicles on the ground. Another approach is the utilization of roadside units (RSUs) as a relay station (RS). In [17], a relay-assisted V2V communications (R-V2VC) scheme has been proposed, which does not require any modification to IEEE 802.11p protocol. In R-V2VC scheme, an RS that has LOS links to two communicating VSs assists the communication. By compensating the large path loss and obtaining the path diversity effect, the PDR of V2V communications improves [17].

However, two main issues prevent the R-V2VC scheme from achieving high reliability. First, packet congestion happens at RS that limits the performance improvement by relay-assist. As traffic becomes higher, the number of packets that RS has to retransmit becomes larger. This leads to a large number of packets waiting in the transmit queue of RS. If the normal relay scheme is employed, the packets may be dropped due to the limited queue size. If the packet drop happens, the gain obtained by relay may be decreased. Consequently, it is crucial to introduce a kind of traffic congestion avoidance methods to RS. Second, R-V2VC scheme still suffers from HT problem, which limits the performance of relay-assist. When RS is located around intersections where LOS propagation between VSs is often unavailable, the packet collision frequently happens at RS due to HTs because VSs cannot carrier sense each other. If packet collision happens at RS, the advantage of R-V2VC becomes smaller.

In addition, in actual environments, multiple RSs may coexist, e.g., each RS is installed at each intersection in urban area. In such a case, to obtain the maximum diversity effect among RSs while minimizing the drawback such as packet congestion due to relayed packets from multiple RSs, a sophisticated RS cooperation scheme should be developed.

1.2.2 Contributions

The main contributions of this dissertation are as follows.

1) A packet payload combining relay (PCRL) scheme is proposed to deal with the congestion issue at RS. In the scheme, multiple V2V packet payloads are combined into a single packet and the resultant packet is rebroadcasted once the channel becomes idle. Analytical and simulated results show that the proposed PCRL scheme can remarkably alleviate the congestion issue and improve the relaying performance.

2) An improved PCRL scheme with sectorized receiving RS (SR-V2VC/PCRL) is proposed in order to alleviate the congestion issue as well as mitigate the effect of HT problem. A theoretical model is derived to evaluate the performance of the proposed scheme considering both straight street and intersection scenarios. The model takes into account the effect of multiple HTs and fading. Numerical results show that the reliability of V2V communications is significantly improved by the proposed scheme.

3) Performance of the proposed SR-V2VC/PCRL scheme is evaluated in an urban scenario that consists of multiple intersections. The employed performance metric is broadcast packet delivery rate (BPDR). After theoretically analyzing the effectiveness of the sectorized receiving scheme under multiple interference sources, large-scale simulations are conducted to evaluate performance of SR-V2VC/PCRL scheme. It is shown that the SR-V2VC/PCRL remarkably improves BPDR of V2V communications. SR-V2VC/PCRL scheme even performs better when employing higher-order modulation for V2V communications and relay transmission.

4) A highly reliable network coding (NC) based PCRL scheme with a payload sorting and selection algorithm (PCRL-NC) is proposed to solve the congestion issue at RSs due to the increased traffic in urban environments. The proposed PCRL-NC for SR-V2VC scheme (SR-V2VC/PCRL-NC) is evaluated by theoretical analysis and large-scale simulations. Numerical results show that by employing the proposed algorithm for the encoding process, the disadvantage of normal NC is alleviated while the congestion issue is effectively mitigated. As a result, the proposed SR-V2VC/PCRL-NC remarkably improves the reliability of V2V communications even under very high traffic conditions.

1.3 Outline of the Dissertation

This dissertation consists of 7 Chapters, which are outlined in Fig. 1.4. Fig. 1.5 shows the technology map for this dissertation. The organization is described as follows:

- **Chapter 1** gives the introduction about the dissertation that contains the research background, the motivations and the contributions.
- **Chapter 2** gives a brief introduction about the technical background of vehicular communication systems for ITS safety support applications. The PHY and MAC layer protocol and frequency allocation of ITS applications are also described.
- **Chapter 3** proposes a packet payload combining relay (PCRL) to deal with the congestion issue at RS. An analytical model is derived to evaluate the performance of the proposed scheme. The accuracy of the model is verified by simulation results.
- **Chapter 4** analyzes the performance of the sectorized receiving relay scheme. In order to achieve the potential benefit of relay, the combination of sectorized receiving and payload combining (SR-V2VC/PCRL) is proposed. The analytical expressions of the packet reception rate at RS as well as the PDR of SR-V2VC/PCRL are derived. Computer simulations are conducted to confirm the validity of the theoretical derivation.

- **Chapter 5** evaluates the performance of the SR-V2VC/PCRL scheme in urban environment with multiple intersections by using large-scale simulations. Then an adaptive modulation and coding for the direct V2V communications is proposed.
- **Chapter 6** proposes a network coding based PCRL (PCRL-NC) scheme with a payload sorting and selection algorithm to further mitigate the congestion issue at RS under high traffic conditions.
- **Chapter 7** summarizes the dissertation.

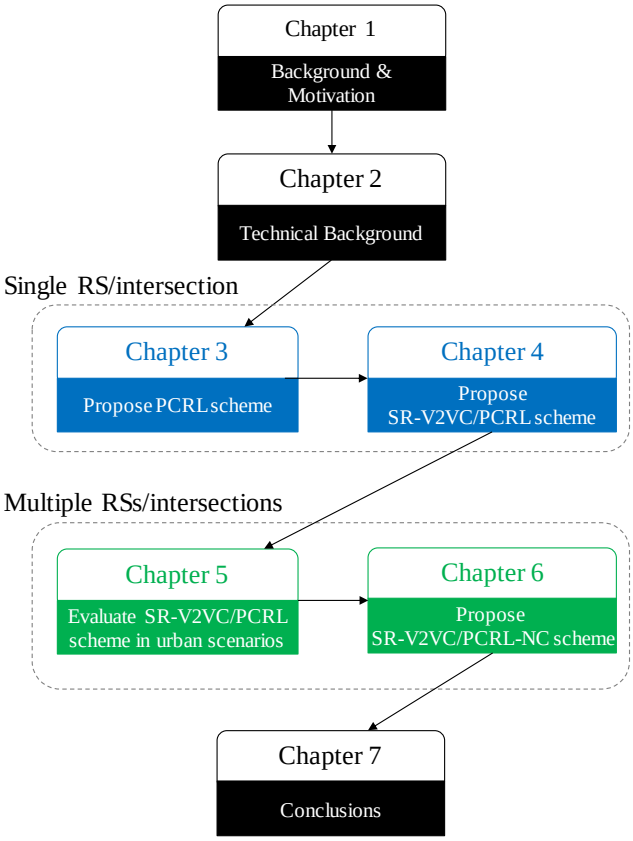

Fig. 1.4: Outline of the dissertation.

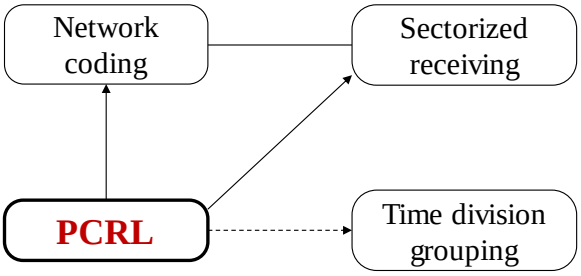

Fig. 1.5: Technology map for this dissertation.

Chapter 2. Technical Background

This chapter explains about the technical background of the research in this dissertation. Two types of ITS related applications and the communications requirements are introduced. Next, the PHY/MAC layer specifications of IEEE 802.11p protocol to support such applications are provided. Then, the frequency allocations in the eastern and western countries are investigated. Finally, the propagation models at the intersection are presented.

2.1 Application Descriptions and Requirements for Communication

Two categories of applications can be enabled by wireless communication technologies in A-ITS: safety and non-safety applications.

2.1.1 Safety Applications

Active safety applications highly depend on accurate estimate of the states of neighboring vehicles to correctly predict hazardous crash situations. This will allow timely actions by the driver or autonomous driving control. Furthermore, a vehicle expects to receive enough information on a continuous basis from all its neighboring vehicles to maintain the accurate estimation. Therefore, each vehicle frequently broadcasts beacon messages (or periodic messages) that includes its mobility status (speed, braking status, velocity vector …) to neighboring vehicles of up to a few hundred meters. This is generally obtained from Global Positioning System (GPS) receiver and onboard sensors such as speed meter, and broadcasting the beacons over a single-hop IEEE 802.11p based broadcast channel. On the other hand, if an abnormal

situation such as a hard brake happens, it is necessary to immediately notify the nearby vehicles. In such a case, an event-driven message is generated and disseminated through the vehicular network with high priority. However, this type of message is relatively rare and does not contribute much to the total channel load [27]-[28].

This dissertation focuses on the delivery of beacon messages for safety applications such as intersection collision warning, cooperative forward collision warning and left- and right-turn assistant. The communication requirements needed for the applications to function properly in its mode of operation are listed in Table 2.1 [29]-[32]. The size of a periodic message is usually short as 100 bytes [11], [31]. In the future, more information for necessary automated driving systems and redundant bits necessary for information security may be added, and thus the message size may become larger. Periodic messages are broadcasted with the interval of 100 ms in order to provide up-to-date information [30], [32]. If the latest periodic message is ready to be transmitted, the previous one will be discarded. Thus, the allowable latency for the beacon message is equal to the broadcast interval of 100 ms [32].

Intersection collision warning application warns drivers when a collision at an intersection is probable. By receiving the beacon messages transmitted from others vehicles approaching an intersection, a vehicle can detect the nearby vehicles as well as their position, velocity, and turning status. Based on a warning strategy, application determines when a collision is imminent and issues a warning to the driver. The maximum required range of communications is up to 300 m [30], [32].

Cooperative forward collision warning application is designed to aid the driver in avoiding collisions with the rear-end of vehicles in the forward path of travel. This is an enhancement of the radar-based forward collision warning system. Using the mobility information from the lead vehicles along with its own position and roadway information, a vehicle can determine whether a rear-end collision is likely. The communication range is around 150 m [30], [32].

Left- and right-turn assistant application provides information to drivers about oncoming traffic to help them make a left/right turn at a signalized intersection. The application determines that there is a need for information about approaching traffic near an intersection based upon the driver’s activation of the left/right turn signal. Based on the received beacon messages, the application collects the location and movement

Table 2.1: Examples of safety applications and the requirements [30-32]

Applications	Max. payload size	Transmission interval	Allowable latency	Communication range
Intersection collision warning	100 bytes	100 ms	100 ms	250 ~ 300 m
Cooperative forward collision warning				150 m
Left- and right-turn assistant				250 ~ 300 m

patterns of oncoming vehicles and provides the relevant information to driver. Same as the intersection collision warning application, the maximum required range of communications can be up to 300 m [30], [32].

Other safety applications using event-driven message include approaching emergency vehicle warning and vehicle-based road condition warning. The first one provides the driver a warning to yield the right way to an approaching emergency vehicle. The second application detects marginal road conditions using on-board systems and sensors, and then broadcasts a road condition warning to other vehicles [32].

2.1.2 Non-Safety Applications

While safety applications have ability to reduce traffic accidents and to improve general public safety, the non-safety applications for traffic management, tolling, internet access… provide additional information and value-added infotainment features to the passengers and drivers. These features can create a new driving experience and open new business chances for many companies.

Examples of non-safety applications include intelligent traffic flow control, free-flow tolling, adaptive drivetrain management, green light optimal speed advisory ... In general, non-safety applications may require wider communication range than safety applications. However, the latency requirement is not as stringent as that of safety applications. For example, allowable latency is around one second for the intelligent traffic flow control application [32].

2.2 IEEE 802.11p PHY/MAC Standard

The first version of the IEEE 802.11 standard was published in 1997 and specifies the MAC and PHY layers for wireless local area networks (WLANs). Over the years, the standard was continuously developed and grew, so that numerous amendments were created. One of them is the IEEE 802.11p [8], a variant of IEEE 802.11a that additionally covers the specifics of vehicular communications: highly dynamic environment, low latency, and operation in a reserved frequency band. This section explains about the specifications of PHY and MAC layers of this standard.

2.2.1 Physical Layer Specification

On physical layer, IEEE 802.11p is similar to IEEE 802.11a, with some adaptations to support low-latency and robust vehicular communications. The main differences between these two standards are listed in Table 2.2 [33]. The channel bandwidth in protocol 802.11p is 10 MHz which is half the bandwidth of protocol 802.11a in order to make the signal more robust against fading. Several measurements showed the delay spread of up to 0.8 μs and a Doppler spread of up to 2 kHz due to multipath propagation and the high-speed moving vehicles, respectively [34]-[35]. The longer guard interval of 1.6 μs as well as symbol duration of 8 μs in the IEEE 802.11p standard can effectively mitigate inter-symbol interference (ISI) caused by the delay spread. In addition, the Doppler spread is much smaller than the subcarrier spacing of 156.25 kHz that can alleviate inter-carrier interferences (ICIs). For the same reason, the physical layer convergence protocol (PLCP) preamble duration, the guard time and the fast Fourier transform (FFT) period are 2 times larger than those in the protocol for IEEE 802.11a.

OFDM transmission technique with 64 orthogonal subcarriers is used then each orthogonal frequency subcarrier has spacing of the aforementioned 156.25 kHz. Of 64 subcarriers, 52 carriers are utilized; 4 pilot carriers transmit a fix pattern, the other carriers contain the data. Subcarriers are modulated using binary or quadrature phase shift keying (BPSK/QPSK), 16-quadrature amplitude modulation (16QAM) or 64-quadrature amplitude modulation (64QAM). Forward error correction coding (convolutional coding) is used with a coding rate of 1/2, 2/3 or 3/4. The data rate is thus

Table 2.2: Parameters for PHY layers of IEEE 802.11a and IEEE 802.11p [14]

Parameters	IEEE 802.11a	IEEE 802.11p	Changes
Channel bandwidth	20 MHz	10 MHz	Half
Subcarrier spacing	312.5 kHz	156.25 kHz	Half
Data rate (Mbps)	6, 9, 12, 18, 24, 36, 48, 54	3, 4.5, 6, 9, 12, 18, 24, 27	Half
Symbol duration	4 μs	8 μs	Double
Guard time	0.8 μs	1.6 μs	Double
FFT period	3.2 μs	6.4 μs	Double
Preamble duration	16 μs	32 μs	Double

two times less than that in the IEEE 802.11a standard.

Fig. 2.1 shows the 802.11p frame format. It contains three parts: preamble, signal field and the data symbol parts. The PLCP preamble part at the beginning contains training sequence information used by the receiver for frequency correction and channel estimation. The following PLCP header contains information on the modulation/coding rate of subcarriers, the length of the transmission, and other additional information and sent with the basic data rate of 3 Mbps. It means that the length of the signal field is fixed at 8 μs for every frame. Finally, the data symbols part contains the IEEE 802.11 headers, the payload data to be transmitted and some other information.

2.2.2 MAC Layer Specification

A fundamental difference of IEEE 802.11p compared to the others IEEE 802.11 protocols designed for wireless LAN systems is the ability to communicate outside the context of a basic service set (BSS) to enable communication in an ad-hoc manner in a highly mobile network. The authentication and association processes in the normal IEEE 802.11 would last too long in the situation of communication between two vehicles with opposing driving direction. Thus, they are omitted in the IEEE 802.11p PHY/MAC protocol.

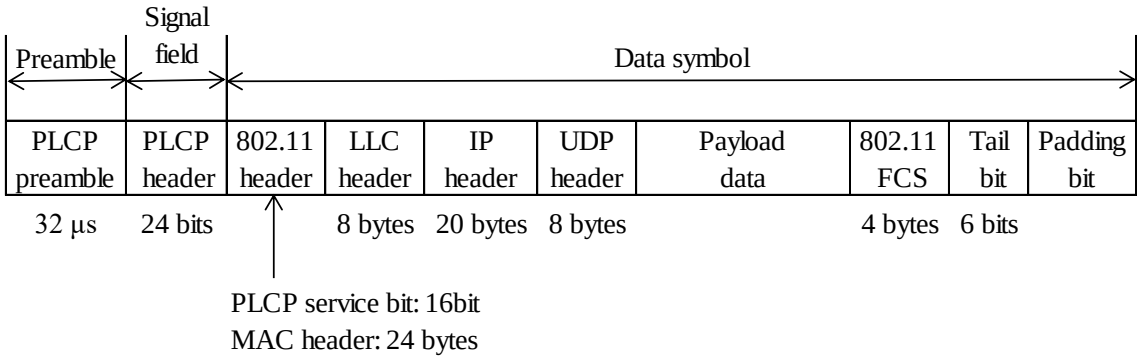

Fig. 2.1: IEEE 802.11p frame format

This section explains about the main procedures of IEEE 802.11 MAC layer protocol using distributed coordination function (DCF). The DCF is the basis of the standard CSMA/CA access mechanism [36]. Under this method, a node will sense the shared channel before transmitting. If the channel is sensed as idle for greater than an amount of time called Distributed Inter Frame Space (DIFS), then the node will transmit immediately (Fig. 2.2(a)). On the other hand, if an on-going transmission is detected, the node suspends its transmission and evokes a backoff procedure to void collision (Fig. 2.2(b)). The node first sets the backoff timer T_b, which can be expressed

$$T_b = CW \times \delta \quad \textbf{(2.1)}$$

where CW is a random integer number selected within the backoff range [0, CW_{max}] with the contention window (CW) size CW_{max} and δ is the unit timeslot. When the channel becomes idle for a DIFS period, the backoff timer starts to decrement. The node will transmit its packet immediately when the timer reaches zero. On the other hand, if any transmission is sensed during the backoff, the decrement process is suspended until the channel becomes idle again. Moreover, the premise of resuming decrement of the backoff timer is that the channel stays free for the duration of a DIFS interval.

Table 2.3 shows the main parameters of MAC layer for IEEE 802.11a and IEEE 802.11p protocol. The length of slot time and DIFS for IEEE 802.11p is 13μs and 58 μs, respectively, longer than those of IEEE 802.11a. The minimum and maximum contention window sizes are 15 and 1023, respectively. However, if we consider vehicular broadcast communications, there has no retransmission then the minimum and maximum contention window sizes are the same.

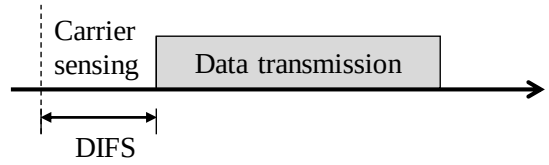

(a) Immediate access when channel is idle

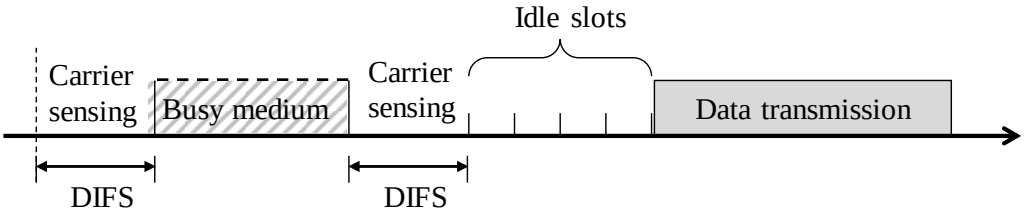

(b) Defer the transmission when channel is busy

Fig. 2.2: IEEE 802.11 channel access method

Table 2.3: Parameters for MAC layer of IEEE 802.11a and IEEE 802.11p

Parameters	IEEE 802.11a	IEEE 802.11p
Slot time	9μs	13μs
DIFS	34 μs	58 μs
Minimum contention window size	15	15
Maximum contention window size	1023	1023

Carrier sense (CS) is used to determine if the medium is idle or busy. CS is composed of two separate and distinct functions, Clear Channel Assessment (CCA) and Network Allocation Vector (NAV). CCA is physical CS which listens to received energy on the radio interface. NAV is virtual CS which is used by stations to reserve the medium for mandatory frames. CCA indicates a busy medium for the current frame, whereas NAV reserves the medium as busy for the future frames that required to be transmitted. Typically, NAV is used for the reservation of control frames from RSUs as in [14], and is not considered in this dissertation.

There are two common ways of detecting an incoming transmission by CCA. Preamble detection is the simplest method. Since each transmission begins with a unique preamble sequence, it is highly likely that there is an incoming transmission if

the station decodes a preamble. The other method is energy detection. Just before a transmission, the station makes its CS decision with a comparison between the instantaneous RSSI (Received Signal Strength Indicator) and a fixed threshold called carrier sense level (CSL). If the RSSI reading is greater than CSL, the channel is sensed as busy, and otherwise the channel is sensed as idle.

However, CS performance is not always perfect. This may result in HT problem [37]-[38]. Fig. 2.3 illustrates the situation. Two transmitters, nodes B and C, are out of the communication range of each other. The intended recipient of their transmissions, node A, is within their communication ranges. The transmitters B and C may try to communicate with node A simultaneously, but cannot detect the interference. As a result, packet collision may happen at node A. The HT problem depends on CSL, the communication environment and the number of competing nodes. In vehicular environments, attenuation losses due to fast fading and shadowing prevent the node from achieving high probability of CS success. When the number of competing nodes increases, the number of nodes tries to transmit packets becomes large which results in high probability of simultaneous transmissions.

Under the event of collision, one of the multiple overlapping packets can be successfully received owing to the presence of capture effect [17], [39]. This happens when the power ratio of one packet to the others plus noise is higher than a required Carrier-to-Interference-and-Noise power Ratio (CINR) value. The required CINR value

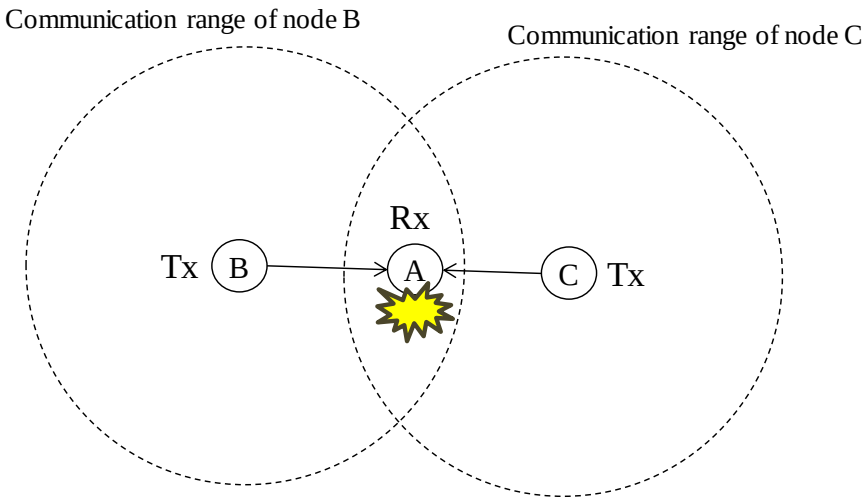

Fig. 2.3: Hidden terminal (HT) problem

depends on the data rate. The IEEE 802.11p defines eight different data rates between 3 and 27 Mbps [8]. The data rates of 6 Mbps or higher are generally assumed for V2V communications [40]-[41]. Their required CINRs are listed in Table 2.4. Higher data rates result in shorter transmission time, but require higher CINR to successfully receive the packets.

2.3 Frequency Band Allocations

The ITS frequency bands allocations in Europe, the North America and Japan are summarized in Fig. 2.4. A frequency band centered at 5.8 GHz is specified based on the ITU-R Recommendation M.1453-2 [42]. In Europe, the frequency band 5795-5815 MHz is used for road transport and traffic telematics (RTTT) applications. The frequency band 5,875-5,925 MHz is designated to ITS safety applications and the objective with the non-safety applications in the band 5,855-5,875 MHz is to provide non-safety communication services that would enhance the ITS concept for V2V and V2I communications [43]. In the North America, the frequency band 902-928 MHz is currently used for ITS services such as ETC while a shared bandwidth of 75 MHz frequency band from 5,850 to 5,925 MHz is allocated for DSRC applications in 1999.

Table 2.4: Main candidate data rates for IEEE 802.11p based V2V communications

Data rate (Mbps)	Modulation	Coding rate	Required CINR (dB)
3	BPSK	1/2	7
4.5	BPSK	3/4	8
6	QPSK	1/2	10
9	QPSK	3/4	11
12	16QAM	1/2	15
18	16QAM	3/4	19
24	64QAM	2/3	23
27	64QAM	3/4	24

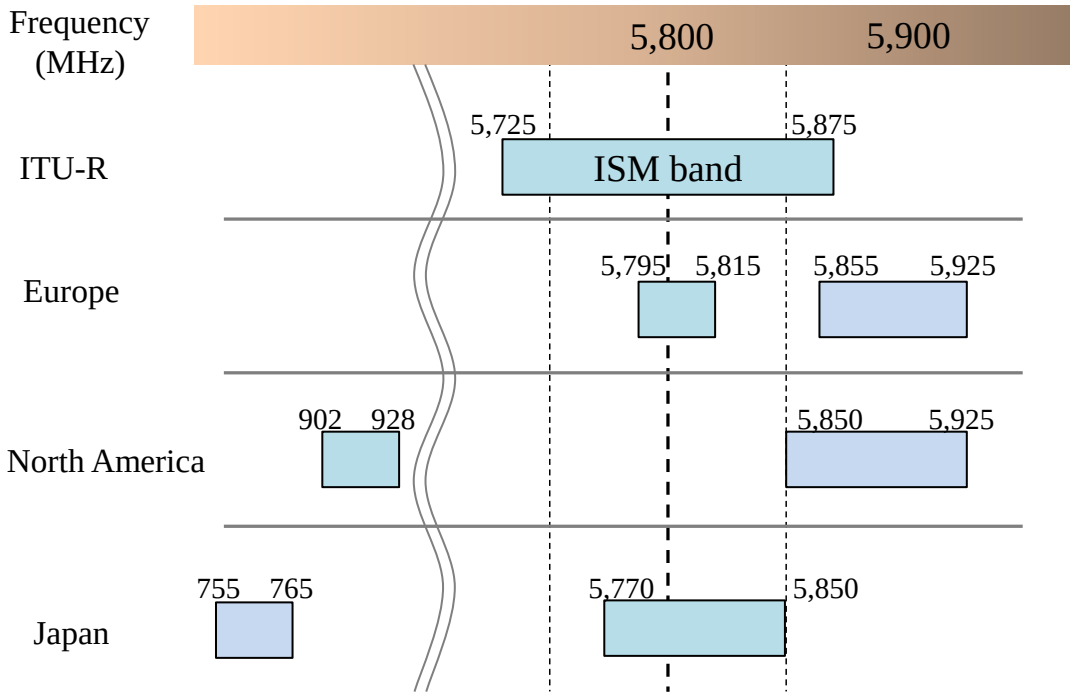

Fig. 2.4: ITS frequency bands allocation

The 5.9 GHz band is divided into eight channels (one control channel with 10 MHz bandwidth, six service channels with 10 MHz bandwidth and one reserve channel with 5 MHz). The safety-related information is transmitted in the control channel, while the service channels are used for traffic management applications, infotainment applications, etc.

In Japan, in addition to the 5.8 GHz band which is currently used for ETC, frequency band 755-765 MHz is allocated for V2V and V2I communications. As summarized in Fig. 2.5, the frequency band centered at 760 MHz was allocated in the past for analogue television broadcasting services. It became available after the digitization of television broadcasting which was completed in April 2013. After a series of tests and road experiments, this band was officially allocated for ITS safety support applications in December 2012 [44]. Since the 760 MHz frequency band has lower propagation and diffraction losses caused by buildings and obstacles than the 5.8 GHz frequency band, the former one is suitable for communications at NLOS area, such as V2V communication at intersections.

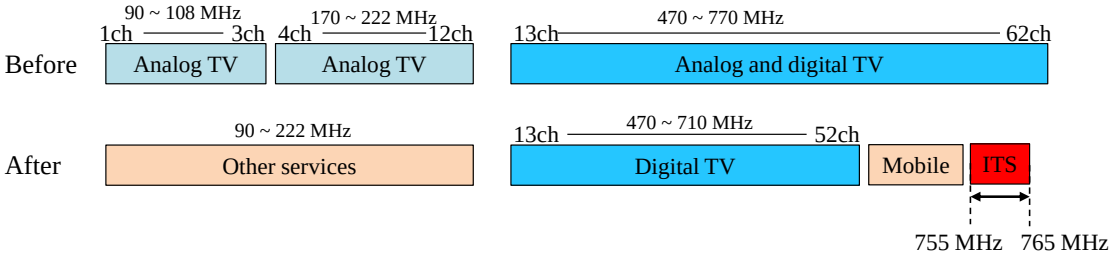

Fig. 2.5: Frequency arrangement regarding 700 MHz range in Japan

2.4 Radio Propagation Model for Intersections

Propagation over paths of length less than 1 km is affected primarily by buildings and trees, rather than by variations in ground elevation. In particular, the effect of buildings is predominant in vehicular environments, especially in urban areas. The corners at intersection are often occupied by buildings, which may block the direct path between transmitting and receiving vehicles. Under such NLOS circumstances, the received signal power may be strongly dropped. On the other hand, if the vehicles are on the same street, and the direct ray between them is unobstructed by obstacles such as buildings, the radio link is considered LOS. In this case, the received power may be much larger than the NLOS case.

Radio propagation in vehicular environments can be typically categorized into these two cases. Thus, two radio propagation models that can predict the propagation losses for wireless transmission around intersections are necessary. Moreover, both 5.8 GHz and 760 MHz are the candidate frequency bands for ITS in Japan. It would be the best that the propagation models can cover the above spectra. One of the promising candidates is ITU-R P.1411-6 [45], which provides methods for estimating path losses in urban and suburban areas over the frequency range from 300 MHz to 100 GHz. The models recommended by the International Telecommunication Unit (ITU) are widely accepted and used for coordination and comparison purpose [46]. Therefore, in this dissertation, the ITU-R P.1411-6 path loss models are employed.

2.4.1 Propagation Model for LOS Situation with Street Canyons

For the frequency range from 300 MHz to 3 GHz, basic transmission loss can be characterized by two slopes and a single breakpoint. An approximate lower bound is given by

$$L_{\mathrm{LOS}} = L_{bp} + \begin{cases} 20\log_{10}\left({}^{d}/_{R_{bp}}\right) & \text{for } d \le R_{bp} \\ 40\log_{10}\left({}^{d}/_{R_{bp}}\right) & \text{for } d > R_{bp} \end{cases} \tag{2.1}$$

where d is the distance between the transmitting and receiving vehicles. R_{bp} is the breakpoint distance and is given by

$$R_{bp} \approx \frac{4h_{\mathrm{t}}h_{\mathrm{r}}}{\lambda} \tag{2.2}$$

where λ is the wavelength. h_{t} and h_{r} are the height of transmitting and receiving antennas, respectively. L_{bp} is a value for the basic transmission loss at the break point, defined as

$$L_{bp} = \left|20\log_{10}\left({}^{\lambda^2}/_{8\pi h_{\mathrm{t}}h_{\mathrm{r}}}\right)\right| \tag{2.3}$$

An approximate upper bound is given by

$$L_{\mathrm{LOS}} = L_{bp} + 20 + \begin{cases} 25\log_{10}\left({}^{d}/_{R_{bp}}\right) & \text{for } d \le R_{bp} \\ 40\log_{10}\left({}^{d}/_{R_{bp}}\right) & \text{for } d > R_{bp} \end{cases} \tag{2.4}$$

The upper bound has the fading margin of 20 dB. In addition, the coefficient before break point is set to 2.5 since that a short distance leads to weak shadowing effect.

Finally, an approximate median bound is given by

$$L_{\mathrm{LOS}} = L_{bp} + 6 + \begin{cases} 20\log_{10}\left({}^{d}/_{R_{bp}}\right) & \text{for } d \le R_{bp} \\ 40\log_{10}\left({}^{d}/_{R_{bp}}\right) & \text{for } d > R_{bp} \end{cases} \tag{2.5}$$

Note that the lower value is used in this dissertation.

2.4.2 Propagation Model for NLOS with Street Canyons

This situation is depicted in Fig. 2.6. Here, we assume that the antenna heights of transmitting and receiving vehicles are below the rooftop level. The propagation loss is given as

$$L_{\mathrm{NLOS}} = -10\log_{10}\left(10^{-L_{\mathrm{r}}/10} + 10^{-L_{\mathrm{d}}/10}\right) \quad \textbf{(2.6)}$$

where L_{r} and L_{d} are the reflection and diffraction losses, respectively. The reflection loss is yielded by nine purely reflections, and is defined by

$$L_{\mathrm{r}} = 20\log_{10}(x_1 + x_2) + x_1 x_2 \frac{1}{w_1 w_2}\frac{3.86}{\alpha^{3.5}} + 20\log_{10}\left(\frac{4\pi}{\lambda}\right) \quad \textbf{(2.7)}$$

where α is the corner angle in rad, and $0.6 < \alpha < \pi$. x_1 and x_2 are the distances from transmitting and receiving vehicles to the intersection center, respectively. w_1 and w_2 are the street widths at the position of the transmitting and receiving vehicles, respectively. These parameters are illustrated in Fig. 2.6. The diffraction loss can be calculated as

$$L_{\mathrm{d}} = 10\log_{10}[x_1 x_2 (x_1 + x_2)] + 2D_{\mathrm{a}} - 0.1\left(90 - \alpha\frac{180}{\pi}\right) + 20\log_{10}\left(\frac{4\pi}{\lambda}\right) \quad \textbf{(2.8)}$$

where

$$D_{\mathrm{a}} = \frac{40}{2\pi}\left[\arctan\left(\frac{x_1}{w_1}\right) + \arctan\left(\frac{x_2}{w_2}\right) - \frac{\pi}{2}\right] \quad \textbf{(2.9)}$$

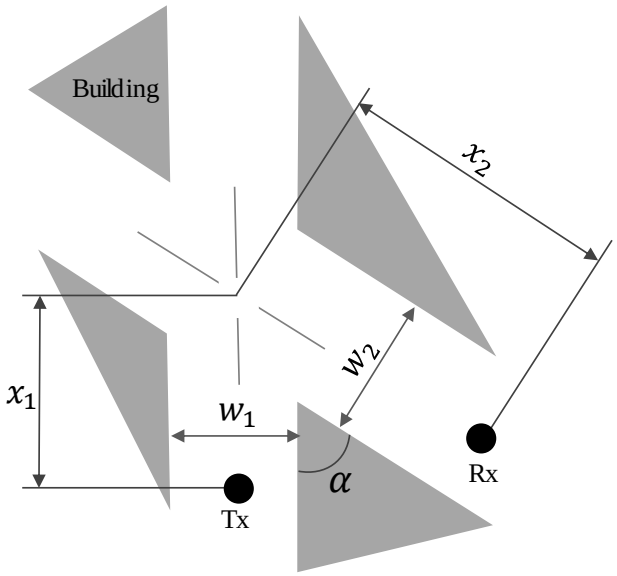

Fig. 2.6: Definition of parameters for NLOS condition

Chapter 3. Relay-Assisted V2V Communications with Payload Combining

This chapter first proposes a packet payload combining relay (PCRL) scheme to alleviate packet congestion issue at RS for relay-assisted V2V communications (R-V2VC) scheme. In addition, a time division grouping (TDG) method is introduced to PCRL scheme in order to mitigate the effect of HT problem. Next, an analytical model is derived to theoretically analyze the packet transmission rate at RS by modeling the backoff process at RS as a Markov chain and using the signal transfer function of the generalized state transition diagram. Finally, computer simulations considering a single intersection scenario are conducted to validate the model as well as confirm the effectiveness of PCRL scheme.

3.1 Introduction

Addition of RS to CSMA/CA based V2V communications can effectively mitigate the effect of shadowing as well as compensate fading loss and thus improve the reliability of V2V communications, especially around intersection environments. The effectiveness of the R-V2VC scheme has been shown in previous works by theoretical analysis and simulations [17], [47]. However, as the number of VSs increases, the number of need-to-be transmitted packets at RS becomes larger. This poses an issue that is not obvious when traffic is very low. At high traffic conditions, it takes RS longer time to contend for its transmission. As a result, the number of awaiting packets in the transmit queue at RS increases. Since the queue size is limited and each packet has its

delay requirement, the packets may need to be dropped. If the packet drop happens, the R-V2VC scheme cannot improve the PDR. Therefore, the potential improvement brought by RS cannot be fully obtained as investigated in [17]. Thus, it is necessary to avoid the packet congestion at RS. Employing dual frequency bands for the R-V2VC scheme was proposed in [17], [47] to solve the congestion issue. However, frequency resources are precious and not always available in many countries.

There are many studies about the performance of CSMA/CA MAC protocol under high traffic conditions. The authors in [48] proposed an adaptive contention window mechanism, which dynamically selects the optimal back-off window according to the estimate of the number of contending stations. Another approach is dynamic optimization on range (DOOR) [49] method which was proposed to improve the whole system performance by partitioning the number of stations into many sub-ranges and calculating the optimal parameters for each sub-range. Although the proposals dynamically adjust the parameters of CSMA/CA, they don't intend to decrease the packet drop due to congestion.

For unicast duplex communication, network coding (NC) [50]-[51] is considered as a solution to reduce air traffic by relay. The principle of NC is to mix two data at an intermediate network node and multicast it to both senders. The senders receive the encoded packets and deduce from it the messages that were originally intended to be received. Regarding vehicular safety communications (VSC) system, a retransmission scheme using NC was proposed [21] to improve the PDR of V2V communications. In the scheme, multiple native V2V packets are encoded with exclusive-or (XOR) operation and the encoded packet is used for retransmission. However, retransmission increases air traffic and is not effective when the number of VSs is large.

In this chapter, a R-V2VC scheme with payload combining relay (R-V2VC/PCRL) is proposed in order to mitigate the packet congestion at RS. An analytical model is derived to theoretically analyze the packet transmission rate at RS by modeling the backoff process at RS as a Markov chain and using the signal transfer function of the generalized state transition diagram. Moreover, a time division grouping method is introduced to the R-V2VC/PCRL scheme for mitigating the HT problem.

3.2 Packet Combining Relay (PCRL) Scheme

3.2.1 Packet Relay-Assisted V2V Scheme

When R-VS is in NLOS condition to T-VS in an intersection environment, performance of the direct communication may be poor due the large shadowing loss. In such a case, the use of RS can compensate the shadowing loss and improve the reliability of V2V communications. As for relaying method, three schemes have been studied: Decode-and-Forward (DF), Amplify-and-Forward (AF) and Compress-and-Forward (CF) [52]. In DF, the RS receives a packet and decodes it, thus eliminating the effects of interferences and noise, before re-encoding and retransmitting the packet. On the contrary, RS in AF and CF schemes do not decode a message, but forward whatever it received (including interferences and noise). The basic principle of AF is that the RS takes the noisy received signal and amplifies it with a gain. The CF scheme forwards a quantized, compressed version of the signal received at the RS. Since V2V communication operates in hi-speed moving environments, it suffers from large Doppler shift that causes error for packet transmission. The worst case is when T-VS and R-VS are facing each other where the relative velocity is doubled (and the Doppler shift also). In this dissertation, DF is employed at the stationary RS to remove the Doppler shift caused by the move of T-VS.

Fig. 3.1 shows the model of the R-V2VC scheme considered in this paper. The T-VS periodically broadcasts its data packets with a transmission interval T_{f} following CSMA/CA mechanism. Since the R-VS can receive the packet via direct and/or relay path, path diversity gain on the MAC layer can be obtained. PDR of the R-V2VC scheme, PDR_{R}, can be calculated as

$$PDR_{\mathrm{R}} = p_{\mathrm{T,R}} + (1 - p_{\mathrm{T,R}}) \cdot q_{\mathrm{T,RS}} \cdot \xi_{\mathrm{RS}} \cdot q_{\mathrm{RS,R}} \qquad \textbf{(3.1)}$$

where $p_{\mathrm{T,R}}$ is the PDR from T-VS to R-VS via the direct path. $q_{\mathrm{T,RS}}$ and $q_{\mathrm{RS,R}}$ are the packet reception rate (PRR) at RS from T-VS and that at R-VS from RS, respectively. ξ_{RS} is the packet transmission rate (PTR) at RS. The second term of Eq. (3.1) represents the path diversity gain. Since RS is installed at a high position at intersection enabling LOS propagation to VSs, the propagation loss between RS and T-VS/R-VS is small, then $q_{\mathrm{T,RS}}$ and $q_{\mathrm{RS,R}}$ are high. If T-VS and R-VS are in the relation of NLOS, the first

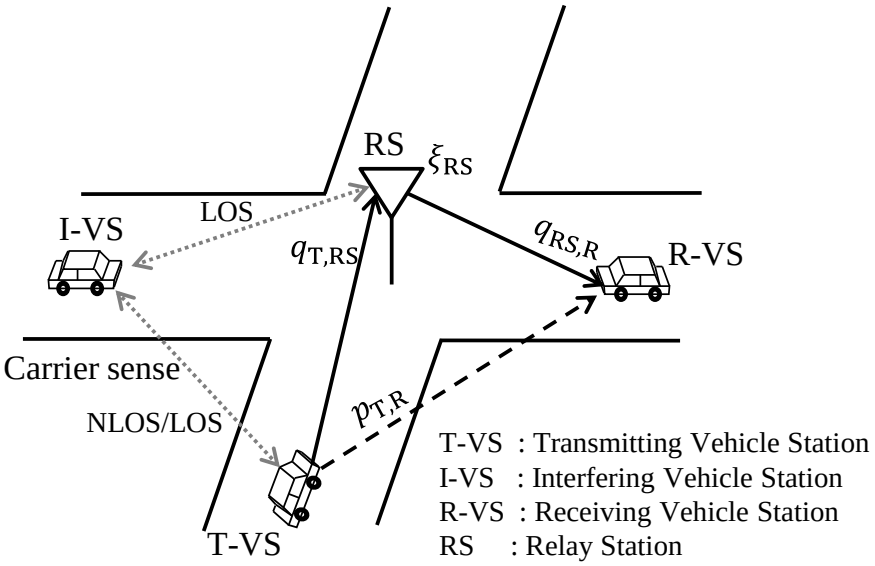

Fig. 3.1: Relay-assisted V2V communications model

term of right hand side in Eq. (3.1) is quite low. In the R-V2VC scheme, the diversity gain increases the PDR. However, packet congestion occurs at the RS in high traffic conditions, resulting in large number of awaiting packets in the transmit queue. A packet will be dropped if its age exceeds its predetermined packet lifetime. If packet drop happens, ξ_{RS} decreases and hence the gain of RS cannot be achieved as expected. For example, if $\xi_{\mathrm{RS}} \approx 0$, the PDR of R-V2VC scheme is close to that of the direct V2V communications (D-V2VC) system, i.e., $PDR_{\mathrm{R}} \approx p_{\mathrm{T,R}}$. Thus, the benefit of introducing RS vanishes. Therefore, it is necessary to increase ξ_{RS}.

3.2.2 Principle of PCRL Scheme

Fig. 3.2 shows the two R-V2VC schemes. Normal relay (RL) scheme in Fig. (a) forwards all received V2V packets individually. Once the channel becomes idle, RL scheme forwards one V2V packet. Although the next packet is ready in the transmit queue, it is not permitted to transmit the packet right after the previous transmission, and RS needs to contend again for the transmission and it will need another waiting time. Moreover, the payload size for vehicular safety application is as small as 100 bytes, and the overhead time ratio in each packet is large [11], [31]. For example, the overhead time ratios for 100-byte payload are 49 % and 56 % if the IEEE 802.11p

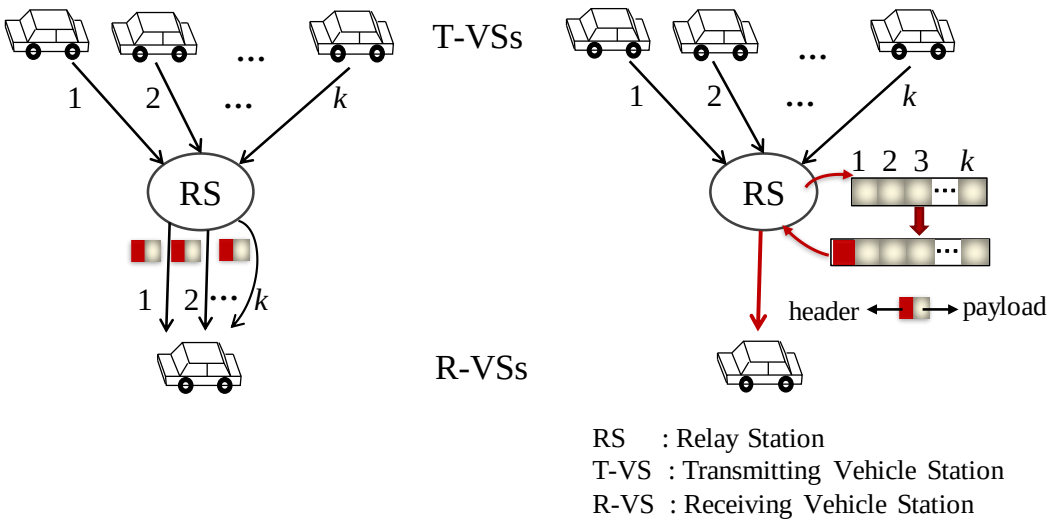

(a) Normal relay (RL) (b) Packet payload combining relay (PCRL)

Fig. 3.2: Packet relay-assisted V2V communications schemes

physical layer of 6 Mbps QPSK and 12 Mbps 16QAM are employed, respectively. Consequently, the RL scheme is not efficient in the sense of air time resource utilization.

The proposed PCRL scheme in Fig. (b) creates a packet with the payload that has been combined from k V2V packet payloads and forwards it once the channel becomes idle. This reduces the number of awaiting packets in the transmit queue, and then increases ξ_{RS}. As a result, the relaying gain is improved.

The number of payload combining k is dynamically determined according to the traffic volume on the roads considering the restrictions on packet size and waiting time. When the k comes up to a predetermined number K, a new combined packet with K payloads is created and sent immediately. K is called the *maximum number of payload combining*. The number K is limited by the maximum payload size of a V2V packet, which is determined by the IEEE 1609 specification [11]. It specifies that the maximum payload length of an IEEE 802.11p frame is 1400 bytes. Considering vehicle safety applications, the normal V2V payload size is 100 bytes [31]. Then K is equal to 14. However, when traffic is low, time for waiting K packets may be longer than transmission interval. In V2V communications for safety applications, each VS broadcasts its packet every transmission interval T_f of 100 ms [14], [31]. The maximum waiting time for packet combining should not exceed T_f. From this view point, the

maximum allowable waiting time $T_{\max}$ should be introduced, i.e., $T_{\max} = \varepsilon T_f$ ($\varepsilon \ll 1$). If the predetermined waiting time $T_{\max}$ counts up before the number of V2V packets reaches K, a packet with the payload combined from less than K V2V payloads is rebroadcasted.

Fig. 3.3 shows the frame format of a combined packet. The difference from a normal packet (see Fig. 2.1) is that the payload data consists of k payloads, not a single V2V payload. In order to correctly retrieve all these payloads, k should be known at the receiver side. Since k depends on the traffic condition, it should be included in every single relayed packet. Currently unused last nine bits in the PCRL service field can be used to convey k to the receiver. In addition, the presence of k can be adopted to indicate a relayed packet. The PCRL scheme then requires little modifications to IEEE 802.11p protocol.

3.2.3 Analysis of Airtime Reduction

Now we analyze the improvement in airtime reduction by replacing RL scheme with PCRL scheme. Let T_{oh} and T_{d} denote the lengths of overhead and data payload of a normal relayed packet, respectively. By sending k packets individually, the total time for relaying transmission is $k(T_{\text{oh}} + T_{\text{d}})$. In the proposed PCRL scheme, transmission time for the combined packet is reduced to $(T_{\text{oh}} + kT_{\text{d}})$. Here, we assume that the T_{oh} keeps the same because the overhead parts of broadcast packets do not include any individual addresses of sender VSs. We then define the airtime reduction rate $\eta(k)$ as

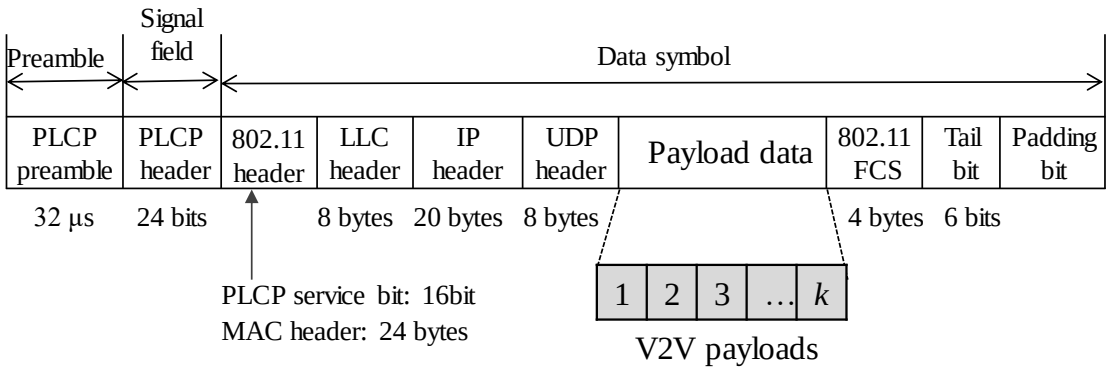

Fig. 3.3: Frame format of combined packet. The number of payload combining *k* can be conveyed in PLCP service field.

$$\eta(k) = \frac{T_{\text{oh}} + kT_{\text{d}}}{k(T_{\text{oh}} + T_{\text{d}})} = \frac{\frac{T_{\text{oh}}}{T_{\text{d}}} + k}{k(\frac{T_{\text{oh}}}{T_{\text{d}}} + 1)} \quad \textbf{(3.2)}$$

Smaller $\eta(k)$ means better in reducing air traffic.

The η depends on the ratio of T_{oh} to T_{d}, which depend on the data transmission rate employed at RS. Fig. 3.4 shows the relationship between η and the number of payload combining k. Two cases of modulation/data rate: QPSK/6 Mbps and 16QAM/12 Mbps for PCRL are compared with QPSK/6 Mbps RL. The airtime reduction rate $\eta^{16\text{QAM}}$ for PCRL using 16QAM/12 Mbps is calculated as the following equation

$$\eta^{16\text{QAM}}(k) = \frac{T_{\text{oh}}^{16\text{QAM}} + kT_{\text{d}}^{16\text{QAM}}}{k(T_{\text{oh}} + T_{\text{d}})} \quad \textbf{(3.3)}$$

As shown in the figure, PCRL scheme using 16QAM/12 Mbps (16QAM-PCRL) for relaying transmission has smaller airtime reduction rate than PCRL scheme using QPSK/6 Mbps (QPSK-PCRL), which means that 16QAM-PCRL scheme is better in the sense of airtime reduction. Since we set the waiting time T_{max}, the average of k is close to K for high traffic conditions and smaller than that for low traffic conditions.

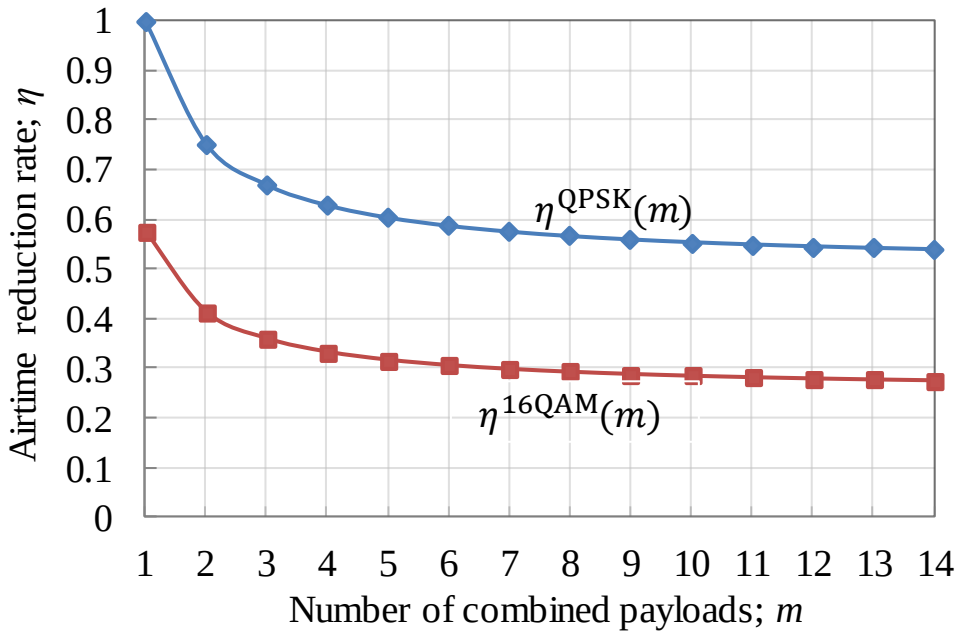

Fig. 3.4: Relationship between η and k

3.2.4 Time Division Grouping (TDG) Method

In general, contention issue is solved by carrier sensing and the back-off mechanism. However, CS is not always perfect in vehicular environments. The propagation on urban streets is known as multipath environment, which causes fading and unstable received signal power. Also, propagation loss for NLOS communication is very large due to diffraction by corner buildings. Thus, VSs that cannot sense each other will be in the situation of HT. As a result, the PRR at RS, $q_{\mathrm{T,RS}}$, may be degraded.

In order to mitigate the HT problem, a time division grouping, i.e. TDG, method was proposed to separate packets sent by the VSs that are in the relation of HT each other [53]. In the method, the grouping of vehicles is based on their locations on the road. There are two kinds of grouping method proposed in the study: direction-based linear grouping and radius-based circular grouping. In this chapter, the combination of PCRL and TDG method is proposed, which employs the linear grouping method, dividing all VSs into four groups by the streets as shown in Fig. 3.5. Each group is assigned to a dedicated transmission time period that doesn't overlap with others. The RS broadcasts grouping information so that a VS can determine its group association from its location. In addition, the time synchronization at VSs and RS can be done by using GNSS (Global Navigation Satellite System). Hence, a moving VS can switch among the groups by following its location obtained by GPS. The TDG method mitigates HT problem then improves the probability $q_{\mathrm{T,RS}}$. Combination of PCRL and TDG improves the PRR and the packet transmission rate at RS, increases the gain of relay-assist and thus improves reliability of V2V communication.

3.3 Analysis Model

In order to analyze the packet transmission rate at RS for the proposed scheme, we first present an approximate probability distribution of MAC layer service time of RS by modeling the backoff process as a Markov chain and using the signal transfer function of the generalized state transition diagram. Then the mean value of MAC layer service time is calculated. After that, the packet transmission rate at RS for the proposed PCRL scheme is derived.

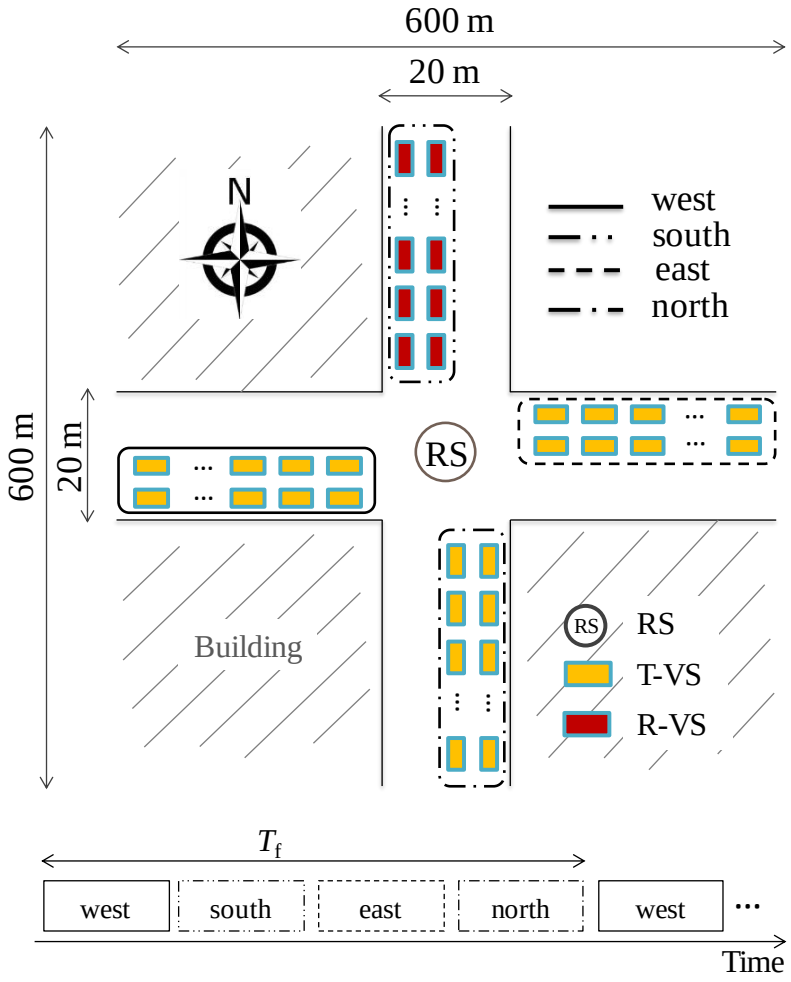

Fig. 3.5: An example of linear TDG with four groups [52]

3.3.1 MAC Layer Service Time of RS

The MAC layer service time (or MAC service time for short) is the time interval from the time instant that a packet becomes the head of the queue and starts to contend for transmission, to the time instant that the packet has been transmitted. The distribution of the MAC service time is a discrete probability distribution because the smallest time unit of the backoff timer is a time slot δ. Let T_s be the non-negative random variable of MAC service time, which has a discrete probability of p_i for T_s being T_i. The probability generating function (PGF) of T_s is given by

$$P_s(z) = \sum_{i=0}^{\infty} p_i z^{T_i} \qquad \textbf{(3.4)}$$

and completely characterizes the discrete probability distribution of T_s. From Eq. (3.4), we have two important properties of PGF as follows

$$\begin{cases} P_s(1) = 1 \\ \mathrm{E}[T_s] = P_s'(1) \end{cases} \tag{3.5}$$

where E[x] denotes the expectation value of x.

We will apply the generalized state transition diagram to derive $P_s(z)$. Let α_c be the channel-in-use time ratio at RS, which is the ratio of time that the RS senses the channel as busy due to the transmissions of VSs. The expression of α_c will be derived later. The transmissions include collision-free process that takes a time T_p for a V2V packet plus DIFS, and collision process that takes a time T_{col}, a random variable representing to the period that the channel is sensed as busy at the RS when packet collision happens. The RS will start its transmission immediately if the channel is sensed as idle. The probability is (1 - α_c). On the other hand, when the backoff process is evoked due to busy channel, the backoff timer has the probability of (1 - α_c) to decrement by one after an slot time δ, the probability of α_{col} to stay at the current state during T_{col} plus DIFS, and the probability of (α_c - α_{col}) to stay at the current state during T_p plus DIFS. The expression of channel-in-use time ratio due to collision process, α_{col}, is derived later. So, the decrement process of backoff timer is a Markov process. The signal transfer function of its generalized state transition diagram is expressed as [54]

$$H_d(z) = \frac{(1-\alpha_c)z^{\delta}}{1-\alpha_{col}z^{\bar{T}_{col}+\mathrm{DIFS}} - (\alpha_c-\alpha_{col})z^{T_p+\mathrm{DIFS}}} \tag{3.6}$$

where $\bar{T}_{col}$ is the mean value of T_{col}. The generalized state transition diagram for transmission process at RS is shown in Fig. 3.6. From the figure, we can derive the $P_s(z)$ as

$$P_s(z) = (1-\alpha_c)z^{T_p^r} + \frac{\alpha_c}{CW}\cdot z^{T_p^r}\cdot \sum_{i=0}^{CW-1}[H_d(z)]^i \tag{3.7}$$

where CW is the contention window size and $T_p^r = T_{oh} + \bar{k}T_d$ is the length of a relayed packet. Here, $\bar{k}$ is the expected value of k. For RL scheme, $\bar{k}$ is 1. To calculate $\bar{k}$ for PCRL scheme, we model the packet arrival process at RS as a Gaussian process with the mean of μ arrivals during T_f and the variance of σ^2 by using continuity correction [55]. In Section 3.4, we will confirm the validity of this model by computer simulations.

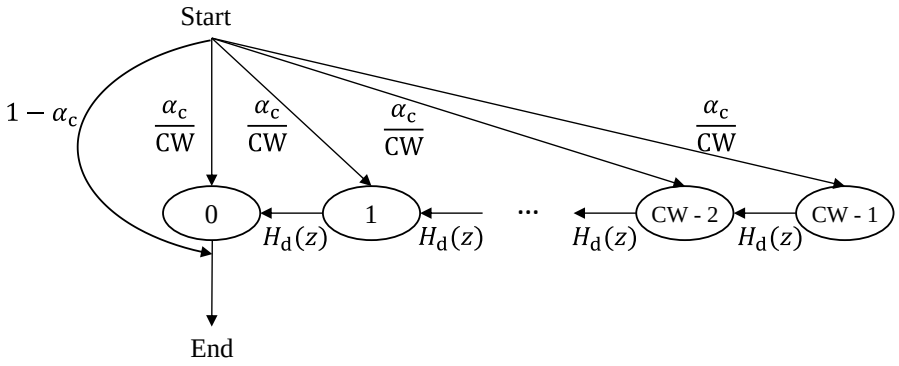

Fig. 3.6: Generalized state transition diagram for transmission process

Given the first packet that has already arrived at the transmit queue, the probability that there are n packets arriving at RS during T_{max} is calculated as

$$p(n) = \int_{n-0.5}^{n+0.5} \frac{1}{\sqrt{2\pi}\frac{T_{\max}}{T_f}\sigma} \exp\left\{ -\frac{\left(x - \frac{T_{\max}}{T_f}\mu\right)^2}{2\left(\frac{T_{\max}}{T_f}\sigma\right)^2} \right\} dx \qquad \textbf{(3.8)}$$

The $\bar{k}$ for PCRL scheme is calculated as

$$\bar{k} = \sum_{n=0}^{K-2} (n+1) \cdot p(n) + \sum_{n=K-1}^{\infty} K \cdot p(n) \qquad \textbf{(3.9)}$$

The first term indicates the situations when the number of packets arriving at RS does not reach K but the waiting time of the first packet reaches T_{max}. The second term indicates the situation when the number of awaiting packets in the transmit queue reaches K before the waiting time of the first packet reaches T_{max}.

The expectation of MAC service time is given as

$$\mathrm{E}[T_s] = P_s'(1) = T_p^r + \alpha_c T_{bo} \qquad \textbf{(3.10)}$$

where T_{bo} is the average time period for the backoff process and is expressed as

$$T_{bo} = \frac{CW-1}{2} \times \left\{ \delta + \frac{\alpha_{col}(\bar{T}_{col} + DIFS) + (\alpha_c - \alpha_{col})(T_p + DIFS)}{1-\alpha_c} \right\} \qquad \textbf{(3.11)}$$

Obviously, T_{bo} does not depend on relaying scheme employed at RS. Some other observations can be obtained from the expression of T_{bo}. When $\alpha_c = 0$ (and thus $\alpha_{col} = 0$), T_{bo} is equal to $(CW - 1)\delta/2$. This is the average backoff time in case that the channel is clear after the backoff procedure is evoked until the timer reaches zero. When $\alpha_c \to 1$,

T_{bo} converges to the infinity. It means that the channel is saturated and RS cannot transmit any packet.

In order to obtain the average time period for the backoff process T_{bo}, we need to derive α_c and α_{col}. Let M_{CS} be the number of VSs in the carrier-sensing range of RS. Knowing that the channel is sensed busy at RS if there is at least one of M_{CS} VSs transmitting its packet, the expression of α_c (the channel-in-use time ratio at RS) can be basically derived as

$$\alpha_c = 1 - \left(1 - \frac{T_p + \text{DIFS}}{T_f}\right)^{N_{CS}} \tag{3.12}$$

To calculate α_{col} (channel-in-use time ratio due to collision process), we assume that at most two packets collide at RS [17]. This results in the maximum T_{col} to be $2T_p$, which gives the average value $\bar{T}_{col}$ of $3T_p/2$. We focus on a T-VS in the sensing range of RS that is transmitting a packet. If there is another VS in the range that fails to sense the transmission of T-VS of interest, RS will sense the channel as busy due to collision process (contrary to collision-free process). Let M_{HT} be the number of HTs on the sensing range of RS. The expression of α_{col} can be derived as

$$\alpha_{col} = \alpha_c M_{HT} \left(\frac{2T_p + \text{DIFS}}{T_f}\right)\left(1 - \frac{2T_p + \text{DIFS}}{T_f}\right)^{M_{HT}-1} \tag{3.13}$$

3.3.2 Expression of Packet Transmission Rate at RS

We consider the packet lifetime of relay packets equal to T_f. Assuming that each relay transmission is independent on the previous transmission at RS. It means that RS has the same opportunity to transmit every relayed packet. By using the MAC service time, we can calculate the maximum number of relayed packets that RS can transmit in a transmission interval T_f as

$$n_t^i = \left\lfloor \frac{(1 - \alpha_c)T_f}{\text{E}[T_s^i]} \right\rfloor \tag{3.14}$$

where T_s^i with $i \in \{\text{RL, PCRL}\}$ is the MAC service time of RS. $\lfloor x \rfloor$ is the largest integer less than or equal to x.

Then, the packet transmission rate at RS for PCRL scheme is expressed as

$$\xi_{\mathrm{RS}}^{\mathrm{PCRL}} = \begin{cases} \bar{k} \cdot n_{\mathrm{t}}^{\mathrm{PCRL}}/\lambda, & \text{for } \lambda > \bar{k} \cdot n_{\mathrm{t}}^{\mathrm{PCRL}} \\ 1, & \text{otherwise} \end{cases} \quad \textbf{(3.15)}$$

Note that the arrival rate λ is also the average number of V2V packets that RS receives in a T_{f} and basically does not depend on the packet forwarding scheme employed at RS. The packet transmission rate at RS for RL scheme can be similarly calculated as Eq. (15) by substituting $n_{\mathrm{t}}^{\mathrm{PCRL}}$ and $\bar{k}$ by $n_{\mathrm{t}}^{\mathrm{RL}}$ and 1, respectively. It can be seen that the packet drop happens when λ exceeds $\bar{k} \cdot n_{\mathrm{t}}^{\mathrm{PCRL}}$ and $n_{\mathrm{t}}^{\mathrm{RL}}$ for PCRL and RL schemes, respectively. The proposed PCRL scheme sends $\bar{k}$ V2V data payloads in a transmission opportunity, and thus can accommodate larger λ.

3.4 Numerical Results

3.4.1 Vehicle Stations Layout and Evaluation Parameters

In order to validate the analysis model and evaluate performance of the proposed scheme for various traffic conditions, computer simulations using the Scenargie network simulator [56] were conducted. The vehicle stations layout is shown in Fig. 3.7. Each street of the crossroads has 20 m width and 600 m length. One RS is placed at the center of the intersection. The total number of VSs *M* is varied from 50 to 300, and all VSs are equally divided into four groups on the streets (we call them north group, west group, south group and east group, respectively). Each street group spreads between 20m and 300m from center of the intersection and VSs in each group are uniformly distributed. For example, if *M* is 200, all VSs in each group are placed on two lanes with 25 VSs per lane, as illustrated in Fig. 3.6. Each VS independently generates packets and then broadcasts them to other VSs by CSMA/CA.

We only consider the balanced vehicle distribution among the streets. However, we may encounter unbalanced vehicle distribution in the practical scenarios. For example, let us consider the scenario when the number of VSs on a certain street (e.g., north street) is much larger than those on the other streets. Since carrier-sensing within a street group may succeed with high probability, the opportunity for a T-VS to get channel access becomes lower, especially when traffic is high. However, from the viewpoint of an R-VS and RS, the collision probability becomes lower due to the

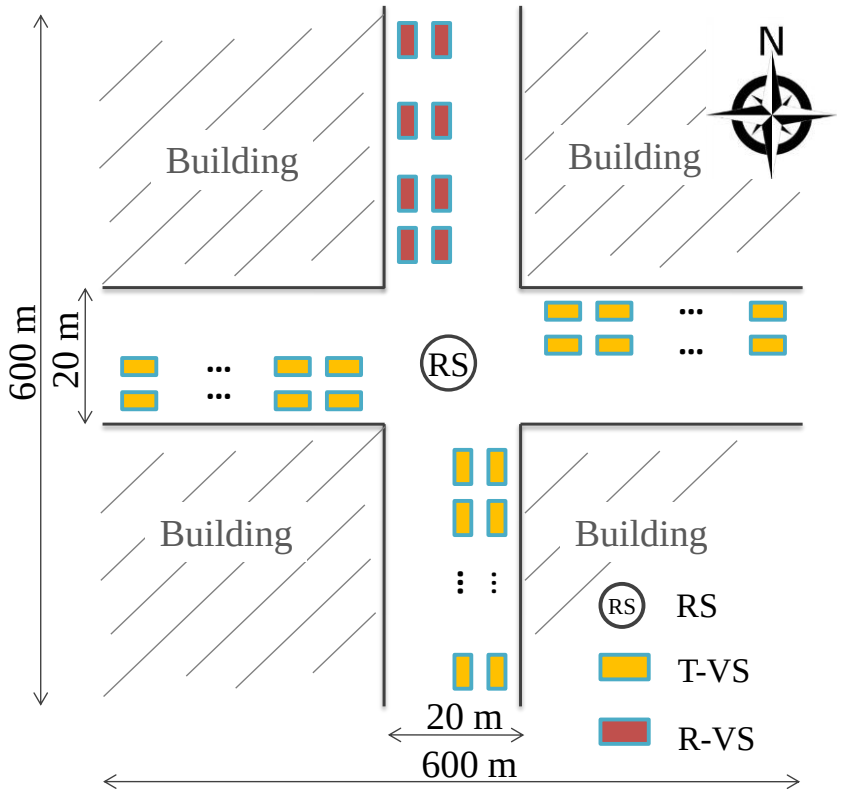

Fig. 3.7: Node layout model

successful carrier-sensing among T-VSs in the street groups. This may result in either higher or lower PDR of the direct V2V communications depending on the number of VSs. This phenomenon happens irrespective of the use of RS. For packet relay transmission, the opportunity for RS to obtain channel access also becomes lower than that in a uniform vehicle distribution. However, even in such a situation, PCRL can efficiently utilize limited chance of channel access. Therefore, PCRL can still improve the PDR performance of V2V communications irrespective of vehicle distribution.

The radio transmission parameters and V2V traffic conditions are shown in Table 3.1 and Table 3.2, respectively. All VSs repeatedly generate packets with the same interval T_f of 100 ms but independent timings and broadcast them to other VSs by CSMA/CA. The 700 MHz frequency band is employed because of its low diffraction loss and propagation loss. The propagation environment is characterized by ITU-R P.1411-6 [45] path loss models which present both LOS and NLOS propagation loss models that take into account shadowing for NLOS caused by buildings around intersection. Rayleigh fading is used as fading model.

Table 3.1: Radio Transmission Parameters

Frequency (Bandwidth)	700 MHz (10 MHz)	
Tx power	18 dBm	
Propagation model	ITU-R P.1411-6 LOS + Rayleigh fading	
Access protocol	IEEE 802.11p (CSMA/CA)	
Data rate/Modulation	VS to VS, VS to RS, RS to VS	RS to VS
	6 Mbps/QPSK	12Mbps/16QAM
CINR threshold	10 dB	15 dB
Packet length (100 byte payload)	264 μs	152 μs
Carrier sense threshold	-82 dBm	
Receiver noise figure	11.8 dB	
Contention window size	64	
VS antenna height	1.5 m	
RS antenna height	6 m	
Omnidirectional antenna gain	0 dBi	

Table 3.2: V2V Traffic Conditions

Packet Type	UDP broadcast packet
Packet Payload Size	100 bytes
Packet Generation Interval: T_f	100 ms

We focus on the R-VSs on the north street for evaluation. Since the layout of the VSs and RS is rotation symmetric by 90 degrees and its multiples, this condition does not loose generality. On the contrary, this condition lets us know what combination of the transmitting and receiving vehicles has good or bad performance. For performance evaluation, we adopt a general quality measure of average broadcast packet delivery rate (BPDR) as the performance metric to provide a general view about performance of the proposed schemes. The BPDR is calculated for a T-VS to the evaluated R-VSs on the north street, and then the average BPDR is obtained by averaging in location of the

T-VS. More details about the impact of the location of T-VS on the performance of PDR will be discussed in the next chapters.

3.4.2 Packet Arrival Process at RS

Fig. 3.8 shows packet arrival probability at RS for T_{max} = 10 ms. We consider two traffic conditions of M = 100 and M = 200. The solid lines are calculated from the Gaussian distribution given in Eq. (3.8) with the mean μ of 72 and 103 arrivals for the M of 100 and 200 vehicles, respectively. The variance σ^2 is 20, which is obtained by least square algorithm to match with the simulated results. Fig. 3.8 clearly shows that the Gaussian distributions well agrees with the simulated ones. Thus, we conclude that the packet arrival process at RS can be modeled as a Gaussian process and hence it is used in the following evaluations.

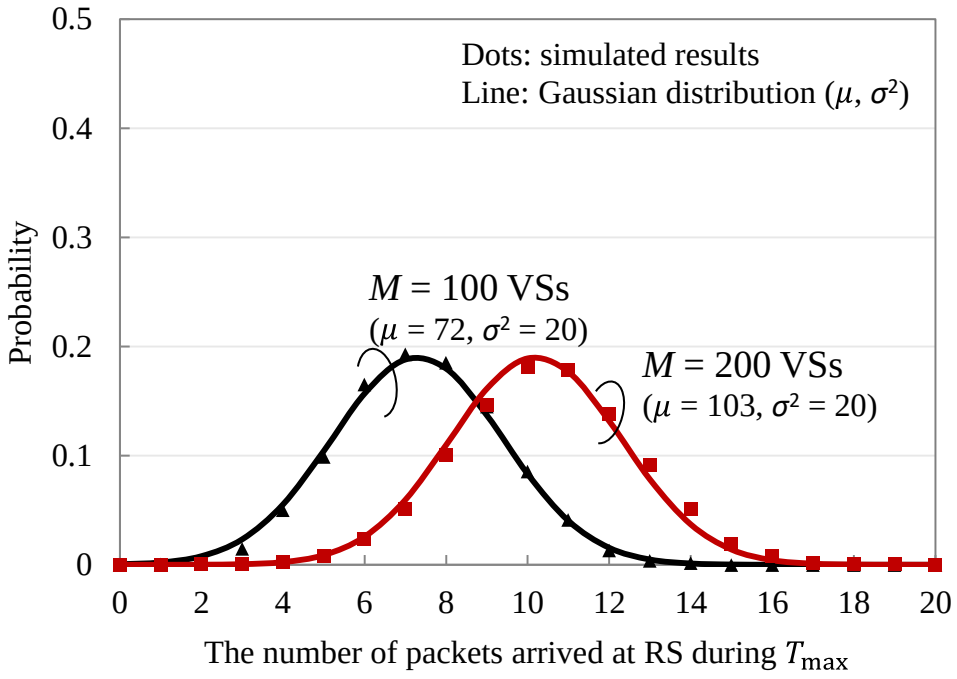

Fig. 3.8: Packet arrival process at RS (T_{max} = 10 ms)

3.4.3 Packet Transmission Rate at RS

Fig. 3.9 shows the theoretical and simulated results of the packet transmission rate at RS for PCRL and RL schemes. For PCRL scheme, T_{max} is set to 10 ms. To calculate the theoretical values from Eq. (3.15), we use the Gaussian process with the mean μ obtained from simulations and the variance σ^2 of 20. In order to calculate α_{col} in Eq. (3.13), we assume that VSs on different streets become HT to each other due to large propagation loss among them. As a result, M_{HT} is assumed to be equal to $3M/4$.

It can be seen from the figure that the theoretical and simulated results well agree with each other for the proposed PCRL. For RL scheme, the theoretical and simulated results agree only when M is less than or equal to 100. Although the theoretical result does not agree well with the simulated one when M is larger than or equal to 150, it describes well the declining trend of the packet transmission rate at RS. It is observed that packet drop appears for RL scheme when M is 150, and it becomes severer as M becomes larger. It decreases to less than 20 % when M is 300. On the other hand, the transmission rate for the proposed PCRL scheme is 100 % regardless of M. This comes from the effect of the proposed PCRL in mitigating congestion issue at RS.

Fig. 3.10 shows the impact of T_{max} and the modulation schemes on the packet transmission rate at RS. The value of T_{max} is set either 5 ms or 10 ms. Packet transmission rate for RL scheme is also presented for reference. When T_{max} = 5 ms, the packet transmission rate for QPSK-PCRL scheme keeps 100 % until M is 230 and becomes lower for the larger M. The degradation is mitigated by employing 16QAM for relay transmission. When T_{max} is set to 10 ms, the packet transmission rate at RS for both QPSK and 16QAM is 100 % irrespective of M. Since the number of V2V payloads to be combined reaches the maximum number of K before T_{max} counts up in high traffic conditions, the transmission rate keeps 100 % for T_{max} of 10 ms or greater. Therefore, it is enough to set T_{max} as 10 ms. It is only 10 % of the transmission interval T_f that is the dominant cause of transmission delay. Hereafter we use T_{max} of 10 ms in the evaluation.

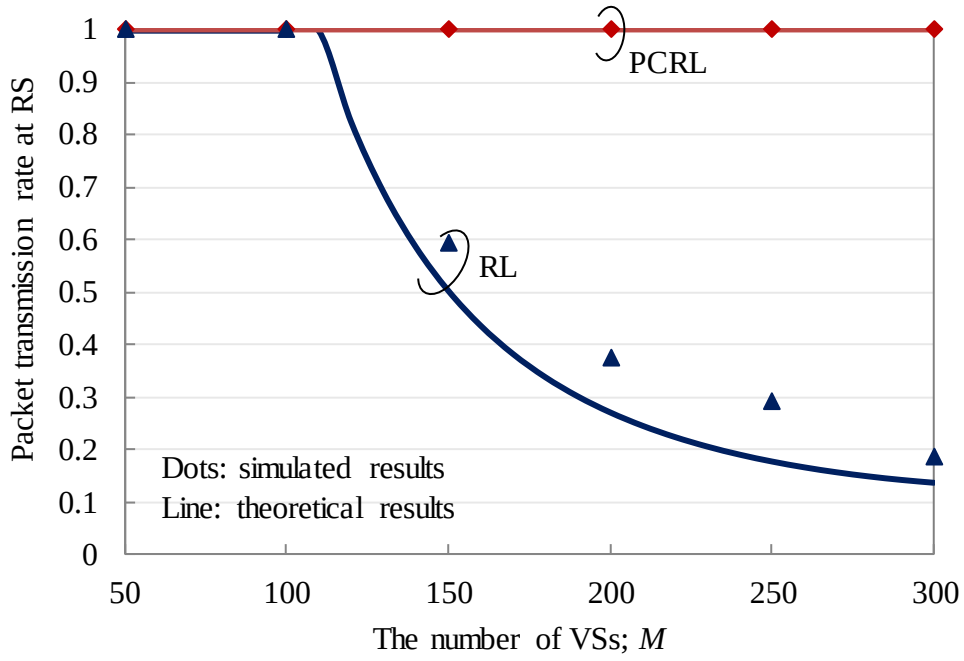

Fig. 3.9: Packet transmission rate at RS (T_{max} = 10 ms)

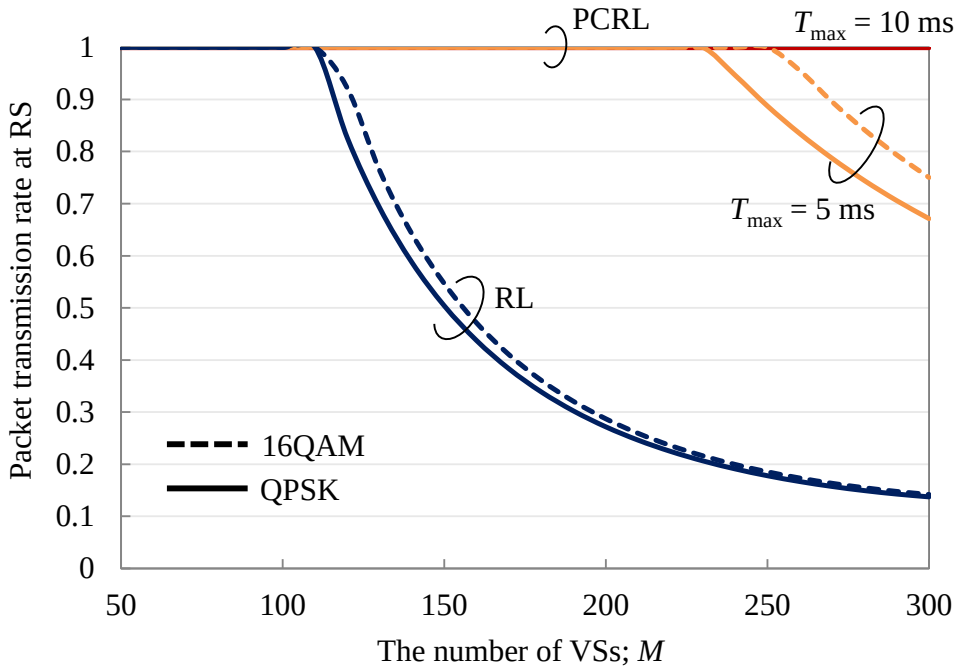

Fig. 3.10: Impact of T_{max} and modulation scheme

3.4.4 Broadcast Packet Delivery Rate (BPDR)

For ITS safety application, V2V cumulative packet reception rate should satisfy 95 % during a vehicle moves 10 m [30]. If vehicle speed is 70 km/h, there are at most 5.14 chances of the reception during the move. Then average packet reception ratio should keep more than 44.2 %.

3.4.4.1 Effect of packet payload combining and 16QAM modulation

In order to evaluate the effect of packet payload combining and 16QAM modulation, average BPDRs of D-V2VC, RL and packet combining relay (QPSK-PCRL and 16QAM-PCRL) schemes were compared.

Fig. 3.11 shows average BPDRs from T-VSs on the west and east streets. Note that the T-VSs are in NLOS conditions with the evaluated R-VSs on the north street. Average BPDR of the D-V2VC scheme is less than 20%, which is caused by shadowing due to buildings at the corner. Addition of an RS around the intersection can effectively mitigate the shadowing issue and thus remarkably increases the BPDR. Performance of relay-assist is further improved by PCRL schemes. Especially, the improvement for large M is more significant, which comes from the effect in improving the packet transmission rate at the RS.

Fig. 3.12 shows average BPDRs from T-VSs on the south street. Average BPDRs of the relay-assisted V2V schemes are higher than that of the direct scheme. This proves that using RS can effectively compensate attenuation loss due to node distance. Same as on the west and east streets in Fig. 3.11, PCRL schemes further improve the relaying performance. However, BPDR of relaying schemes for the south street is higher than that of the west and east streets. The gain comes from the path diversity effect between direct and relayed paths. The diversity effect is further obtained by using 16QAM for relaying transmission. With 16QAM, the probability of packet collisions among V2V packets is lowered.

Note that the average BPDRs from T-VSs on the north street are high for all V2V schemes because of the low propagation loss due to LOS condition between the T-VSs and R-VSs. Figure 3.13 shows average BPDRs from T-VSs on all streets. In general, relay-assist improves performance of V2V communications. PCRL schemes further

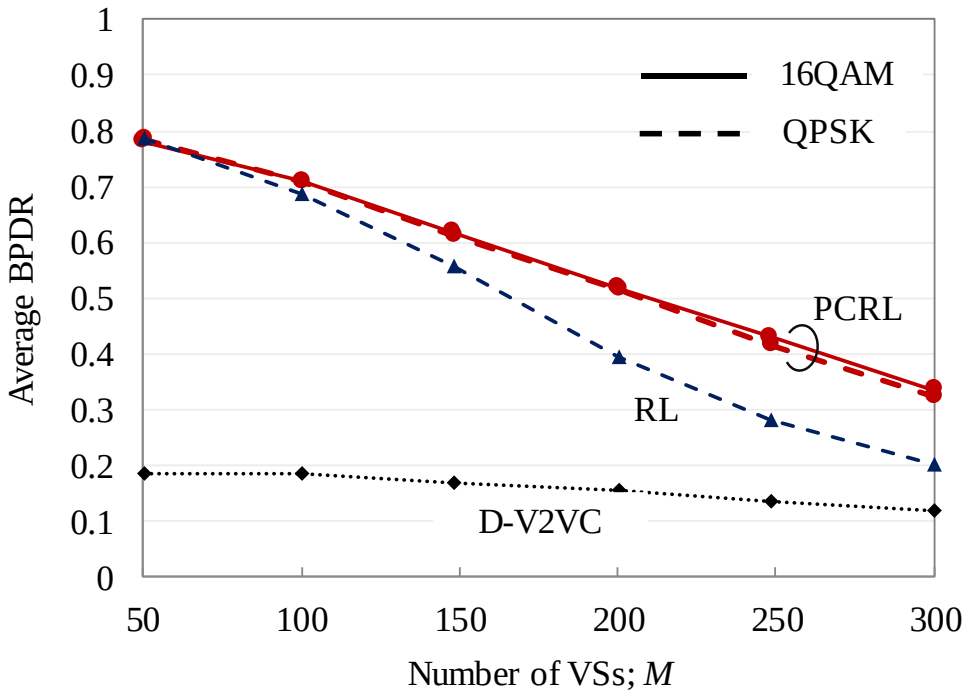

Fig. 3.11: Average BPDR from T-VSs on east and west streets

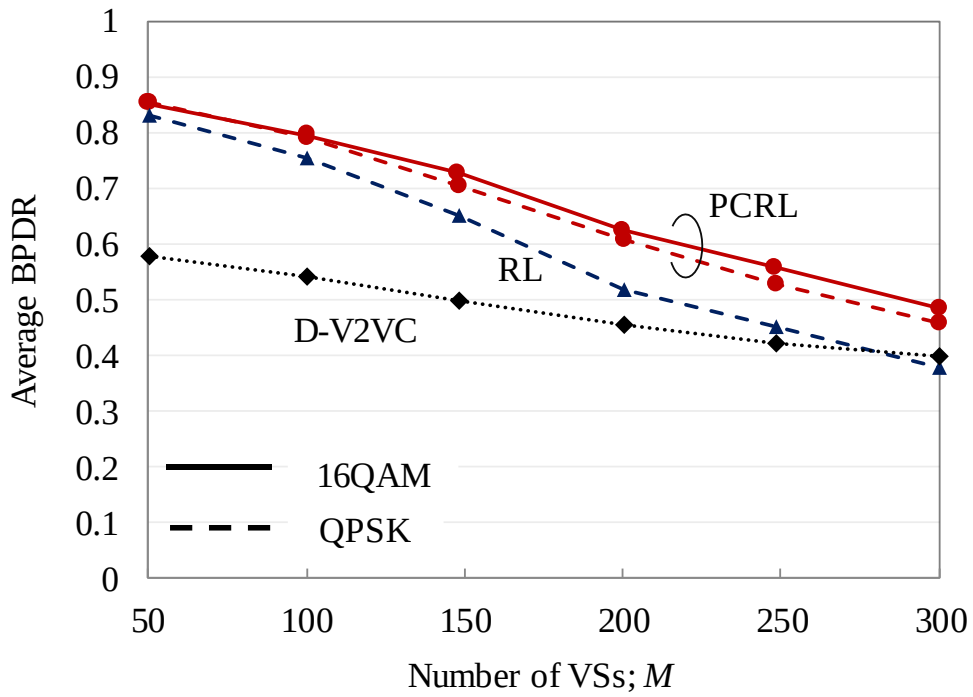

Fig. 3.12: Average BPDR from T-VSs on south street

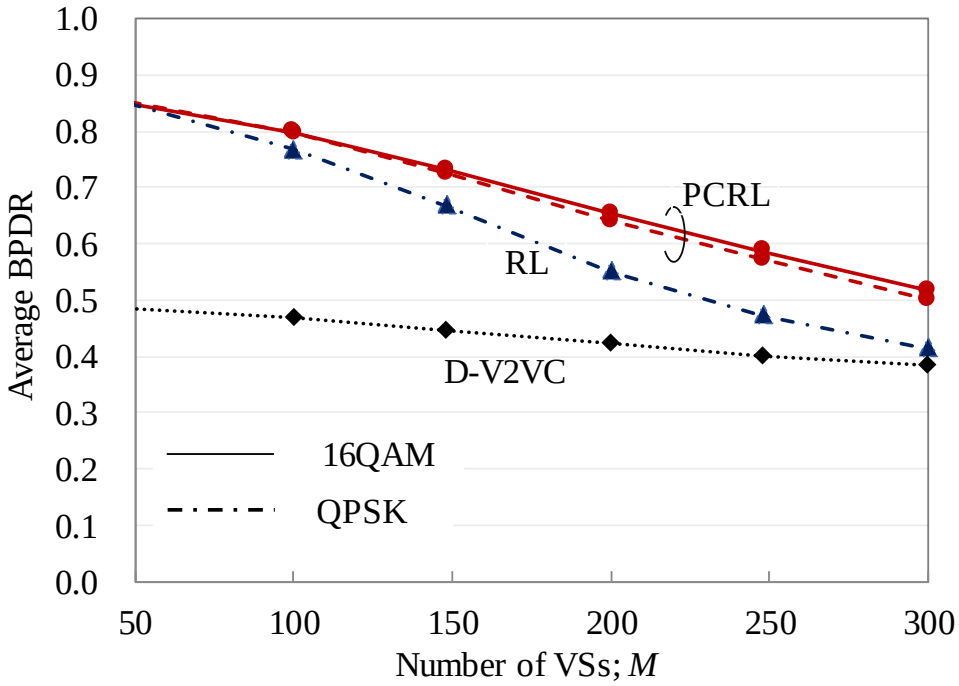

Fig. 3.13: Average BPDR from T-VSs on all streets

improve performance of relay-assist by mitigating the congestion issue, especially in high traffic conditions.

3.4.4.2 Improvement by combination of PCRL and TDG

Fig. 3.14 shows average BPDRs of D-V2VC, RL with and without TDG, and PCRL with TDG schemes for all streets. When *M* is small, Both RL and PCRL with TDG remarkably improve the average BPDRs. This is because the HT problem among different groups can be effectively alleviated by TDG. As *M* increases, the average BPDR of RL with TDG significantly degrades due to the packet congestion issue. On the other hand, PCRL with TDG scheme still provides large improvement over RL with TDG when *M* is large.

The improvement is more significant if 16QAM data modulation is adopted for the proposed PCRL-TDG. When *M* is larger than 100, average BPDR of 16QAM-PCRL with TDG becomes higher than that of QPSK-PCRL with TDG. When *M* is 300 or less, average BPDR of the scheme is 52 % or higher. The proposed 16QAM -PCRL with TDG scheme can accommodate 300 VSs.

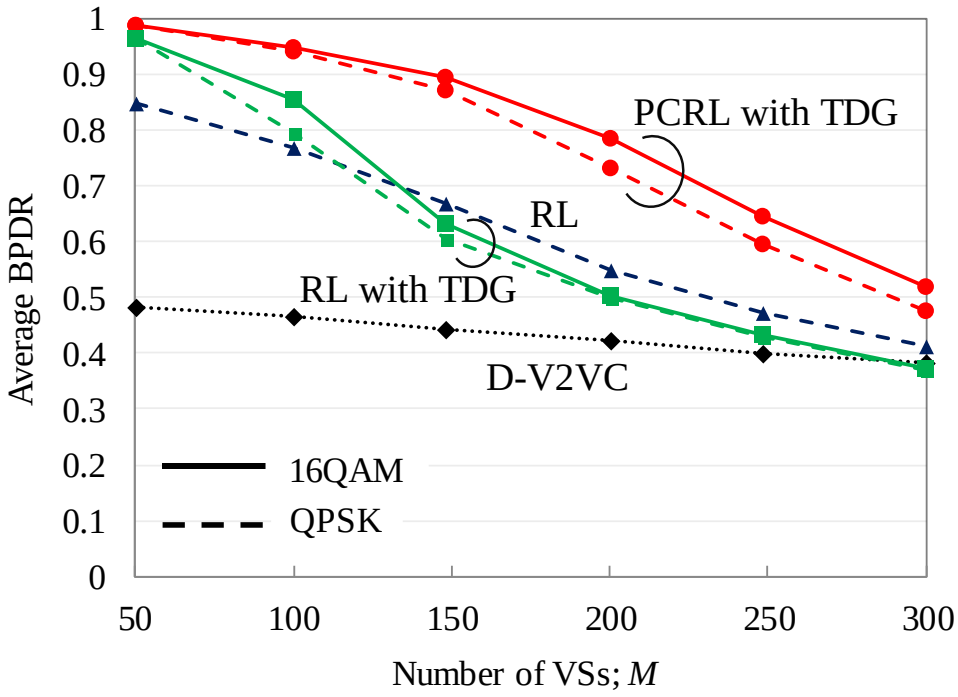

Fig. 3.14: Average BPDR from T-VSs on all streets with TDG

3.5 Chapter Summary

In this chapter, the PCRL scheme has been proposed to alleviate the packet congestion issue at RS. An analytical model is derived to analyze the effectiveness of the proposed scheme in terms of packet transmission rate at RS. Computer simulations are conducted to validate the model and confirm the effectiveness of the proposed PCRL scheme. From the numerical results, the following important observations and conclusions can be obtained:

1) For the RL scheme, when the number of VSs becomes large, packet congestion issue happens at RS that limits performance of relay-assist.

2) For the proposed PCRL scheme, the congestion issue is effectively alleviated and then packet transmission rate at RS increases. As a result, performance of relay-assist is remarkably improved.

3) The packet transmission rate is 100 % for all the number of VSs when T_{max} is 10 ms or longer. In the next chapters, this value of T_{max} will be used in the evaluation.

4) Addition of TDG to the PCRL scheme further mitigates HT problem and then further improves relaying performance, especially when traffic is not too high.

5) When traffic load becomes higher, the division loss that causes contention within a group limits the improvement by relay-assist. Another HT avoidance method is thus needed.

6) Performance of the PCRL with and without TDG schemes is further improved by employing the higher-order modulation of 16QAM for relaying transmission. Unless otherwise stated, the modulation of 16QAM is used for relay from hereafter.

Chapter 4. An Improved Relay-Assisted V2V Communications with Packet Payload Combining and Sectorized Receiving

In the previous chapter, combination of PCRL and TDG was introduced in order to alleviate congestion issue at RS as well as mitigate HT problem. However, it is observed that the TDG method just only works under low traffic conditions, and thus it is necessary to introduce a more effective HT avoidance scheme. This chapter proposes to employ sectorized receiving RS in PCRL scheme (SR-V2VC/PCRL). Then, analytical expression of the PRR at RS and the PDR of SR-V2VC/PCRL is derived. Computer simulations are conducted to confirm the validity of the theoretical derivation as well as the effectiveness of the proposed SR-V2VC/PCRL scheme.

4.1 Introduction

R-V2VC scheme improves the reliability of V2V communication, especially in NLOS environment such as intersections. However, when RS is located around intersections where LOS propagation between VSs is often unavailable, the packet collision frequently happens at RS due to HTs [37]-[38] because VSs cannot carrier sense each other. If packet collision happens at RS, the advantage of R-V2VC becomes smaller. Although a request-to-send/clear-to-send (RTS/CTS) handshake method [57] is well-known to solve the HT problem, the RTS/CTS handshake method cannot be adopted in V2V communication because a packet is broadcasted to a large number of VSs on different locations.

In order to overcome the HT problem in V2V communications, several methods have been studied. In [58], time division multiple access (TDMA) is employed to enable VSs to access the communication channel in turns. A geographical space is divided into a grid and a map defining the relationship between the locations and the time slot assignment is created. Then, the map is shared by all VSs. Therefore, the access order is decided based on their locations. Although this approach realizes collision-free media access, the spectrum efficiency decreases as the number of VSs increases. Another potential solution to improve the PDR of V2V communications is a beam steering technology [59]-[60]. In [60], a directional antenna is introduced to each station in an ad hoc network and the improvement of throughput/capacity is investigated. Although the introduction of directional antenna can improve CINR at the receiver, employing sector antenna on VSs may increase the deployment cost and lead to enlarge the size of antenna. Moreover, its effectiveness in the broadcast V2V communications with a large number of VSs has not been guaranteed.

In [61], the use of sectorized receiving antenna (SRA) at RS was introduced to overcome the HT problem, i.e. SR-V2VC scheme. In the scheme, the packets transmitted from multiple VSs in the relation of HT each other are received separately by different directional antennas at RS. Due to the antenna directivity, the packet collision at RS can be mitigated. In [61], the numerical simulations have been conducted to confirm the superiority of SR-V2VC under the intersection environments. Nevertheless, potential benefit and limitation of the sectorized receiving scheme has not been fully analyzed yet.

The utilization of SRA improves the PRR at RS, and hence the number of the packets to be relayed increases. This may lead to a large number of packets waiting in the transmit queue of RS. Thus, the SR-V2VC scheme suffers from another issue, i.e. packet congestion at RS, especially when traffic load is high. Since the transmit queue size is limited and each V2V packet has its own delay requirement, packet drop may happen due to the congestion issue. If packet drop happens, the achievable gain obtained by SR-V2VC scheme may be limited. Therefore, the potential improvement brought by SR-V2VC cannot be fully obtained as investigated in [61].

In this chapter, SR-V2VC combined with PCRL is proposed which achieves the potential benefit of RS in V2V communications. Hereafter, this scheme is called SR-

V2VC/PCRL, in contrast to the omnidirectional receiving relay-assisted V2V communications scheme combined with PCRL (OR-V2VC/PCRL). Then, analytical expression of the PRR at RS and the PDR of SR-V2VC/PCRL is derived. This is the first attempt to comprehensively evaluate the PDR of SR-V2VC/PCRL. Computer simulations are conducted to confirm the validity of the theoretical derivation.

4.2 V2V Communications System

In the V2V broadcast applications for safe driving support and information exchange for automated driving, each VS broadcasts fixed-size data packets with the generation interval T_{f} to nearby vehicles in order to inform its current mobility status. The average PDR at R-VSs within the transmission range of T-VS is taken as the metric of the communication reliability. Higher quality will be necessary for the information exchange in automated driving systems with less number of repeated transmissions. Thus, it is crucial to increase the PDR. For example, the PDR of 95% is targeted (including the repeated transmissions in the next intervals) within the range of 250 m for the safety driving support [30].

4.2.1 R-V2VC Scheme

As shown in Eq. (3.1), PDR of R-V2VC scheme is expressed as

$$PDR_{\mathrm{R}} = p_{\mathrm{T,R}} + (1 - p_{\mathrm{T,R}}) \cdot q_{\mathrm{T,RS}} \cdot \xi_{\mathrm{RS}} \cdot q_{\mathrm{RS,R}} \qquad \textbf{(4.1)}$$

If packet congestion happens at RS as the number of VSs increases, ξ_{RS} becomes larger and hence the gain of RS may not be achieved as expected. For example, if $\xi_{\mathrm{RS}} \approx 1$, the PDR of R-V2VC is close to that of D-V2VC, i.e., $PDR_{\mathrm{R}} \approx p_{\mathrm{T,R}}$. Thus, the benefit of introducing RS vanishes. Therefore, it is necessary to improve ξ_{RS}.

4.2.2 OR-V2VC/PCRL Scheme

In Chapter 3, it is shown that the introduction of PCRL can greatly improve the packet transmission rate at RS, i.e., $\xi_{\mathrm{RS}} \approx 1$. Thus, for OR-V2VC/PCRL, (4.1) can be

approximated as

$$PDR_{\mathrm{R}}^{\mathrm{OR}} \approx p_{\mathrm{T,R}} + (1 - p_{\mathrm{T,R}}) \cdot q_{\mathrm{T,RS}}^{\mathrm{OR}} \cdot q_{\mathrm{RS,R}} \quad \textbf{(4.2)}$$

where $q_{\mathrm{T,RS}}^{\mathrm{OR}}$ is the PRR at omnidirectional receiving RS. If the channel between T-VS and R-VS is NLOS, high propagation loss between them results in quite low $p_{\mathrm{T,R}}$. On the contrary, the location of RS at the high position enables LOS propagations from T-VS and to R-VS. Therefore, the propagation loss between RS and T-VS/R-VS is smaller than that of direct path. In OR-V2VC/PCRL, the second term in (3.2) increases the PDR. However, $q_{\mathrm{T,RS}}^{\mathrm{OR}}$ may become low due to the HT problem and the gain is limited.

The packets transmitted from other VSs, which are hidden from T-VS, may collide with the packet transmitted from T-VS during its *critical period* [17], [62]. The VSs transmitting the packet during this critical period is referred to as interfering vehicle stations (I-VSs). The packet collision probability at RS depends on both the transmission overlapping probability and CS failure probability among VSs [17].

Let M_{HT} be the number of I-VSs. Let $C_{\mathrm{T,RS}}$ and $C_{\mathrm{I}_i,\mathrm{RS}}$ be the instantaneous received power of the signals transmitted from T-VS and the ith I-VS ($1 \le i \le M_{\mathrm{HT}}$) at RS, respectively. The PRR at RS is defined as [63]-[66]

$$q_{\mathrm{T,RS}}^{\mathrm{OR}} = \Pr\left(\frac{C_{\mathrm{T,RS}}}{\sum_{i=1}^{M_{\mathrm{HT}}} C_{\mathrm{I}_i,\mathrm{RS}} + N} \ge \Gamma_{\mathrm{CINR}} \right), \quad \textbf{(4.3)}$$

where N is the thermal noise power and Γ_{CINR} is the required CINR threshold for successful packet reception. Considering flat Rayleigh fading channel, the probability density function (PDF) of the instantaneous received power is written by

$$f(x) = \frac{1}{\sigma^2} \exp\left(-\frac{x}{\sigma^2} \right), \quad \textbf{(4.4)}$$

where σ^2 is the mean of the instantaneous received power x. The PRR at RS can be calculated as

$$\begin{aligned} q_{\mathrm{T,RS}}^{\mathrm{OR}} &= \int_0^\infty \int_0^\infty \cdots \int_0^\infty \left(\int_{\left(\sum_{i=1}^{M_{\mathrm{NT}}} C_{\mathrm{I}_i,\mathrm{RS}} + N \right) \Gamma_{\mathrm{CINR}}}^{\infty} \left(f\left(C_{\mathrm{T,RS}}\right) \prod_{i=1}^{M_{\mathrm{NT}}} f\left(C_{\mathrm{I}_i,\mathrm{RS}}\right) \right) dC_{\mathrm{T,RS}} \right) dC_{\mathrm{I}_k,\mathrm{RS}} \cdots dC_{\mathrm{I}_2,\mathrm{RS}} dC_{\mathrm{I}_1,\mathrm{RS}} \\ &= \exp\left(-\frac{N\Gamma_{\mathrm{CINR}}}{\sigma_{\mathrm{T,RS}}^2} \right) \prod_{i=1}^{M_{\mathrm{NT}}} \left(\frac{1}{1 + \Gamma_{\mathrm{CINR}} \frac{\sigma_{\mathrm{I}_i,\mathrm{RS}}^2}{\sigma_{\mathrm{T,RS}}^2}} \right). \end{aligned} \quad \textbf{(4.5)}$$

Here, $\sigma^2_{\mathrm{T,RS}}$ and $\sigma^2_{\mathrm{I}_i,\mathrm{RS}}$ are the average received signal power of T-VS and that of the *i*th I-VS at RS, respectively, and they are obtained as

$$\sigma^2_{\mathrm{T,RS}} = \frac{P_{\mathrm{t}} G_{\mathrm{t}} G_{\mathrm{r}}^{0}}{L_{\mathrm{V,RS}}\left(d_{\mathrm{T,RS}}\right)}, \tag{4.6a}$$

$$\sigma^2_{\mathrm{I}_i,\mathrm{RS}} = \frac{P_{\mathrm{t}} G_{\mathrm{t}} G_{\mathrm{r}}^{0}}{L_{\mathrm{V,RS}}\left(d_{\mathrm{I,RS}}\right)}, \tag{4.6b}$$

where G_{t} and $G_{\mathrm{r}}^{\mathrm{o}}$ are the omnidirectional transmit and receive antenna gains, respectively. P_{t} is the common transmit power. $L_{\mathrm{V,RS}}(d)$ is the propagation loss between a VS and RS which is a function of distance d and the path loss model. Substituting (4.6a) and (4.6b) into (4.5) yields

$$q^{\mathrm{OR}}_{\mathrm{T,RS}} = \exp\left(-\frac{N\Gamma_{\mathrm{CINR}}}{\sigma^2_{\mathrm{T,RS}}}\right)\prod_{i=1}^{M_{\mathrm{NT}}}\left(\frac{1}{1+\Gamma_{\mathrm{CINR}}\dfrac{L_{\mathrm{V,RS}}\left(d_{\mathrm{T,RS}}\right)}{L_{\mathrm{V,RS}}\left(d_{\mathrm{I,RS}}\right)}}\right). \tag{4.7}$$

It can be seen from (4.5) that the PRR at RS is an increasing function over $\sigma^2_{\mathrm{T,RS}}$ and a decreasing function over the ratio $L_{\mathrm{V,RS}}(d_{\mathrm{T,RS}})/L_{\mathrm{V,RS}}(d_{\mathrm{I,RS}})$.

4.2.3 SR-V2VC/PCRL Scheme

The block diagram of the proposed SR-V2VC/PCRL in a four-corner intersection environment is shown in Fig. 4.1 (For the straight road environment, two-sector receiving antenna is employed.). The received packets at different sectors are input to a common receiving queue in RS. If the same packet is received by multiple sectors, only one of them will be stored and the others are discarded in order to prevent packet duplication and save airtime. The duplication can be detected by comparing the sender address and IDs of the packets. After that, a number of *k* packet payloads are processed by PCRL. Then, the resultant packet is rebroadcasted from RS by using an omnidirectional transmitting antenna.

When an omnidirectional receive antenna (ORA) is employed at RS, the PRR of the packet transmitted from T-VS at RS, $q^{\mathrm{OR}}_{\mathrm{T,RS}}$, may be degraded due to the interference from I-VSs. If $q^{\mathrm{OR}}_{\mathrm{T,RS}} \approx 0$ due to the interference, the benefit of RS is lost. Therefore, it is

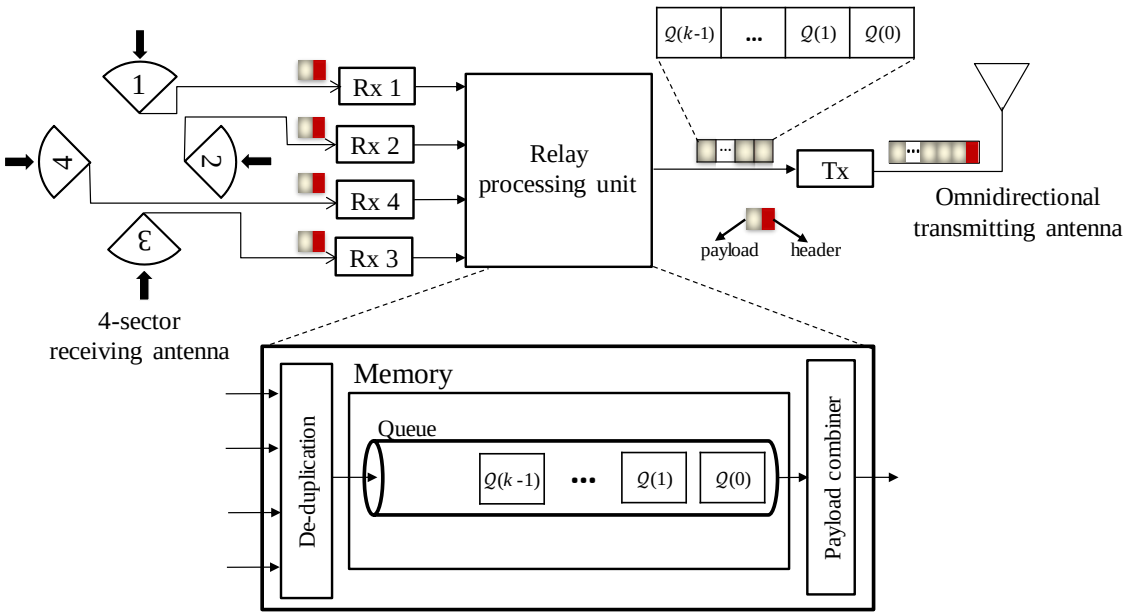

Fig. 4.1: Block diagram of RS with a sectorized receiving antenna

necessary to avoid such situations. SRA at RS can decrease the ratio $\sigma^2_{\mathrm{I}_i,\mathrm{RS}}/\sigma^2_{\mathrm{T,RS}}$ and thus improve the PRR at RS.

Fig. 4.2 illustrates the situation when two VSs (T-VS and I-VS) are approaching the intersection. Since the path between I-VS and T-VS is blocked by a building, I-VS becomes an HT from T-VS. If RS is equipped with ORA, the packet reception error may happen due to the huge interference from I-VS (Fig. (a)). The problem becomes more significant in high traffic conditions. In such a situation, OR-V2VC cannot improve the PDR. Fig. (b) illustrates the situation when RS is equipped with a four-sector receiving antenna in a four-corner intersection environment. Since I-VSs are often on the different streets from T-VS, the packets transmitted from T-VS and I- VS will be received by different sectors at RS. Thus, the interference from I-VS can be effectively mitigated. However, due to the non-zero gain of back-lobe and side-lobe of practical antennas, the packet transmitted from I-VSs may slightly interfere with the packet transmitted from T-VS.

Let F_{B} and F_{S} denotes the front-to-back ratio (FBR) and front-to-side ratio (FSR) of SRA, respectively. Let M_{F}, M_{S} and M_{B} be the number of I-VSs whose signals are received at the main-, the side- and the back-lobe of the directional antenna facing to

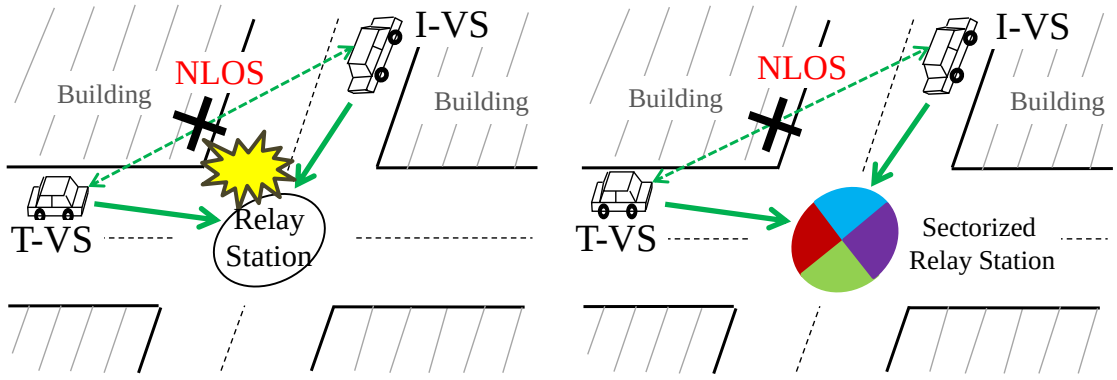

(a) OR-V2VC (b) SR-V2VC

Fig. 4.2: Packet reception at RS when there is I-VS

T-VS, respectively. If I-VS is coming in the opposite direction, the average received power from I-VS at the sector antenna which is facing to T-VS is expressed as

$$\sigma^2_{\mathrm{I,RS}} = \frac{P_{\mathrm{t}} G_{\mathrm{t}} \dfrac{G^{\mathrm{s}}_{\mathrm{r}}}{F_{\mathrm{B}}}}{L_{\mathrm{V,RS}}\left(d_{\mathrm{I,RS}}\right)}. \tag{4.8}$$

In the case that I-VS is coming from the left or right side of the sector antenna facing to T-VS, $\sigma^2_{\mathrm{I,RS}}$ can be obtained similarly as (4.7) by substituting F_B with F_S. The PRR when there are at least one or more than one I-VS is then calculated as

$$q^{\mathrm{SR}}_{\mathrm{T,RS}} = \exp\left(-\frac{N\Gamma_{\mathrm{CINR}}}{\sigma^2_{\mathrm{T,RS}}}\right)\times \prod_{i=1}^{M_{\mathrm{F}}}\left(\frac{1}{1+\Gamma_{\mathrm{CINR}}\dfrac{L_{\mathrm{V,RS}}\left(d_{\mathrm{T,RS}}\right)}{L_{\mathrm{V,RS}}\left(d_{\mathrm{I}_i\mathrm{,RS}}\right)}}\right)\prod_{i=1}^{M_{\mathrm{S}}}\left(\frac{1}{1+\dfrac{\Gamma_{\mathrm{CINR}}}{F_{\mathrm{S}}}\dfrac{L_{\mathrm{V,RS}}\left(d_{\mathrm{T,RS}}\right)}{L_{\mathrm{V,RS}}\left(d_{\mathrm{I}_i\mathrm{,RS}}\right)}}\right)\prod_{i=1}^{M_{\mathrm{B}}}\left(\frac{1}{1+\dfrac{\Gamma_{\mathrm{CINR}}}{F_{\mathrm{B}}}\dfrac{L_{\mathrm{V,RS}}\left(d_{\mathrm{T,RS}}\right)}{L_{\mathrm{V,RS}}\left(d_{\mathrm{I}_i\mathrm{,RS}}\right)}}\right). \tag{4.9}$$

Comparing (4.9) and (4.7), it can be seen that the received CINR can be increased by employing sectorized receiving scheme when I-VSs are on the different streets with T-VS. The degree of the improvement relies on FBR and FSR of the sector antenna.

4.3 Performance Analysis

4.3.1 CSMA/CA collision model

In the V2V beacon broadcast application for safety driving support, each VS transmits a packet with the length of T_p, which is much shorter than the packet generation interval T_f. For example, T_f and T_p are 100 ms and less than 0.3 ms, respectively [17]. Thus, the most probable case is that only one vehicle has the scheduled transmission overlapping with that of T-VS. Therefore, we analyze the case that a focused T-VS accompanies with one I-VS [17]. Employed CSMA/CA collision model has four nodes: T-VS, R-VS, RS and I-VS. R-VS receives data packets from T-VS via direct and/or relayed paths as shown in Fig. 3.1. In the analytical model, the packet transmissions are performed based on the following assumptions:

- Both T-VS and I-VS periodically broadcast data packets with the same time interval T_f, which is large enough to guarantee that the interactions of transmissions only happens in the same time interval. The scheduled transmissions of I-VS and T-VS are supposed to overlap with each other.

- The wireless channel is modelled as Rayleigh slow-fading channel. Note that LOS path may be blocked by large vehicles even if the T-VS and the R-VS are on a straight road. The transmission time of a V2V packet T_p is short relative to the coherence time of the fading channel. Thus, the received power of a packet is approximated to be constant during carrier sensing or reception.

- RS and VSs can reciprocally carrier-sense each other. This is reasonable assumption because RS is located at the height of traffic lights and thereby there is an LOS between RS and VSs.

4.3.2 PRR at RS and PDR at R-VS

Let us denote the probability that I-VS carrier-senses the transmission of T-VS by p_{CS}, which is also the probability that T-VS can detect the transmission of I-VS due to the reciprocal channel between them. p_{CS} can be calculated as the probability that the

detected power is above a predetermined threshold during a CS period. Here, the detected power is defined as the sum of instantaneous signal power $C_{\mathrm{T,I}}$ and noise power N during the CS period. Thus, p_{CS} can be calculated as

$$\begin{aligned} p_{\mathrm{CS}} &= \Pr\left(C_{\mathrm{T,I}} + N \geq \overline{P}_{\mathrm{CS}}\right) = \int_{\overline{P}_{\mathrm{CS}}-N}^{\infty} f\left(C_{\mathrm{T,I}}\right) dC_{\mathrm{T,I}} \\ &= \exp\left(-\frac{\overline{P}_{\mathrm{CS}} - N}{\sigma_{\mathrm{T,I}}^2}\right), \end{aligned} \tag{4.10}$$

where $\overline{P}_{\mathrm{CS}}$ is the CS threshold power level and $\sigma_{\mathrm{T,I}}^2$ is the average received power of T-VS at I-VS, which is given by

$$\sigma_{\mathrm{T,I}}^2 = \frac{P_{\mathrm{t}} G_{\mathrm{t}} G_{\mathrm{r}}^0}{L_{\mathrm{V,V}}\left(d_{\mathrm{T,I}}\right)}, \tag{4.11}$$

where $L_{\mathrm{V,V}}(d)$ is the propagation loss between VSs.

The PRR at RS is calculated as

$$q_{\mathrm{T,RS}}^i = p_{\mathrm{CS}} \cdot \tilde{q}_{\mathrm{T,RS}}^i + \left(1 - p_{\mathrm{CS}}\right) \cdot \bar{q}_{\mathrm{T,RS}}^i , \tag{4.12}$$

where $i \in \{\mathrm{OR}, \mathrm{SR}\}$, $\tilde{q}_{\mathrm{T,RS}}^i$ and $\bar{q}_{\mathrm{T,RS}}^i$ are the probabilities of successful packet reception at RS without interference and with interference, respectively. $\bar{q}_{\mathrm{T,RS}}^i$ is calculated from (4.7) for OR-V2VC and from (4.9) for SR-V2VC. To calculate $\tilde{q}_{\mathrm{T,RS}}^i$, letting $\sigma_{\mathrm{I,RS}}^2$ be zero in (4.6) gives

$$\tilde{q}_{\mathrm{T,RS}}^i = \exp\left(-\frac{N\Gamma_{\mathrm{CINR}}}{\sigma_{\mathrm{T,RS}}^2}\right). \tag{4.13}$$

Note that we assumed perfect carrier-sensing between RS and VSs, hence the PRR at R-VS from RS $q_{\mathrm{RS,R}}$ is similarly calculated as (4.13) by substituting $\sigma_{\mathrm{T,RS}}^2$ by $\sigma_{\mathrm{RS,R}}^2$.

Next, the PDR at R-VS via the direct path, $p_{\mathrm{PDR}}^{\mathrm{D}}$, is given by

$$p_{\mathrm{PDR}}^{\mathrm{D}} = q_{\mathrm{T,R}} = p_{\mathrm{CS}} \cdot \tilde{q}_{\mathrm{T,R}} + \left(1 - p_{\mathrm{CS}}\right) \cdot \bar{q}_{\mathrm{T,R}} , \tag{4.14}$$

where $\tilde{q}_{\mathrm{T,R}}$ and $\bar{q}_{\mathrm{T,R}}$ are the PRR at R-VS via the direct path without and with interference, and can be similarly calculated as (4.13) and (4.7), respectively. By substituting (4.12), and (4.14) into (4.2), the PDR of R-V2VC, p_{PDR}^i with $i \in \{\mathrm{OR}, \mathrm{SR}\}$, is obtained.

$$\begin{aligned} p_{\mathrm{PDR}}^i = {} & p_{\mathrm{CS}} \left\{ \tilde{q}_{\mathrm{T,R}} + \left(1 - \tilde{q}_{\mathrm{T,R}}\right) \cdot \tilde{q}_{\mathrm{T,RS}}^i \cdot q_{\mathrm{RS,R}} \right\} + \\ & \left(1 - p_{\mathrm{CS}}\right) \left\{ \bar{q}_{\mathrm{T,R}} + \left(1 - \bar{q}_{\mathrm{T,R}}\right) \cdot \bar{q}_{\mathrm{T,RS}}^i \cdot q_{\mathrm{RS,R}} \right\}. \end{aligned} \tag{4.15}$$

In order to evaluate the PDR, the locations of T-VS, R-VS, and I-VS should be considered. In the actual road environments, I-VS becomes an HT in a probabilistic way. Since propagation loss fluctuates due to fading, a VS can become I-VS temporally and comes back as a normal VS if CS succeeds. Therefore, we should consider all possibilities of I-VS generation on the road for averaging in time and location. Averaging in time is already taken into account by (4.10) to obtain average CS success probability. In the analysis, we consider the averaging of the PDR over location which depends on road environments. In the following subsections, we consider two representative road scenarios, i.e., straight road and intersection.

The radio transmission parameters used for analysis is the same to those in Table 3.1. A two-sector and a four-sector receiving antenna are employed at RS for the straight road scenario and the intersection scenario, respectively. The peak gain of each directional antenna is set to 6 dBi. For simplicity, we only consider the case that FBR and FSR are equal. In this section, FBR and FSR are set to 20 dB. In the following analysis, we assume that no packet drop happens at RS due to the introduction of PCRL. The impact of packet drop on the performance will be evaluated in Section 4.4.2.

4.3.3 Straight road scenario

For the straight road environment, we consider the model illustrated in Fig. 4.3. In this model, RS is located at the origin of the x-axis, and equipped with two-sector receiving antenna. T-VS, R-VS, and I-VS are placed along the road according to their x-coordinates, which are expressed as x_T, x_R and x_I, respectively.

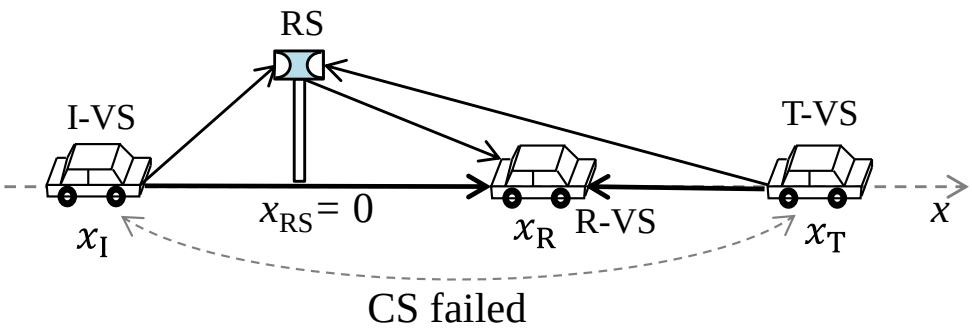

Fig. 4.3: Node layout model for straight road scenario

4.3.3.1 PRR at RS

Fig. 4.4 shows the PRRs at RS as a function of x_T and x_I when ORA and SRA are employed. The figure clearly shows that the PRR severely degrades in a certain area. Hereafter we call the area *severe HT area* where the PRR is less than 50 %. In general, the *severe HT area* is in the opposite side of RS to T-VS where I-VS seldom carrier-senses transmission of T-VS. The area is wide and deep for ORA. When x_T = 300 m, the PRR drops to 6 % at the worst location. This degradation can be alleviated by the use of SRA. The *severe HT area* is narrower and the worst PRR is increased to 39 %.

When I-VS is located at the same side as T-VS (i.e., x_I > 0 m), the PRR is high for both schemes because T-VS and I-VS can carrier-sense each other.

4.3.3.2 Average PDR

From the results of the previous subsection, we focus on the case where the average PDR is severely degraded, i.e., x_T = 300 m. At first, we analyze the case that R-VS is located at x_R = 0 m. In this case, the packet transmitted from RS can be always successfully received by R-VS due to low propagation loss (i.e., $q_{RS,R}$ = 1). Fig. 4.5 shows the average PDRs of D-V2VC, OR-V2V/PCRL, and SR-V2V/PCRL, as a function of the location of I-VS.

When I-VS is located in the opposite side of RS with respect to T-VS, T-VS and I-VS hardly carrier-sense each other. Thus, the average PDR of D-V2VC is low due to the frequent packet collision at R-VS. Although OR-V2V/PCRL improves the average PDR for the same side as T-VS, the minimum PDR for the opposite side is still lower than 10 % when I-VS is located at x_I = -200 m. This is due to packet collision at RS (refer to Fig. 4.4 (a)). On the other hand, SR-V2V/PCRL remarkably increases the average PDR for most of I-VS locations. This confirms the effect of the proposed sectorized receiving scheme in mitigating HT problem.

When I-VS is located at the same side as T-VS, CS almost succeeds. However, the average PDR of D-V2VC is less than 73 % due to the large attenuation loss between T-VS and R-VS. On the other hand, the average PDRs of OR-V2V/PCRL and SR-V2V/PCRL are high and close to 100 % when I-VS is located near T-VS. This shows that RS effectively compensates propagation loss and fading.

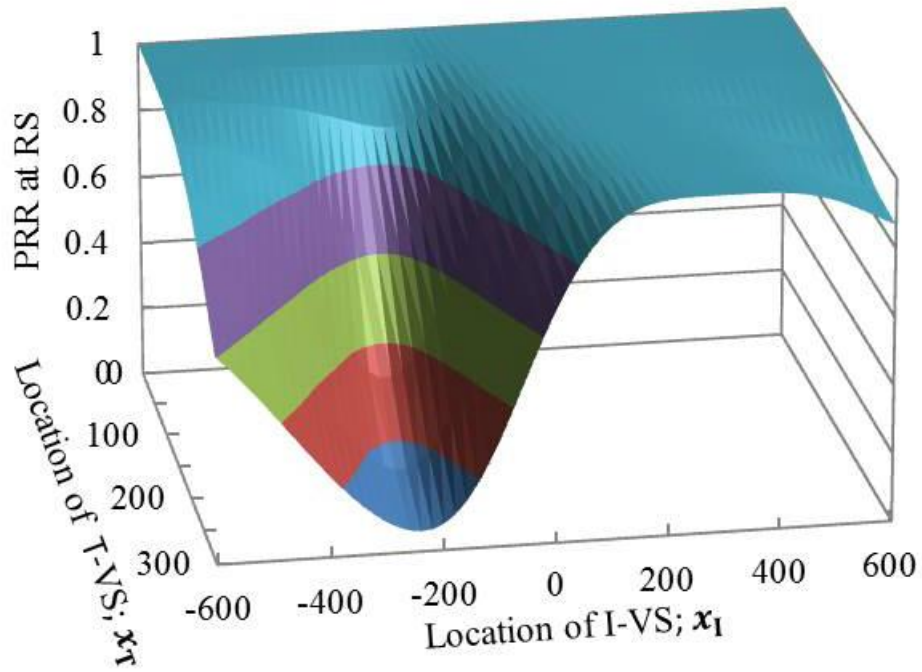

(a) ORA

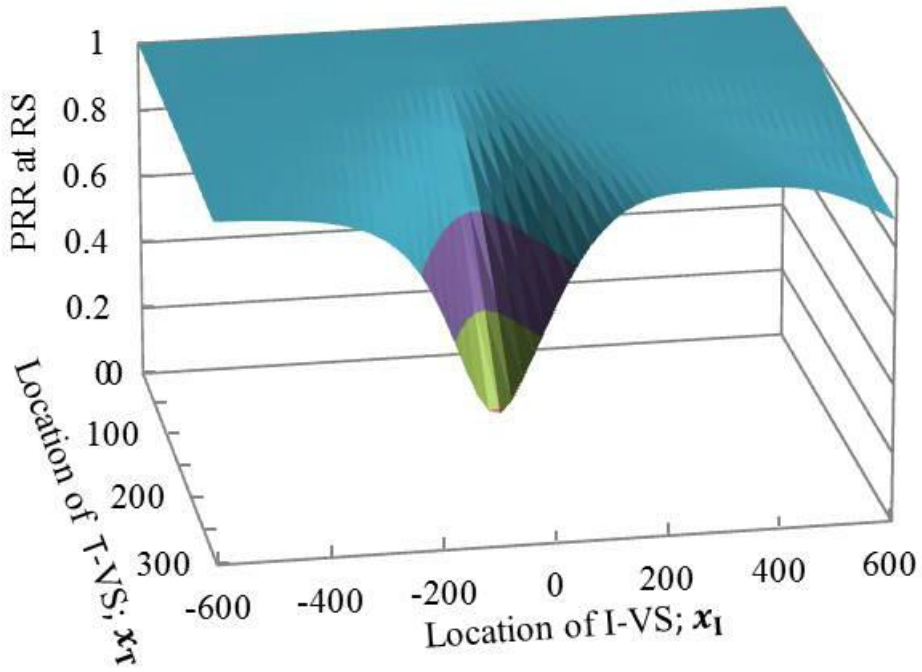

(b) SRA

Fig. 4.4: PRR at RS under straight road environment

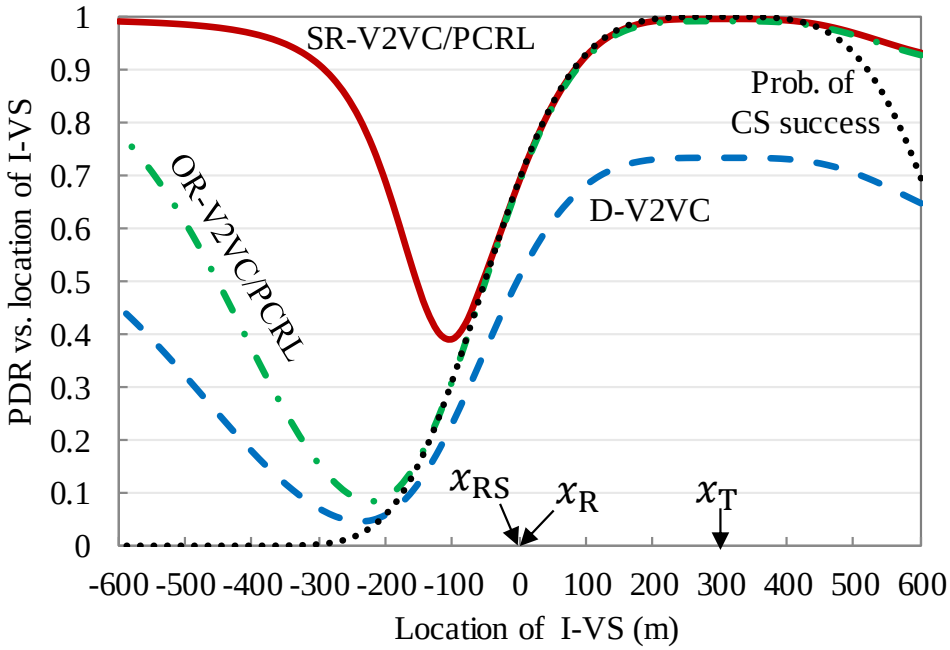

Fig. 4.5: PDR vs. location of I-VS (x_T = 300 m, x_R = 0 m)

As we mentioned above, I-VS becomes an HT in a probabilistic way. Thus, it is necessary to consider all possibilities of I-VS generation on the road by averaging (4.14) and (4.15) with respect to x_I. Fig. 4.6 shows the impact of the location of R-VS on the PDR averaged over I-VS location. Although we assume that I-VS location is uniformly distributed on the road, non-uniform distribution of VSs can be analyzed by considering the vehicle density distribution. When R-VS is located near T-VS, the average PDR is high regardless of V2V communication schemes. As R-VS moves away from T-VS, the average PDR of D-V2VC decreases due to path loss and HT problem. It is lower than 50 % when the distance between T-VS and R-VS is 300 m. Although OR-V2VC/PCRL improves the average PDR by path diversity gain, the packet reception at RS still suffers from HT problem. This packet collision negatively offsets the improvement obtained by employing RS. Thus, the average PDR becomes lower than 70 % when the communication distance is 300 m. On the other hand, SR-V2V/PCRL can effectively mitigate the interference from the HTs while providing full path diversity gain and hence achieves the average PDR higher than 88 % irrespective of the location of R-VS.

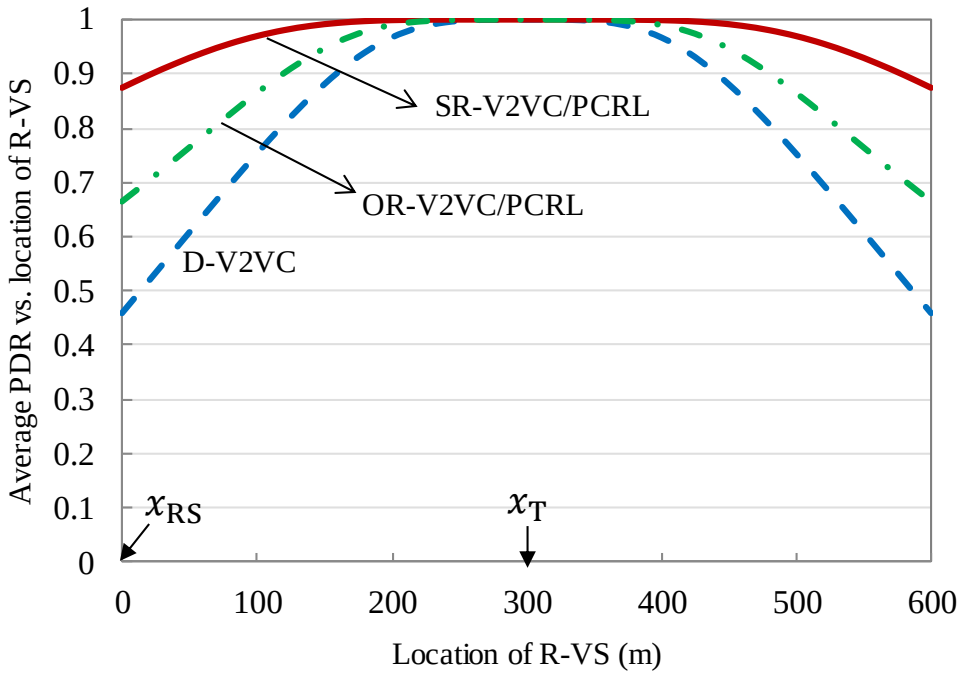

Fig. 4.6: IVS-area averaged PDR vs. location of R-VS (x_T = 300 m)

4.3.4 Intersection Scenario

Next, we consider the intersection environment illustrated in Fig. 4.7. In this model, RS is placed at the intersection center where we set the origin of the *xy*-plane. In an actual implementation, the RS can be located anywhere as far as LOS condition satisfies for four streets. Effect of RS location offset will be discussed in Section 4.4. T-VS is placed on the horizontal road with $x_T > 0$ m. We only focus on NLOS condition between I-VS and T-VS. I-VS is placed on the vertical road with *y*-coordinate of y_I.

4.3.4.1 PRR at RS

Fig. 4.8 shows the PRRs at RS with ORA and SRA. When T-VS is located around the intersection, I-VS can carrier-sense the transmission of T-VS with high probability. Thus, packet collision at RS can be avoided by CSMA/CA. Even if the CS fails, high receiving power from T-VS at RS can lead to successful reception. As a result, the PRR for both OR-V2V/PCRL and SR-V2V/PCRL are sufficiently high for this situation. However, when T-VS moves away from the intersection, frequent CS failure happens

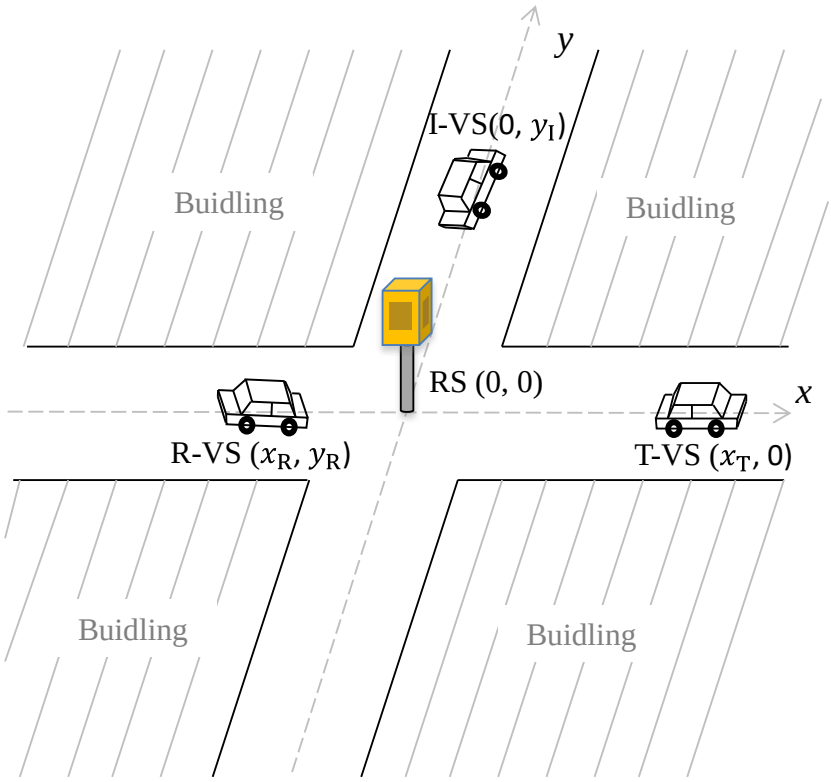

Fig. 4.7: Node layout model for intersection scenario

due to larger propagation loss. This results in severe packet collision at RS. For OR-V2V/PCRL, the *severe HT area* expands over a wide area of I-VS location (Fig. (a)). On the other hand, it is remarkably reduced by SR-V2V/PCRL (Fig. (b)). This is because the interference power from I-VS is mitigated by employing SRA at RS.

4.3.4.2 PDR when T-VS and R-VS are in LOS

Let us first consider the case that the channel between T-VS and R-VS is LOS. Fig. 4.9 shows the PDR of three V2V communication schemes. When I-VS is located around the intersection, the channel between T-VS and I-VS is LOS. In such a situation, the average PDRs are mainly determined by their CS success rate. When y_I > 50 m, the channel between T-VS and I-VS becomes NLOS and they cannot carrier-sense each other. Therefore D-V2VC is strongly affected by the HT and hence the average PDR severely drops. The average PDR of OR-V2VC is still low over a wide range of I-VS location due to the decrease in PRR at the RS (see Fig. 4.8(a)).

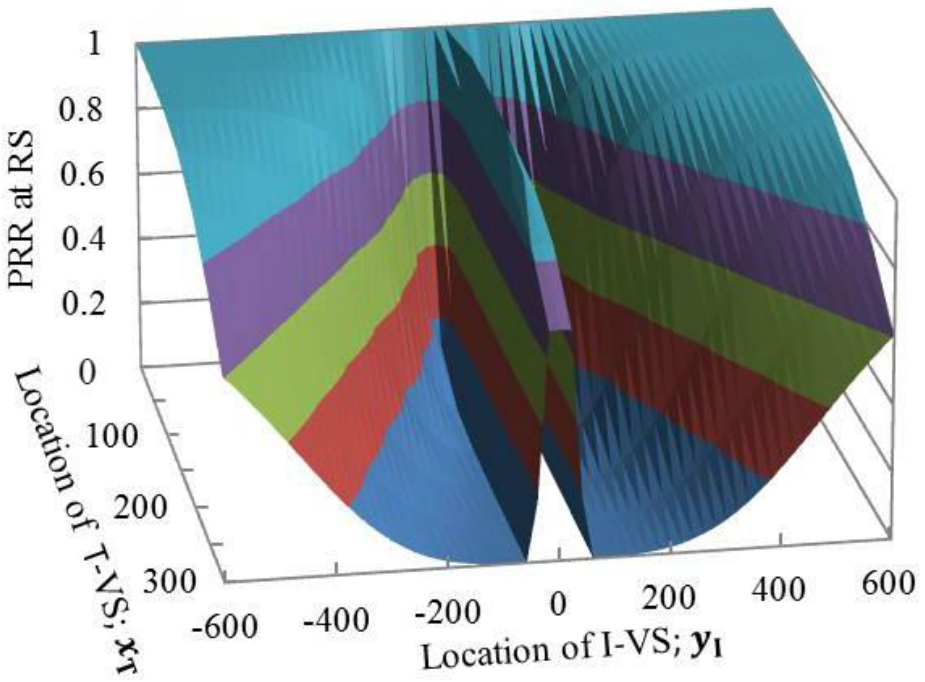

(a) ORA

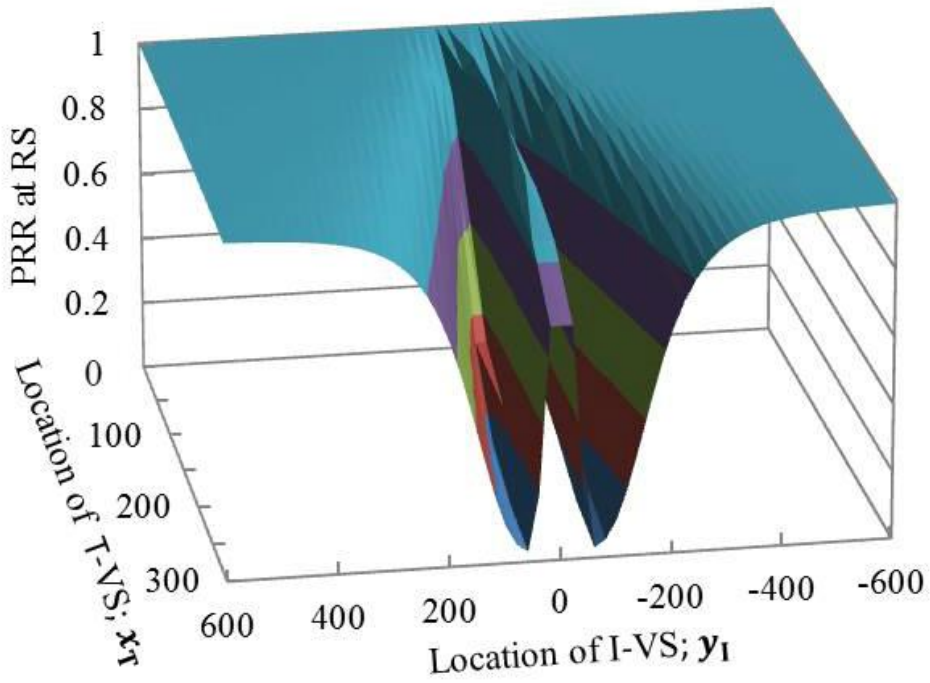

(b) SRA

Fig. 4.8: PRR at RS under intersection environment

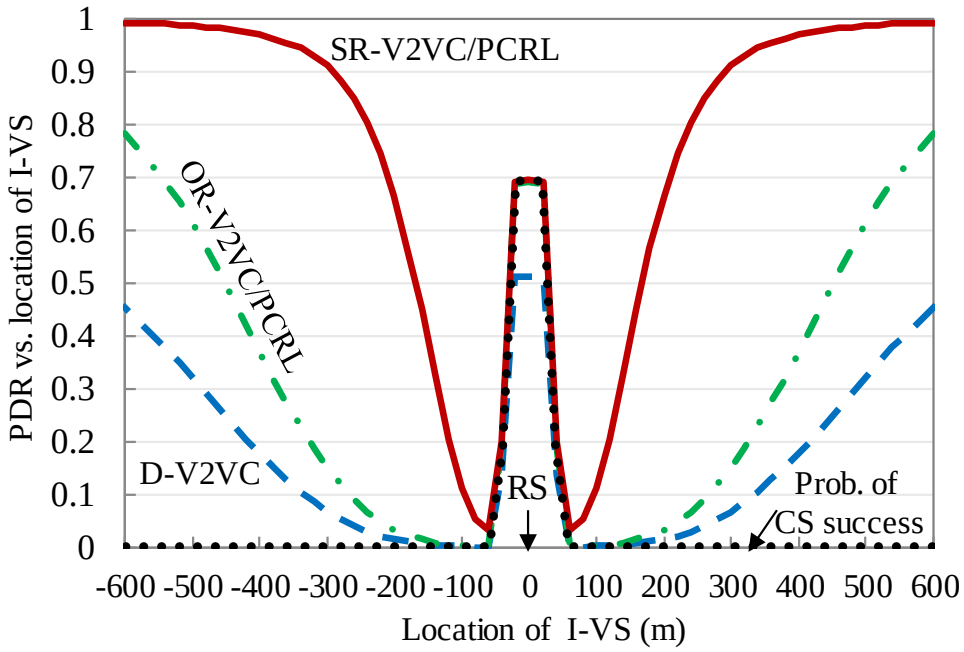

Fig. 4.9: PDR vs. location of I-VS when T-VS and R-VS are in LOS condition x_R ($x_R = y_R = 0$ m, $x_T = 300$ m)

For $y_I = \pm 50$ m from the intersection center, the average PDRs severely decrease regardless of V2V communication schemes. The reason for this can be explained as follows. In this location, CS is not possible due to the NLOS condition between T-VS and I-VS. Furthermore, the distances among I-VS, R-VS, and RS are very short. Then interference power is very strong at R-VS and RS, hence it cannot receive weak signal from T-VS.

Fig. 4.10 shows the impact of the location of R-VS on the PDR averaged over the location of I-VS. We consider R-VS is located on the horizontal road within an area from 0 to 600 m. When R-VS is located near T-VS, the average PDRs of three V2V communication schemes are as high as 100 %. When the distance becomes larger, the PDR of D-V2VC decreases. OR-V2VC/PCRL slightly improves the PDR, while the improvement obtained by SR-V2VC/PCRL scheme is remarkable. Particularly, when R-VS is around the intersection center, the average PDR of D-V2VC is as low as 20 %. The average PDR of OR-V2VC/PCRL is around 34 %, while that of SR-V2VC/PCRL is higher than 77 %.

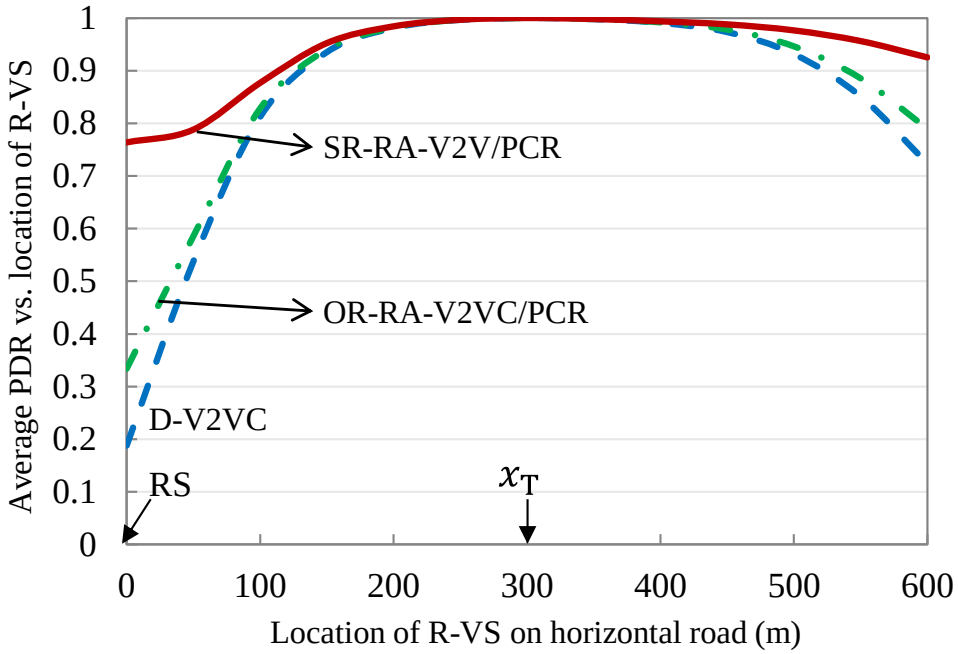

Fig. 4.10: IVS-area averaged PDR vs. location of R-VS (x_T = 300 m)

4.3.4.3 PDR when T-VS and R-VS are in NLOS

Next, let us consider the situation where there is no LOS between T-VS and R-VS. The location of T-VS x_T is set to 200 m. R-VS is located on the vertical road with the y-coordinate y_R of 100 m. The total distance between T-VS and R-VS via the intersection center is 300 m, which is the same distance for the LOS case.

Fig. 4.11 shows the PDRs of the three V2V communication schemes. In D-V2VC, the propagation loss due to shadowing is significant and the average PDR is 0 % regardless of I-VS location. Relay-assisted schemes remarkably improve the PDR even in the NLOS condition. Particularly, SR-V2V/PCRL improves the PDR to more than 90 % when I-VS is 200 m away from the RS.

Let us consider the case that I-VS is located around the intersection center and there is LOS between T-VS and I-VS. The PDRs of R-V2VC schemes for $x_T = 200$ m are higher than that for $x_T = 300$ m in Fig. 10. This is because the CS success rate of T-VS transmission at I-VS is higher than that for the farther location.

Fig. 4.12 shows the impact of the location of R-VS on the PDR averaged over the location of I-VS. R-VS is assumed to be located on the vertical road within an area from

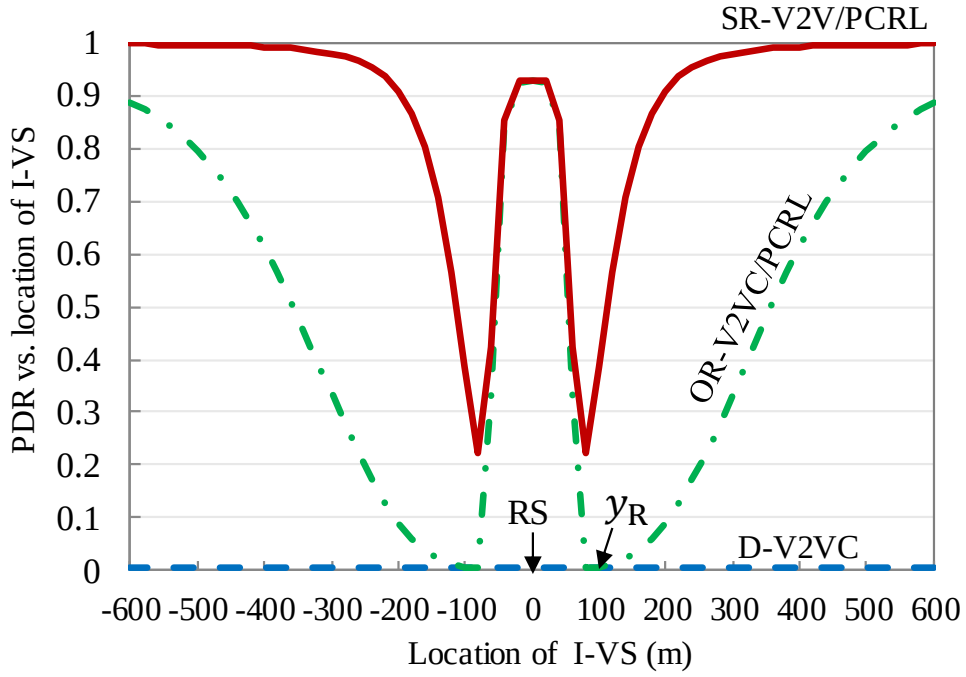

Fig. 4.11: PDR vs. location of I-VS when T-VS and R-VS are in NLOS condition (x_R = 0 m, y_R = 100 m, x_T = 200 m)

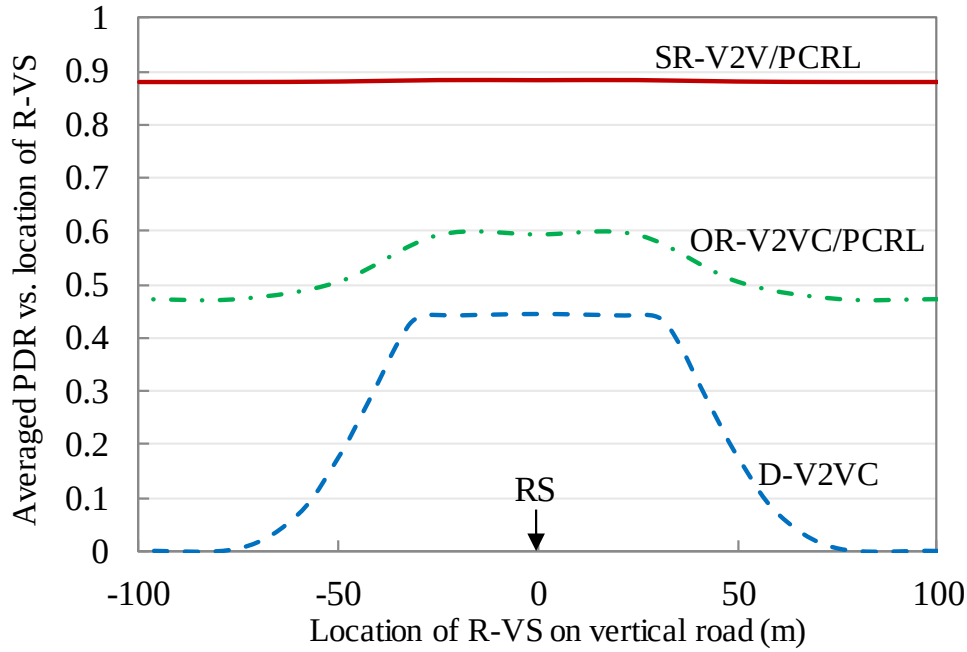

Fig. 4.12: IVS-area averaged PDR vs. location of R-VS (x_T = 200 m)

-100 m to 100 m. When R-VS is located near the intersection center, the effect of shadowing and HTs is moderate and the average PDR of D-V2VC is around 45 %. It rapidly drops down when R-VS is move away from the intersection. R-V2VC schemes improve the average PDR, particularly when the location of R-VS is farther away from the intersection center. However, the average PDR of OR-V2VC/PCRL scheme is still less than 60 % regardless of the location of R-VS due to the effect of HT (see Fig. 4.11). On the other hand, SR-V2VC/PCRL significantly improves the average PDR around 88 % regardless of R-VS locations.

4.4 Numerical Simulation of Large-Scale System

The HT problem happens more severely around an intersection where the presence of buildings introduces the shadowing effect. Therefore, we further investigate the effectiveness of the proposed SR-V2VC/PCRL in an intersection environment by means of large-scale computer simulation. For performance evaluation, we adopt the more general quality measure of BPDR as the performance metric.

4.4.1 Simulation set up

In the previous section, the PDR of the packet transmitted from T-VS to a specific R-VS has been studied. In this section, we consider the scenario when T-VS broadcasts a data packet to multiple R-VSs in the area that the T-VS is expected to cover. Computer simulations are conducted using Scenargie network simulator [56]. Fig. 4.13 shows the node layout. Each road has 1200 m length and 20 m width, with four lanes. All VSs are uniformly distributed with an interval of 25 m in the same lane. It means that there are 392 VSs in the simulation area and the vehicle density is 160 VSs/km. T-VS of interest is located on the horizontal road, same as the analysis in Section 4.3.4. The three V2V communication schemes are compared in terms of the BPDR, which is calculated for the evaluation area of interest that spans ±250 m from T-VS. Only R-VSs in the evaluation area are taken into account for the BPDR calculation. The evaluation area is defined as

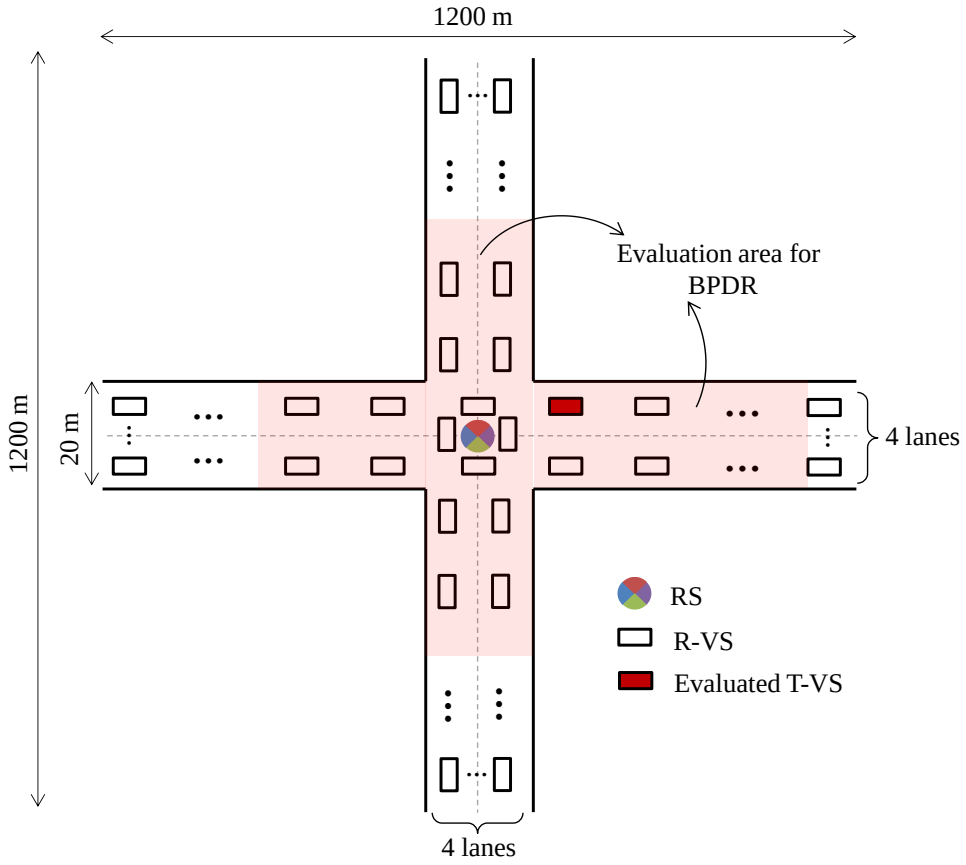

Fig. 4.13: Node layout for intersection environment

$$E_{\mathrm{PDR}} = \left\{ (x, y) \;\middle|\; \left(|x_{\mathrm{T}} - x| + |y_{\mathrm{T}} - y| \right) \le 250 \right\}. \qquad \textbf{(4.16)}$$

where $(x_{\mathrm{T}}, y_{\mathrm{T}})$ is the location of the T-VS. The evaluation area in Fig. 4.13 is shown by highlighted in pink-color.

An RS employing SRA with four sectors is employed considering four-corner intersection. Unless otherwise stated, the RS installed at the center of the intersection. The peak antenna gain of SRA is 6 dBi. FBR and FSR of sector antenna units have options of three different values, i.e., 14 dB, 20 dB and the infinite. The radiation pattern of a sector antenna unit for the case of FBR and FSR of 20 dB is shown in Fig. 4.14.

The radio transmission parameters and the traffic conditions for the V2V communications are the same as those in Table 3.1. As an observation from the previous chapter, 16QAM/12 Mbps is employed for relaying transmission.

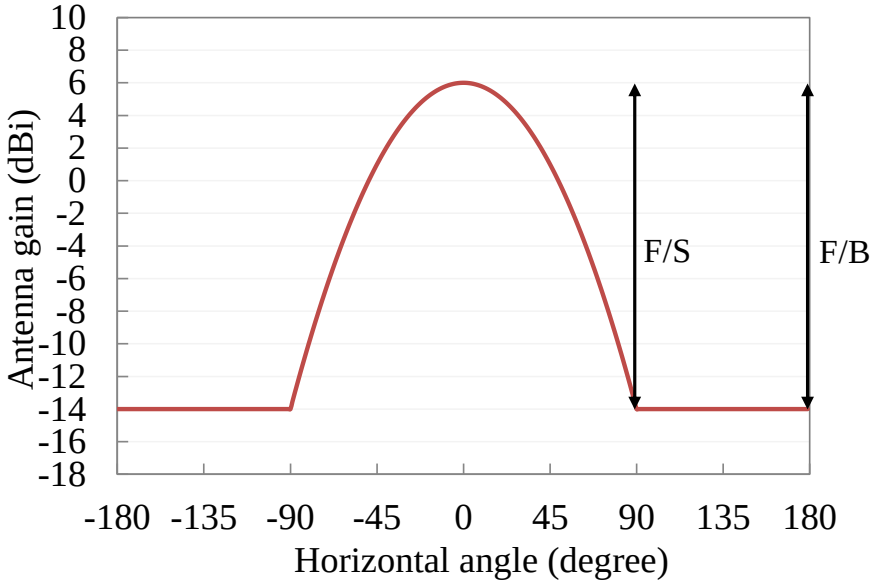

Fig. 4.14: Horizontal radiation pattern of sector antenna unit

4.4.2 Simulation Results

4.4.2.1 PRR at RS

Fig. 4.15 shows the PRRs at RS when the ORA and SRA are employed. When T-VS is near RS, the PRRs are high. However, the PRR at RS with ORA rapidly drops when T-VS is far from RS. This is because the effect of HT becomes severer with the increased distance between RS and T-VS (refer to Fig. 4.8 (a)). The area where the PRR of higher than 90 % has ±70 m range for the omnidirectional scheme. The area is remarkably improved by employing the sectorized receiving RS and the higher improvement is obtained by higher FBR and FSR. The area is ±120 m range for FBR and FSR of 14 dB, and ±150 m for the higher FBR and FSR of 20 dB.

For the ideal case of infinite FBR and FSR, the effect of HTs on the vertical road as well as on the opposite side of RS to T-VS is negligible, and then the PRR is as high as more than 90 % for all locations of T-VS. These results show that SRA is quite effective to mitigate the HT problem.

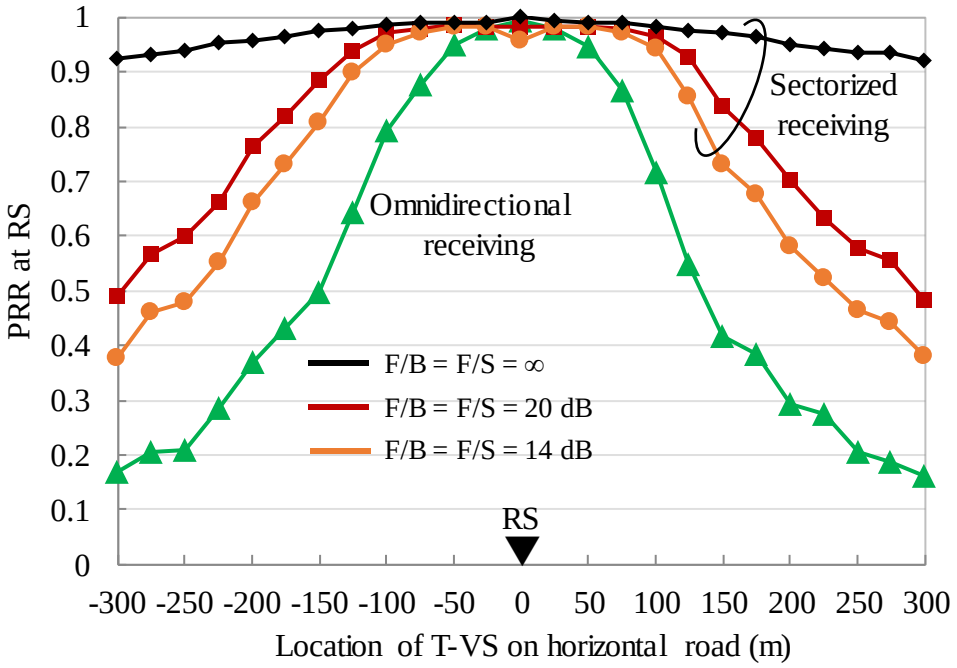

Fig. 4.15: PRR at RS under intersection environment

4.4.2.2 Effect of RS Location on PRR at RS and BPDR Performance

We see the case when the location of RS is set at the corner edge of the intersection. Fig. 4.16 shows the PRR at RS for this case. The PRR when RS locates at the intersection center is also presented for comparison. Here, the separation of the SRA is set to 20 dB. It can be seen from the figure that there are little differences between the two cases of RS locations. This is mainly due to two reasons. First, LOS propagation is still available between RS and VSs when RS locates at the corner edge. Second, the beam width of the sector antenna unit is wide enough to ignore the changes in receiving angle at each antenna unit, especially for T-VS locating far from the RS.

Fig. 4.17 shows the BPDR when the location of RS is set at the corner edge of the intersection. Same as the case of PRR, BPDR in this case is almost same to that in the case of RS locating at the intersection center. From these observations, we set the location of RS at the intersection center from hereafter.

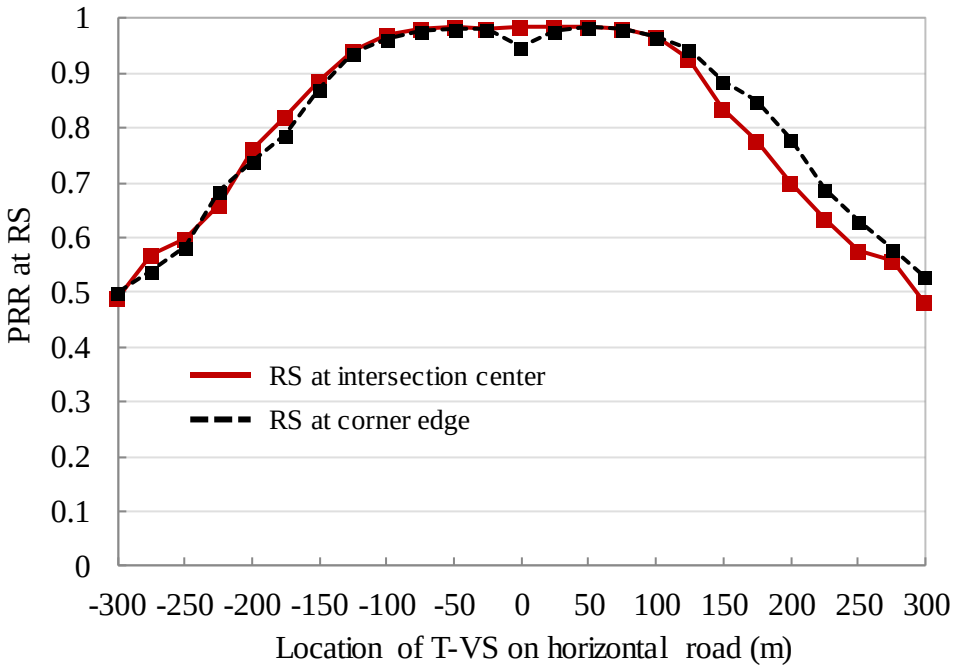

Fig. 4.16: Effect of RS location on PRR at RS

(F/B = F/S = 20 dB)

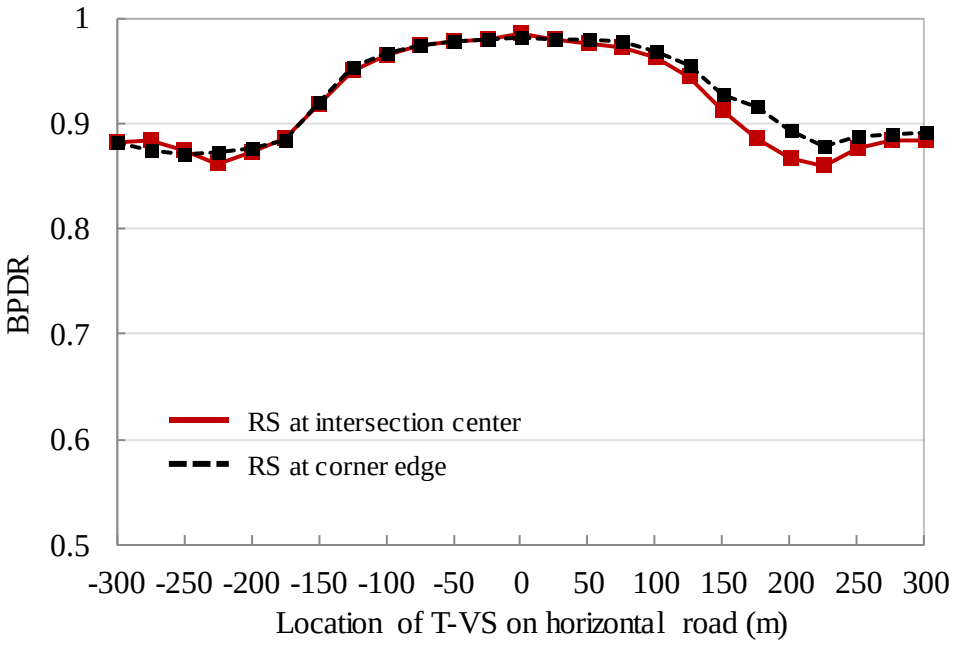

Fig. 4.17: Effect of RS location on BPDR

(F/B = F/S = 20 dB)

4.4.2.3 Effectiveness of SR-V2VC/PCRL on BPDR

First, we evaluate the impact of the packet drop at RS. Fig. 4.16 shows the BPDRs of the three V2V communication schemes. For the SR-V2V scheme, we study the case that both FBR and FSR are 20 dB. Fig. 4.16 clearly shows that the BPDR dramatically drops due to the frequent packet congestion if PCRL is not employed at RS. We have confirmed that more than half of V2V packets are dropped. As a result, the gain of the RA-V2V schemes without PCR is low and the improvement in BPDR is quite small. On the other hand, the packet congestion problem is completely mitigated by employing PCR at RS, thus BPDR is remarkably improved.

When T-VS is near the intersection center, most R-VSs in the evaluation area are in LOS condition. Therefore, the BPDRs are very high for both OR-V2VC/PCR and SR-V2VC/PCR schemes. For D-V2VC, the area-average BPDR is around 88 %. The difference of around 10 % is owing to the path diversity effect of the relay-assisted schemes.

When T-VS is moved away from the intersection center, the BPDR of D-V2VC remarkably decreases. It is around 70 % when T-VS is separated by 150 m from RS.

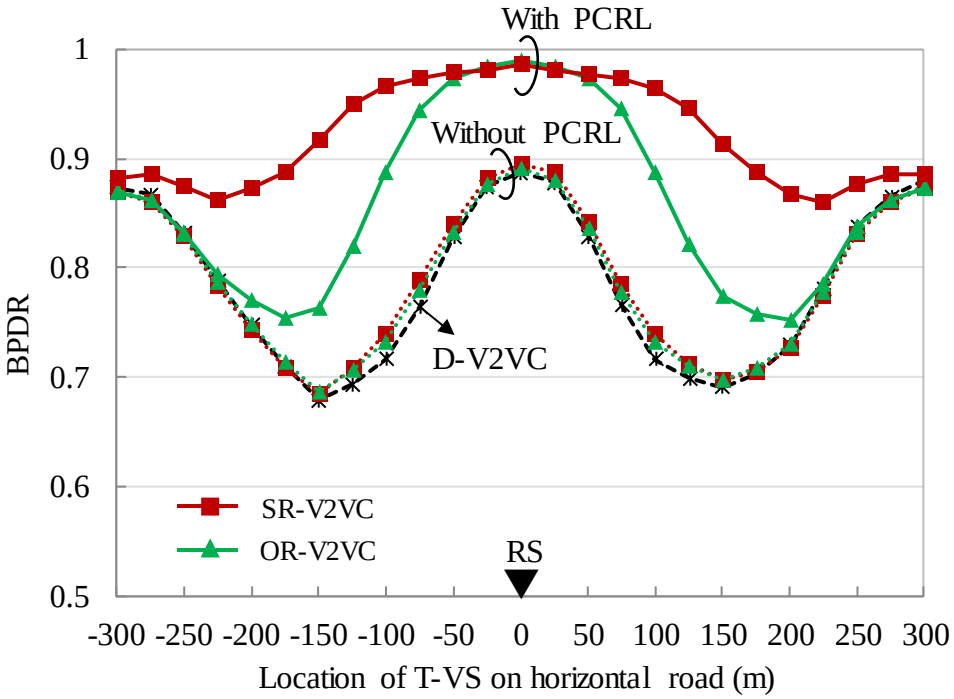

Fig. 4.18: BPDR under intersection environment

This is mainly due to the drop of the BPDR to NLOS R-VSs on the vertical road. Although OR-V2VC/PCRL improves the BPDR when T-VS is around the intersection center, the BPDR rapidly decreases as T-VS moves away from RS. This is due to the decrease of the PRR at RS as shown in Fig. 4.15. On the other hand, the proposed SR-V2VC/PCRL further improves the BPDR even when T-VS is far from the intersection center. For example, the BPDR is improved by 15 % when the distance between T-VS and RS is 150 m.

When T-VS moves farther, the BPDR of D-V2VC recovers to 87 % when T-VS is 300 m away from the intersection center. This is because T-VS and R-VS in the evaluation area are on the same straight road and in LOS condition. Meanwhile, the improvement by OR-V2VC/PCRL is little in this region. This is due to the drop in the PRR at RS. The proposed SR-V2VC/PCR keeps the highest BPDR for all location of T-VS.

Next, we investigate the impact of FBR and FSR on the performance of SR-V2VC/PCRL scheme. Fig. 4.17 shows the BPDR of the proposed scheme when both FBR and FSR are set to 14 dB, 20 dB and the infinite. For practical FBR/FSR values of

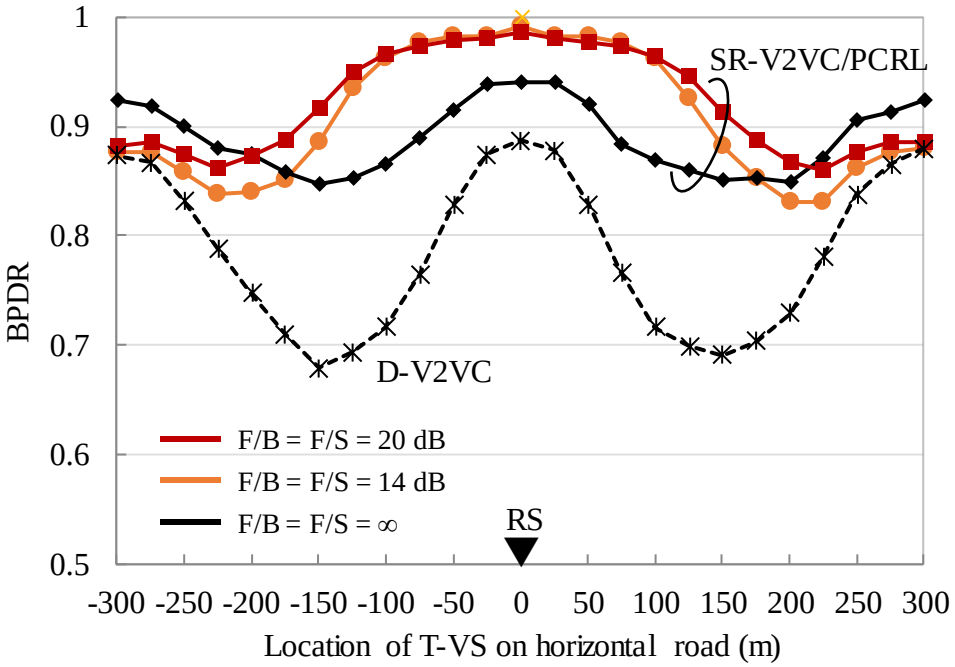

Fig. 4.19: BPDR of SR-V2VC/PCRL with various FBR/FSR

14 dB and 20 dB, the BPDR is improved as FBR/FSR increases. The BPDR slowly deteriorates when T-VS is farther than 120 m from RS. The difference between FBR/FSR values of 14 dB and 20 dB is less than 4% and BPDR keeps higher than 80 % for all locations of T-VS even for the FBR/FSR of 14 dB. Therefore, the proposed SR-V2VC/PCRL is also effective for sector antenna with low FBR/FSR as 14 dB.

When the FBR/FSR are infinite, BPDR of the proposed SR-V2VC/PCRL decreases. This is because of the congestion issue at RS due to the improved PRR. However, the BPDR still keeps much higher than that of D-V2VC scheme. The congestion issue is further discussed in the next chapters.

4.5 Chapter Summary

In this chapter, an improved PCRL scheme with sectorized receiving RS has been proposed. Performance of the proposed SR-V2VC/PCRL scheme is first theoretically analyzed considering both straight street and intersection scenarios. Next, computer simulations are conducted to confirm the superiority of the scheme considering an intersection environment with a large number of VSs. From the results, the following conclusions can be drawn:

1) The combination of PCRL and the sectorized receiving scheme effectively mitigates the effect of HT problem as well as alleviate the congestion issue at RS. Consequently, the reliability of V2V communications improves.

2) Performance of the SR-V2VC/PCRL scheme relies on the separation of the sector antenna, i.e. FSR and FBR. Higher separation provides higher PRR at RS. By employing PCRL, the potential improvement brought by the sectorized receiving scheme is fully obtained for practical values of FBR and FSR.

3) For the ideal case of sector antenna, the congestion issue still happens at RS due to the large number of received V2V packets that need to be relayed. More details will be discussed in the next chapters.

Chapter 5. Packet Relay-Assisted V2V Communication Scheme with Multiple Relay Stations in Urban Environment

In chapter 4, it has been shown that the relay-assisted V2V scheme employing payload combining and sectorized receiving RS, i.e. SR-V2VC/PCRL scheme can remarkably improve the reliability of V2V communications by alleviating the congestion issue as well as mitigating HT problem at RS. Effectiveness of the scheme has been evaluated considering a single intersection environment. In this chapter, performance of the proposed SR-V2VC/PCRL scheme is studied in urban environments with multiple intersections. First, interference from relaying transmissions to V2V communications is investigated. Next, cooperation among RSs is discussed and evaluated to exploit the benefit of relay-assist. Finally, the use of higher-order modulation for V2V and relay transmission is proposed to further remedy the congestion issue at RSs due to the increased air traffic.

5.1 Introduction

High reliability is one of the most important requirements in V2V broadcast communications for safety support applications. Relay-assisted V2V communication employing sectorized receiving RS and payload combining, i.e. SR-V2VC/PCRL, has been proposed to improve the reliability of V2V communications. In the scheme, packets transmitted from multiple VSs in the relation of HT each other are received separately by different sectors at RS. Due to the antenna directivity, the packet collision at RS can be mitigated, and hence the PRR at RS improves. In addition, multiple V2V

packets are forwarded in a single transmission chance by the PCRL scheme, then the congestion issue at RS is effectively mitigated. Therefore, the packet transmission rate at RS remarkably increases. It has been shown in the previous chapter that the improvement brought by the proposed SR-V2VC/PCRL scheme is remarkable in single intersection scenario.

In the real world, urban environment including multiple intersections is the most common scenario, and evaluating the performance of V2V communications under such a scenario is essential for the future deployment of vehicle safety communications. There are some works focusing on urban environment with multiple intersections. In [67], the effects of buildings on the performance of V2V communications at urban environment with multiple intersections are studied. The work considered three different intersection layouts, i.e. urban closed intersection where the four corners are occupied by buildings, urban half-open intersection where two corners are occupied, and urban open intersection where LOS propagation between vehicles can be available due to the absence of buildings. The presence of building not only reduces the communication range, but also increases the number of HTs that affects the performance of V2V communications. In [68], a rateless-coded scheme for infrastructure-to-vehicle communications in an urban environment was proposed. In the scheme, an RSU is deployed at an intersection to provide on-demand large file download to surrounding vehicles. By employing a systematic raptor codes, the rateless-coded scheme can achieve better performance than the traditional ARQ (Automatic Repeat reQuest) scheme. However, all the previous works do not investigate performance of relay-assisted V2V communications in urban environment with multiple intersections. Since almost intersections have a building at each four corners [69], relay-assist is a promising solution to solve the shadowing problem.

Considering SR-V2VC/PCRL scheme in urban environment, each intersection should be covered by an RS. In such a situation, interference from RSs to V2V transmission should be investigated because of their frequent relaying transmissions. In addition, RSs should cooperate with one another to obtain the largest diversity gain. In this chapter, effect of sectorized receiving scheme is studied for a city environment considering interferences from other RSs. Next, cooperation among RSs is discussed and evaluated to exploit the benefit of relay-assist. Then, the utilization of higher-order

modulation for V2V and relaying transmission is proposed to mitigate the congestion issue at RSs due to the increased air traffic load. Finally, performance of SR-V2V/PCRL scheme for urban environment with nine intersections is analyzed by means of large-scale computer simulations.

5.2 Effect of Multiple RSs for SR-V2VC/PCRL Scheme in Urban Environment

5.2.1 PRR at RS5 Suffering from Interferences of Other RSs

First, we estimate the probability that relaying transmissions overlap with a V2V transmission. Consider an urban scenario model shown in Fig. 5.1. The scenario is modelled by a Manhattan grid, where the road structure comprises of evenly spaced horizontal and vertical roads. Each RS is installed at each intersection. The distance between two adjacent RS is d_{RS}. The T-VS that locates between RS5 and RS6 on the horizontal road H2 as shown in the figure is broadcasting a data packet to other VSs according to CSMA/CA. Others VSs and RSs may become HTs if they cannot carrier-sense the on-going transmission of T-VS.

The broadcast process considered in this dissertation is based on CSMA/CA mechanism where a VS trying to transmit a packet senses the channel for ongoing transmissions. If the channel is sensed as busy, then the VS performs a random back-off mechanism to prevent collision. However, under high traffic conditions, it is shown that CSMA/CA behavior breaks down to an ALOHA-like transmission pattern [70]. A fundamental reason for CSMA-based protocol to behave like ALOHA is the finite granularity of the contention window size since there exists a non-negligible probability that nodes may choose the same back-off counter. Further, all nodes with a zero back-off counter at the end of the previous transmission transmit simultaneously without performing CSMA to each other. These nodes include the new arrivals that chose a zero back-off counter and also the nodes from previous slots that decrease their back-off counters to zero.

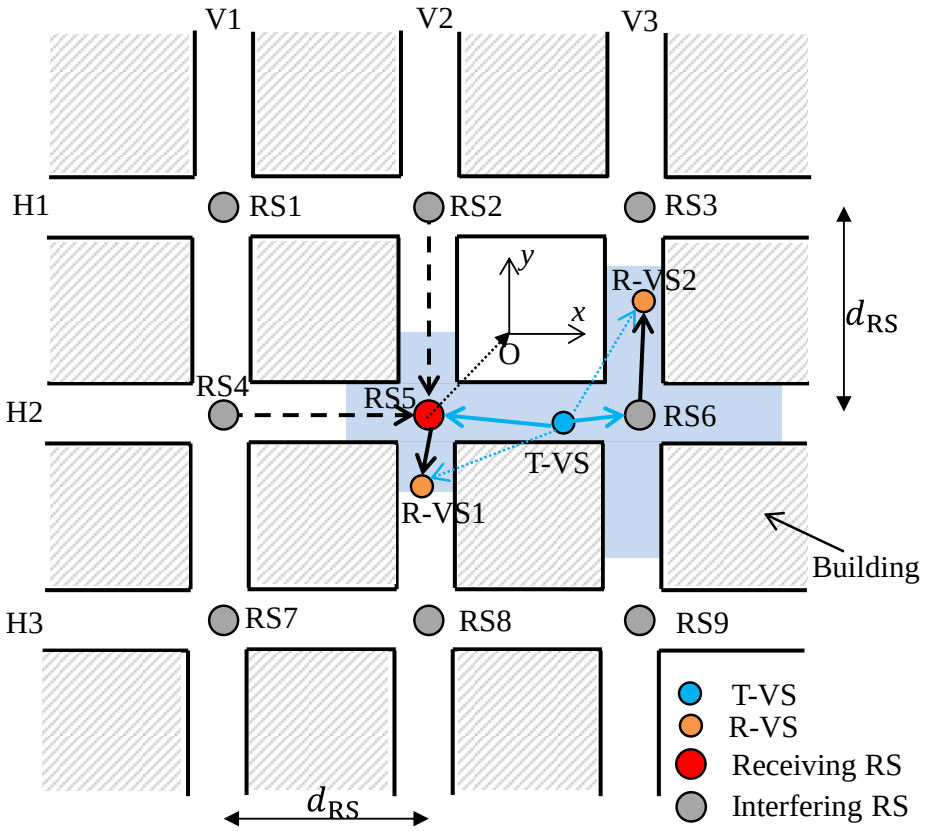

Fig. 5.1: Analysis model

We then assume that there is no carrier sensing mechanism or CS always fails in our estimation in this section. Therefore, the probability of packet collision can be represented by the overlapping probability that the scheduled transmission periods of others VSs and RSs overlap with that of the T-VS. Assume that there are M VSs that generate data packets periodically with the same transmission interval T_f. The packet generation timings of VSs are assumed to be independent and uniformly distributed in the transmission interval. The probability that the scheduled transmission periods of k (k is an integer value that satisfy $1 \leq k \leq M$-1) VSs overlap with that of TVS is given by [71]

$$p_{ov}^{V,V}(M,k) = \binom{M-1}{k}\left(\frac{2T_p}{T_f}\right)^k\left(\frac{T_f-2T_p}{T_f}\right)^{M-1-k} \quad \textbf{(5.1)}$$

where T_p is the duration required for a data packet transmission of V2V communications. The probability that packet collision occurs at RS5 among the T-VS and others VSs is then given by

$$p_c^{V,V}(M) = \sum_{k=1}^{M-1} p_{ov}^{V,V}(M,k) = 1 - \left(1 - \frac{2T_p}{T_f}\right)^{M-1} \quad \textbf{(5.2)}$$

Let M_{RS} denote the number of RSs. Contrary to VSs that are supposed to broadcast one packet in a T_f, an RS may transmit multiple packets depending on the number of received V2V packets as well as the transmitting scheme employed at RS. Let N_R denote the average number of relayed packets that an RS transmits during a T_f. When sectorized receiving scheme is employed, the PRR at RS is improved then N_R increases. N_R also depends on the covering area of the RS. Let T_r denote the transmission time of a relayed packet. Note that if PCRL scheme is employed, T_r is much longer than T_p, then only one of the N_R relayed packets of the RS may collide with the transmission of T-VS. The probability that the scheduled transmission periods of k ($1 \le k \le M_{RS}$) RSs overlap with that of T-VS is given by

$$p_{ov}^{R,V}(M_{RS},k) = \binom{M_{RS}}{k}\left(N_R \frac{T_r + T_p}{T_f}\right)^k \left(1 - N_R \frac{T_r + T_p}{T_f}\right)^{M_{RS}-k} \quad \textbf{(5.3)}$$

Note that the transmission process at RS is initiated when at least one V2V packet has been received. It means that the next relayed packet will be sent after at least a period of (T_p + T_r). As a result, RS cannot transmit more than $\lfloor T_f/(T_r + T_p) \rfloor$ relayed packets in a T_f. This guarantees that the probability is always smaller than 1. Here, $\lfloor x \rfloor$ is the largest integer less than or equal to x. The probability that packet collision occurs at RS5 among the T-VS and others RSs is thus given by

$$p_c^{R,V}(M_{RS}) = \sum_{k=1}^{M_{RS}} p_{ov}^{R,V}(M_{RS},k) = 1 - \left(1 - N_R \frac{T_r + T_p}{T_f}\right)^{M_{RS}} \quad \textbf{(5.4)}$$

If we focus on the transmission from T-VS to RS5, HTs on the roads other than V2 and H2 have little effect on the transmission. Fig. 5.2 shows the overlapping probability between T-VS and others VSs/RSs on V2 and H2. Here, we assume that the RSs employ PCRL scheme and use 16QAM/12 Mbps for transmission. In addition, the

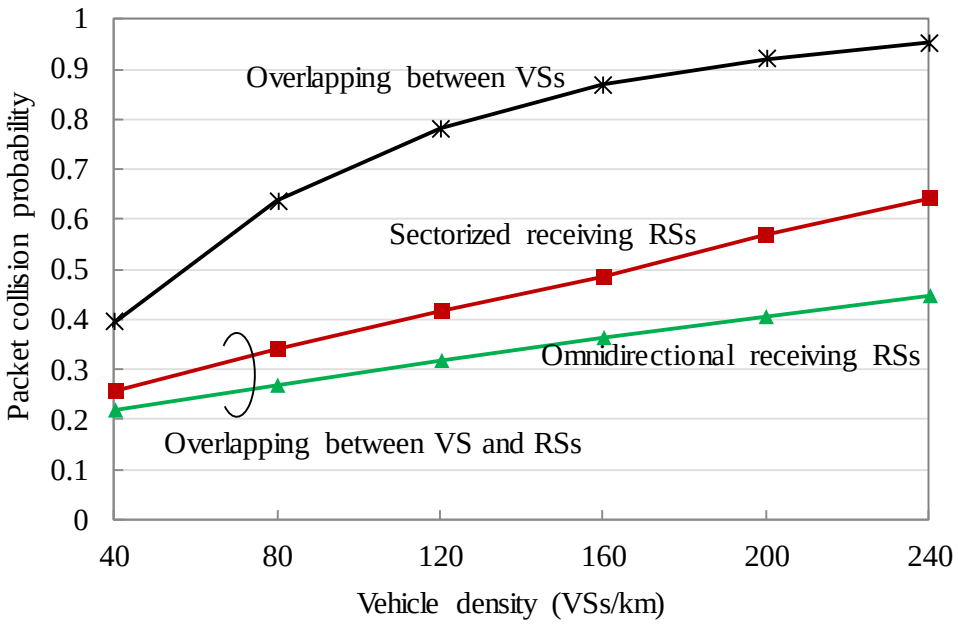

Fig. 5.2: Packet collision probability between T-VS and other VSs and between T-VS and RSs

(T_p = 0.264 ms, T_f = 100 ms, d_{RS} = 300 m)

radius of receiving area at each RS is set to d_{RS}. Finally, the average PRRs at omnidirectional and sectorized receiving RS are set as 0.4 and 0.7, respectively.

It can be observed from the figure that the probability of packet collision between the T-VS and RSs is quite significant, around half of that between T-VS and other VSs. This is due to the frequent transmission of the RSs. The probability becomes large as the number of VSs increases. When the sectorized receiving scheme is employed, the probability of packet collision is higher than that of the omnidirectional scheme. This is due to the improved PRR at RSs.

We now then investigate the effect of relaying transmission on V2V communications. To evaluate the effectiveness of the sectorized receiving scheme in mitigating HT problem, we assume that packet collision due to HT has already happened at RS5. By utilizing Eq. (4.7) and (4.7), we can calculate the PRRs at RS5 under multiple interference sources. Fig. 5.3 show the PRR under one interferer of RS2, two interferers of RS2 and RS4, and three interferers of RS2, RS4 and RS8. Here, the PHY and MAC parameters used for the calculation are the same to those in Table 3.1. If omnidirectional

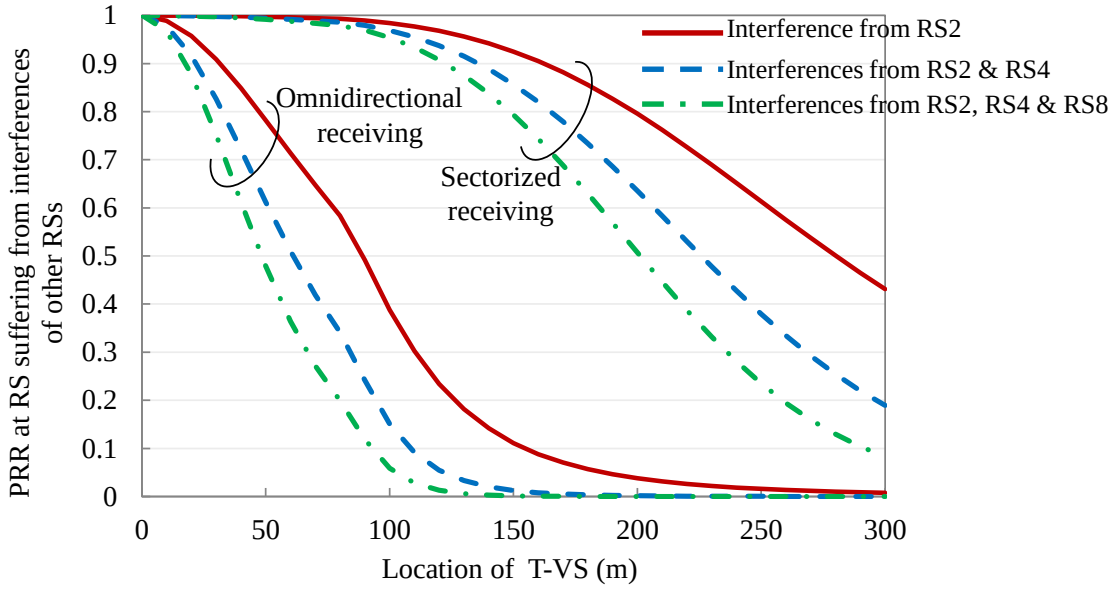

Fig. 5.3: PRR at RS5 suffering from interferences of other RSs

(FBR = FSR = 20 dB, d_{RS} = 300 m)

receiving scheme is employed at RS5, the PRR rapidly drops when the distance between T-VS and RS5 is larger than 25 m. This low PRR will results in bad relaying performance of the omnidirectional receiving scheme. On the other hand, sectorized receiving remarkably improves the PRR. The PRR keeps higher than 90 % when the distance from T-VS to RS5 is 120 m or shorter. When T-VS locates farther from RS5, the PRR decreases. The PRRs are below 80 % when the distance from T-VS to RS5 is 200 m. When the distance is 300 m, the PRR under interference from only RS2 is down to 45 % while that under three interference sources of RS2, RS4 and RS8 is even lower than 10 %. In the next subsection, we will discuss about the cooperation among RSs to deal with this problem.

5.2.2 Cooperation among Sectorized RSs

We have showed that the PRR at RS5 under interferences from other RSs degraded significantly when the location of T-VS is 100 m or more. In such a case, RS6 can also receive and relay the packet from T-VS. If multiple RSs forward the same packet received from T-VS, the RS diversity effect can be obtained which may improve relaying performance.

Consider an R-VS in the communication range of T-VS as shown by blue-color in Fig. 5.1. Let $q_{\mathrm{T,RS}_i}$ and $q_{\mathrm{RS}_i,\mathrm{R}}$ denote the PRR at RS_i from T-VS and that at R-VS from RS_i ($1 \le i \le 9$), respectively. The PDR from T-VS to R-VS can be expressed as

$$PDR_{\mathrm{R}} = p_{\mathrm{T,R}} + (1 - p_{\mathrm{T,R}}) \left\{ 1 - \prod_{i=1}^{9} \left(1 - q_{\mathrm{T,RS}_i} \cdot \xi_{\mathrm{RS}_i} \cdot q_{\mathrm{RS}_i,\mathrm{R}} \right) \right\} \qquad \textbf{(5.5)}$$

Since $q_{\mathrm{T,RS}_i}$ with $i \in \{1,2,3,7,8,9\}$ and with i=4 may be very low due to the NLOS propagation loss and long-distance path loss, respectively, Eq. (5.5) can be approximated as

$$PDR_{\mathrm{R}} \approx p_{\mathrm{T,R}} + (1 - p_{\mathrm{T,R}}) \left\{ 1 - \prod_{i=5}^{6} \left(1 - q_{\mathrm{T,RS}_i} \cdot \xi_{\mathrm{RS}_i} \cdot q_{\mathrm{RS}_i,\mathrm{R}} \right) \right\} \qquad \textbf{(5.6)}$$

Furthermore, if R-VS is at the location of R-VS1, which is NLOS to T-VS as shown in Fig. 5.1, the PDR by direct path is poor ($p_{\mathrm{T,R}} \approx 0$). Since R-VS1 is also in NLOS condition to RS6, $q_{\mathrm{RS}_6,\mathrm{R}}$ is low ($q_{\mathrm{RS}_6,\mathrm{R}} \approx 0$). Then the PDR by relay-assist from T-VS to R-VS1 mainly depends on performance of RS5, which is in LOS to both T-VS and R-VS1. Similarly, for the case that R-VS is at the location of R-VS2 (Fig. 5.1), the PDR from T-VS to R-VS2 mainly depends on RS6. In such a way, the RS diversity effect is obtained. In order to fully achieve the benefit of the diversity effect, it is necessary to set the coverage area of two adjacent RSs to overlap with each other. However, large coverage area of RSs leads to the increase in air traffic by relay, and may affect the performance of V2V communications. We will discuss about the effect of overlapping rate in Section 5.4.

5.3 Effect of High Data Rate for V2V Communications

One question arises here that how to deal with the congestion issue, not only at RSs but also in V2V communications. There are many previous works dealing with the channel congestion problem in vehicular communications. In [72], the authors proposed an adaptive message rate algorithm called LIMERIC to maximize channel throughput through distributed message-rate control. The proposed method adaptively adjusts message rates or T_{f} to keep the channel load at or below a target level. CBR (Channel

Busy Ratio), which is defined as the proportion of time that the channel is sensed as busy, is employed as the channel load metric. Other congestion and awareness control protocols such as PULSAR [73], INTERN [74] adapt the transmission parameters based on the channel load levels measured by means of the CBR.

Another approach in reducing CBR is making use of higher data rates. It is generally assumed that the default modulation/data rate for periodic message dissemination in V2V communications is IEEE 802.11p QPSK/6 Mbps. In [40], the authors showed that the 6 Mbps data rate results in the highest PDR performance except when the channel is either slightly loaded or saturated. The PHY layer of IEEE 802.11p defines 8 data rates (ranging from 3 to 27Mbps) that can be dynamically selected on a per packet basis. However, there is a trade-off when using higher data rates. High data rates reduce the packet duration and hence CBR becomes lower. In addition, since the packet length is shortened, the overlapping probability among V2V packets decreases. This may result in reducing HT problem. Fig. 5.4 shows the effectiveness of high data rates in reducing the overlapping probability, which is calculated by Eq. (5.2). Higher data rates result in lower overlapping probability. The effectiveness has tendency to become saturated as the data rate increases.

A drawback of high data rates is the high required CINR (refer to Table 2.4). In [41], the authors suggest that the disadvantage of high data rates can be compensated by increasing transmission power levels. Using this strategy, it is shown that 6 Mbps is not (always) the optimum data rate for beaconing in vehicular communications. However, augmenting transmit power may in turn increase the interference range. Moreover, emission power of more than 10 mW/1 MHz is not allowed in Japan [14]. Then the maximum transmit power for 10 MHz bandwidth is limited by 20 dBm.

Another approach to overcome the drawback of using high data rates is to employ sectorized receiving RSs. The decrease in communication range when using high data rates can be compensated by relay-assist. Furthermore, in the event of packet collisions, the high required CINR can be covered by the sectorized receiving scheme. Hence, the benefit of employing high data rate can be fully obtained by the SR-V2VC/PCRL scheme. In this chapter, the effectiveness of using high data rate in high channel load conditions is studied.

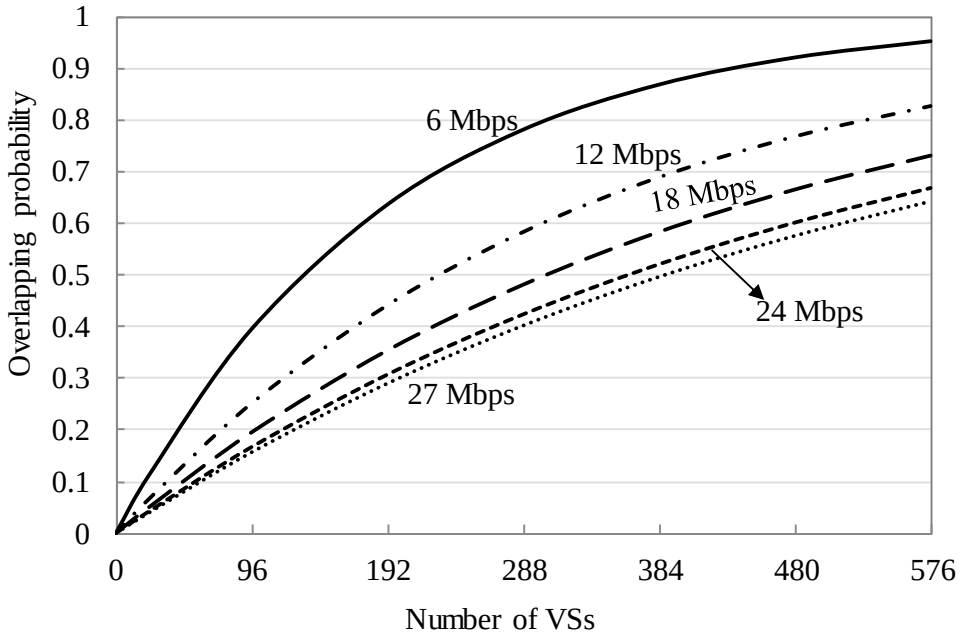

Fig. 5.4: Effectiveness of high data rate in reducing overlapping probability

(Payload data size; 100 bytes, T_f = 100 ms)

5.4 Evaluation by Simulations

5.4.1 Node Layout Model and Simulation Set Up

In order to evaluate performance of the SR-V2VC/PCRL scheme, computer simulations using Scenargie network simulator [56] were conducted. Fig. 5.5 shows the road layout with nine intersections and the corresponding horizontal and vertical roads. The inter-RS distance d_{RS} is set to 300 m. Each road has 1200 m length and 20 m width. All VSs are uniformly distributed on the roads with the distance of 25 m between two adjacent VSs in a lane (vehicle density is 40 VSs /km·lane). If the numbers of lanes are 2 and 4, the vehicle densities are 80 VSs /km and 160 VSs/km, and the total numbers of VSs in the simulation area are 588 and 1176, respectively.

Three V2V schemes of D-V2VC, OR-V2VC/PCRL and SR-V2VC/PCRL are compared in terms of BPDR and average information delivery delay. The BPDR is calculated for R-VSs in the evaluation area of interest shown by highlighted in blue-

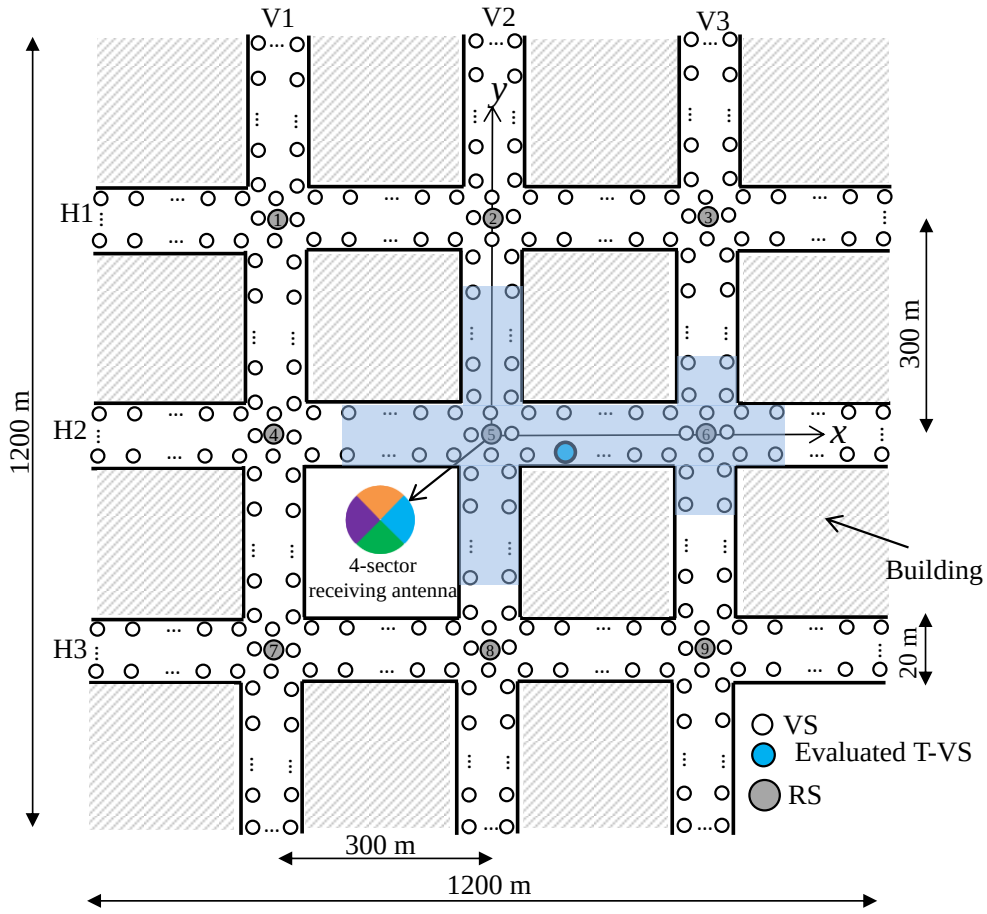

Fig. 5.5: Node layout model

color. T-VS of interest is located on the horizontal road H2, same as the analysis in the previous section. The information delivery delay is defined as how long does it take to receive the latest information correctly from the T-VS of interest at an R-VS. This is important from the point of view of a safety support application which may be tracking the behaviors of surrounding VSs to identify any abnormal situations. The average delivery delay is then calculated for all R-VSs in the evaluation area. Note that the delivery delay does not simply indicate the delay of a single packet transmission, but includes latency originated by MAC layer contention, PHY packet transmission, and repeated transmissions. Ideally, if the R-VS can receive every packet from T-VS, the information delivery delay can be as short as 10 ms, the duration of MAC service time under moderate traffic conditions [75].

One RS equipped with four sectorized receiving antenna is installed at the center of

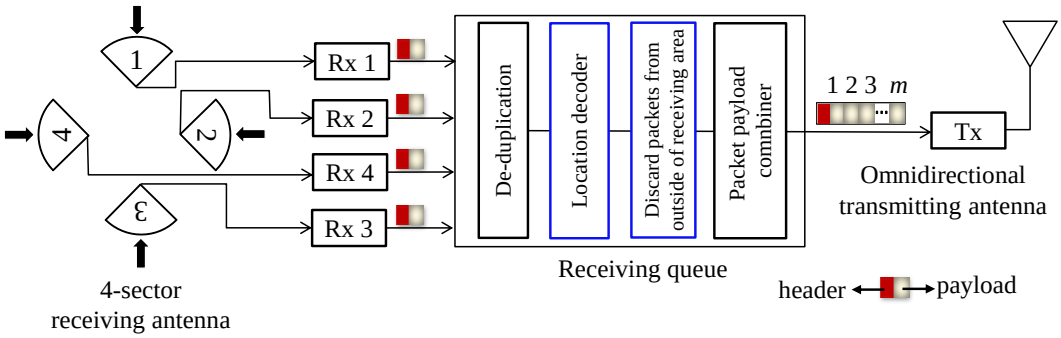

Fig. 5.6: Block diagram of RS for SR-V2VC/PCRL scheme in urban scenarios

each intersection. The configuration of the sector antenna is the same to the previous chapter. The values of FBR and FSR are set to 20 dB. The origin of *xy*-plane is set at RS5. Unless otherwise stated, we set covering area of each RS as a circle with the center at the RS and the radius of 225 m. The block diagram of a RS in a four-corner intersection environment is shown in Fig. 5.6. By decoding location information included in V2V packets, the RS calculates the distance to the sender of the packets and discards those coming from the outside of its covering area. In addition, relayed packets from the other RSs are also ignored.

The radio transmission parameters and traffic conditions for V2V communications are the same as those in Table 3.1 and 3.2. Unless otherwise stated, QPSK/6 Mbps and 16QAM/12 Mbps are employed for V2V and relaying transmission, respectively.

5.4.2 Simulation Results

5.4.2.1 PRR at RS and BPDR Performance

First, we study the effect of the sectorized receiving scheme in mitigating HT problem in urban environments. Fig. 5.7 shows the PRR at RSs when the ORA and SRA are employed. The vehicle density is set to 80 VSs/km. It can be seen from the figure that effectiveness of the sectorized scheme in mitigating HT problem keeps high in urban environments with multiple interferences sources from VSs and RSs. The areas that the PRR is higher than 90 % have the total of less than 450 m length for the omnidirectional scheme, while those for the sectorized scheme have more than 1000 m length.

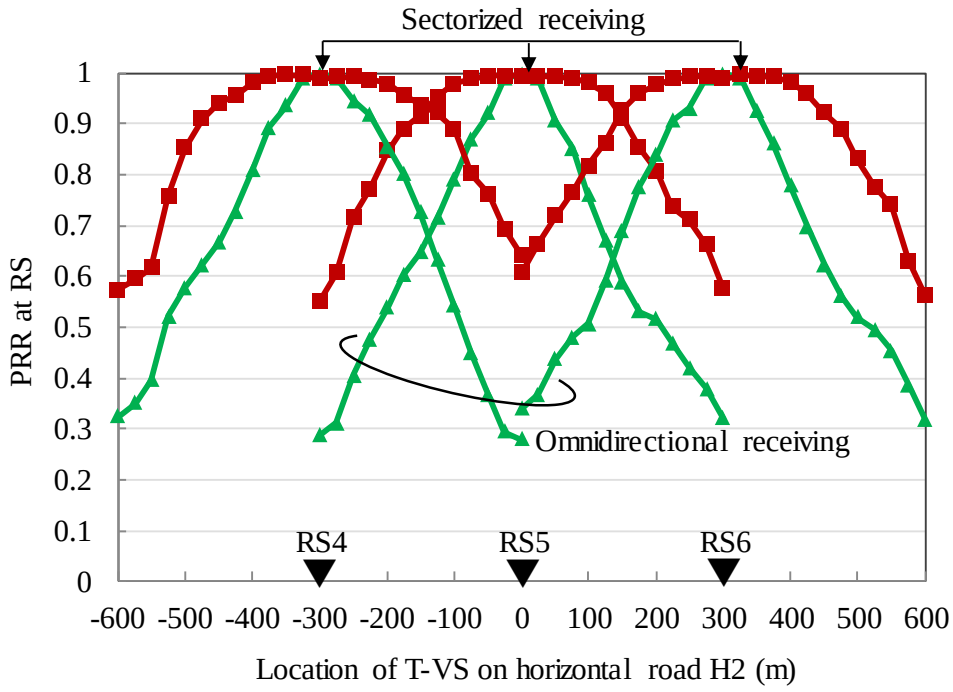

Fig. 5.7: PRR at RSs

(Vehicle density; 80 VSs/km)

Especially, when T-VS locates between two sectorized RSs, the PRR at the nearer RS is always higher than 92 %. This may result in high RS diversity effect.

Fig. 5.8 shows the BPDR performance of the three V2V schemes for the same vehicle density. When T-VS locates near RS5 and the intersection center, most R-VSs in the evaluation area are in LOS to T-VS, and thus the BPDRs are high for the three V2V schemes. Without relay-assist, BPDR is around 90 %. It is further improved to around 98 % by using RSs. This comes from the effect of relay-assist in compensating attenuation loss and fading. When the distance of T-VS from RS5 increases, BPDR of D-V2VC scheme significantly decreases. It is down to around 70 % for T-VS at the intermediate point, 150 m away from RS5. This is mainly because of shadowing, which degrades the BPDR from T-VS to NLOS R-VSs on the vertical roads. OR-RA-V2VC/PCRL scheme compensates the shadowing loss, and improves the reliability of V2V communications. BPDR of the scheme at the intermediate point is improved 14 %

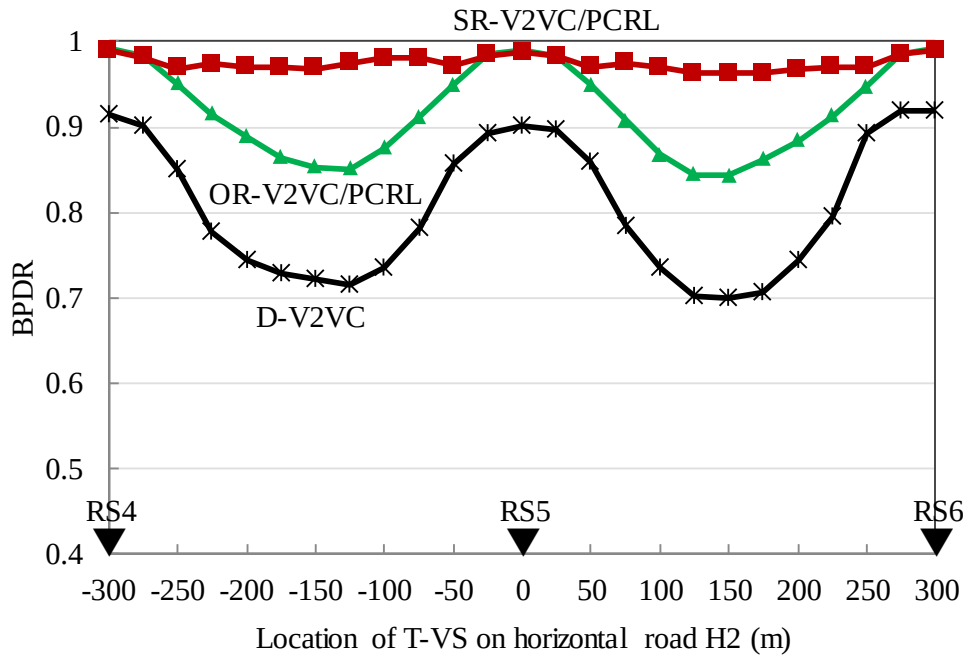

Fig. 5.8: Performance of SR-V2VC/PCRL scheme

(Vehicle density; 80 VSs/km)

by the scheme. However, the scheme till suffers from HT problem at RSs, and thus does not perform well when T-VS moves far from the RSs. The proposed SR-V2VC/PCRL scheme further mitigates the effect of HT problem, highly achieves RS diversity effect, and then remarkably improves the BPDR performance. BPDR of the scheme is higher than 96 % for all locations of T-VS. This shows the effectiveness of the scheme in urban environments with multiple RSs/intersections scenario.

Fig. 5.9 shows the BPDRs of the SR-V2VC/PCRL scheme for four cases of covering radius by each RS. When the covering radius is set to 150 m, there is no overlap of covering area by neighboring RSs. BPDR of the scheme severely degrades at the intermediate point. This is because the RS diversity effect cannot be obtained in this case. When the covering radius is set to 225 m, the areas around the intermediate points are covered by two RSs, and BPDR of the scheme is improved around 10 % than the case of 150 m. The gain comes from the RS diversity effect.

When the covering radius is set to 300 m, all the areas are covered by two RSs. However, the BPDR is almost the same to that when the covering radius is 225 m. When we do not restrict the covering area of RSs, the BPDR slightly decreases. This

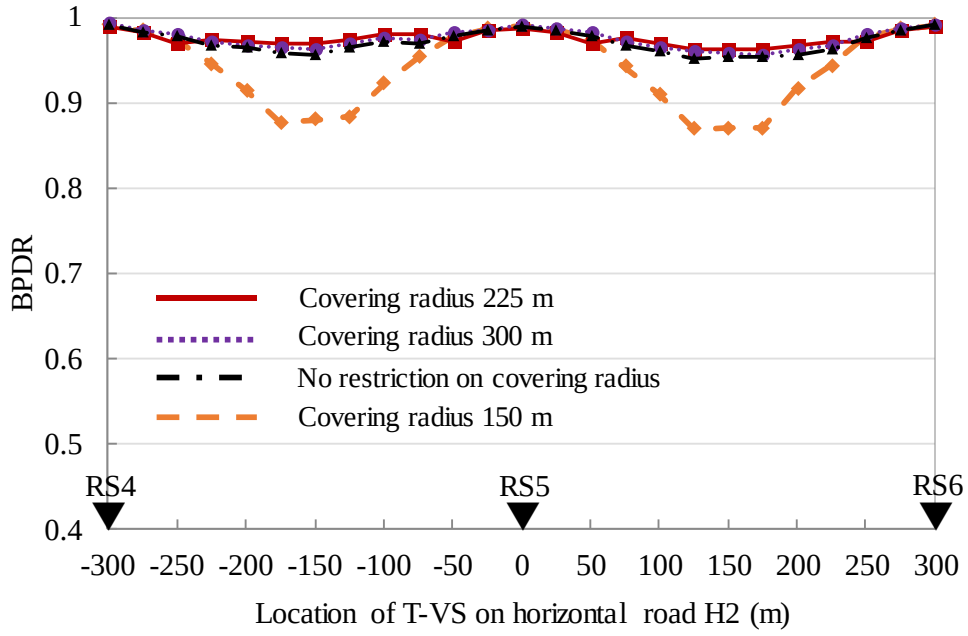

Fig. 5.9: Effect of covering radius at RSs

(Vehicle density; 80 VSs/km)

shows that it is necessary to set the coverage area at RSs to reduce relaying traffic.

5.4.2.2 Performance Under Higher Vehicle Density

In this subsection, we consider the case when the number of VSs is doubled, i.e., the vehicle density is 160 VSs/km. Fig 5.10 shows the effect of covering radius at RSs for SR-V2VC/PCRL scheme. Same to the previous subsection, no RS diversity can be obtained when the covering radius is set to 150 m, and thus the BPDR at the intermediate point drops. When the covering radius is set to 225 m, BPDR at the intermediate point is improved around 8 % than the case of 150 m owing to the RS diversity effect.

When covering radius is set to 300 m, the packet congestion happens at RS that degrades the performance of the proposed scheme. The BPDR of this case is lower than that of the case of 225 m for all locations of T-VS. The degradation is more significant when we do not restrict the coverage area of RSs. From the above observations, the radius of covering area of each RS is set to 225 m hereafter to obtain the largest diversity gain as well as reduce the air traffic by relay.

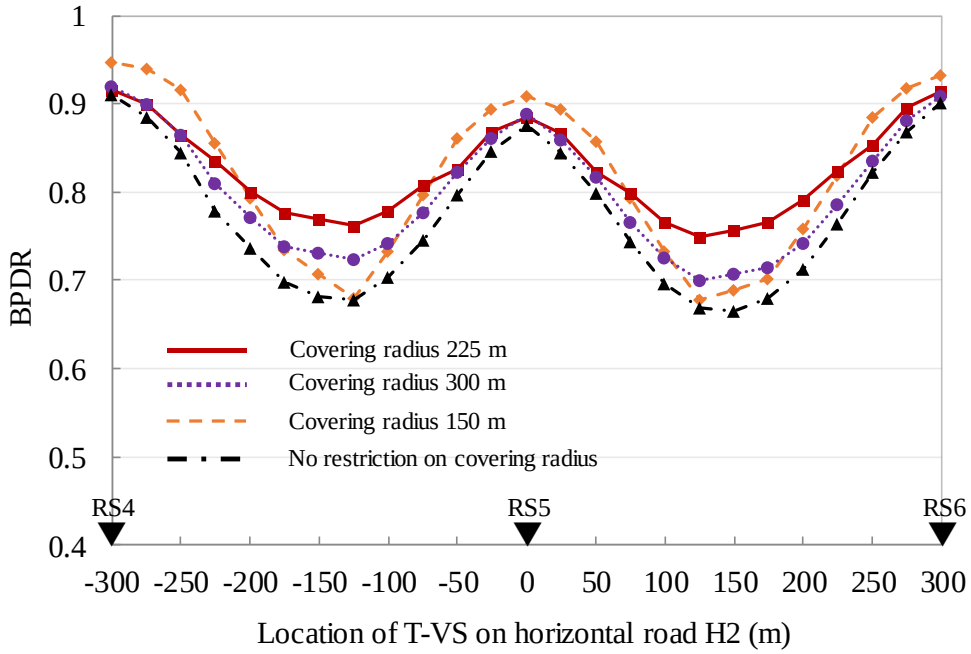

Fig. 5.10: Effect of covering radius at RSs under higher traffic conditions

(Vehicle density; 160 VSs/km)

Next, we investigate the effect of high data rates under high traffic load conditions. Fig. 5.11 shows the BPDR of D-V2VC scheme when the vehicle density is doubled from the previous subsection. Three cases of data rates of 6 Mbps, 12 Mbps and 18 Mbps are considered. Comparing Fig. 5.8 and 5.11, it can be seen that performance of D-V2VC scheme degrades as the traffic increases. This is due to the increase in number of HTs. By employing the higher data rate of 12 Mbps, the decrease in the overlapping probability results in reducing the number of HTs. Hence, BPDR increases, especially when T-VS locates around the intermediate point, where transmission from the T-VS of interest to R-VSs in its evaluation area suffers from HT problem at most.

When the data rate is set to 18 Mbps or higher, the higher receiving sensitivity leads to the decrease in communication range. As a result, the BPDR for the case of 18 Mbps is lowest among the three cases of data rates.

Fig. 5.12 shows the BPDR of SR-V2VC/PCRL scheme for the same vehicle density. BPDR of D-V2VC scheme for the data rates of 12 Mbps is also presented for reference. When the V2V data rate is set to the default 6 Mbps, although the SR-V2VC/PCRL

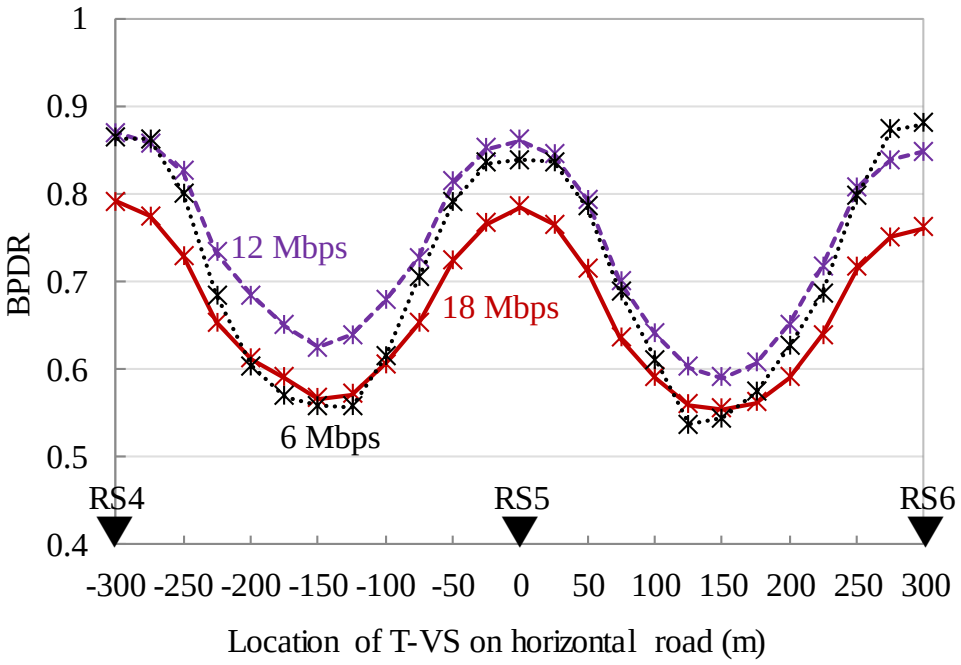

Fig. 5.11: Effect of employing high data rates for direct V2V communications

(Vehicle density; 160 VSs/km)

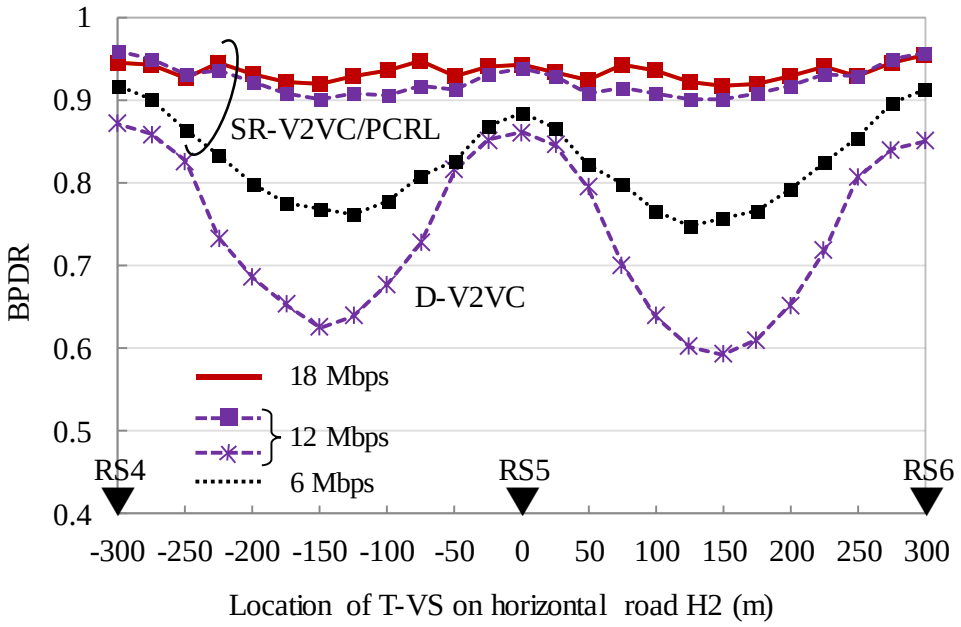

Fig. 5.12: Effect of high data rates in relay-assisted V2V communications

(Vehicle density; 160 VSs/km)

scheme improves the BPDR, it still lower than 80 % at the intermediate point. This is due to the packet congestion issue that causes packet drop at RSs, and thus limits the improvement by relay-assist. When the V2V data rate is set to 12 Mbps, the packet length of a V2V packet is shortened from 264 μs to 152 μs that reduces the channel busy ratio. As a result, the congestion issue is alleviated and the BPDR is higher than 90 % regardless of T-VS locations. This value of BPDR indicates that every R-VS in the evaluation of T-VS can receive packets from T-VS after two times of transmissions with the probability of higher than 99 %.

When the data rate of 18 Mbps is employed for V2V and relaying transmissions, since the high required CINR can be compensated by relay-assist, the BPDR is even improved. It is higher than 92 % for all locations of T-VS. This shows the effectiveness of employing high data rate for relay-assisted V2V communications.

5.4.2.3 Average Information Delivery Delay

In this section, we investigate the average information delivery delay of V2V communications. Since the delivery delay may be larger under high traffic load conditions, we study the case of vehicle density of 160 VSs/km.

For D-V2VC, there has a situation that an R-VS in the evaluation area of T-VS of interest cannot receive any packets from T-VS during a simulation run due to the effect of shadowing. In such a case, we ignore the R-VS in th calculation of the average delivery delay. Fig. 5.13 shows the average delivery delay for D-V2VC and SR-V2VC/PCRL. Two data rates of 6 Mbps and 12 Mbps are considered for V2V transmission. For SR-V2VC/PCRL, the covering radius is set to 225 m. Without relay-assist, the average delivery delay is as small as 25 ms when T-VS locates around the intersection, but it rapidly increases as T-VS moves far from the intersection center. When T-VS is at the intermediate point, the average delivery delay is larger than 120 ms for the data rate of 6 Mbps. This is due to the drop in BPDR as shown in Fig. 5. 11. If BPDR is low, R-VSs in the evaluation area may often fail to get updated the latest mobility information from T-VS every transmission frame, T_f. It means that the R-VSs have to wait for the following packets from the T-VS with the same or correlated information, resulting in the increase in delivery delay. Employing the higher data rate

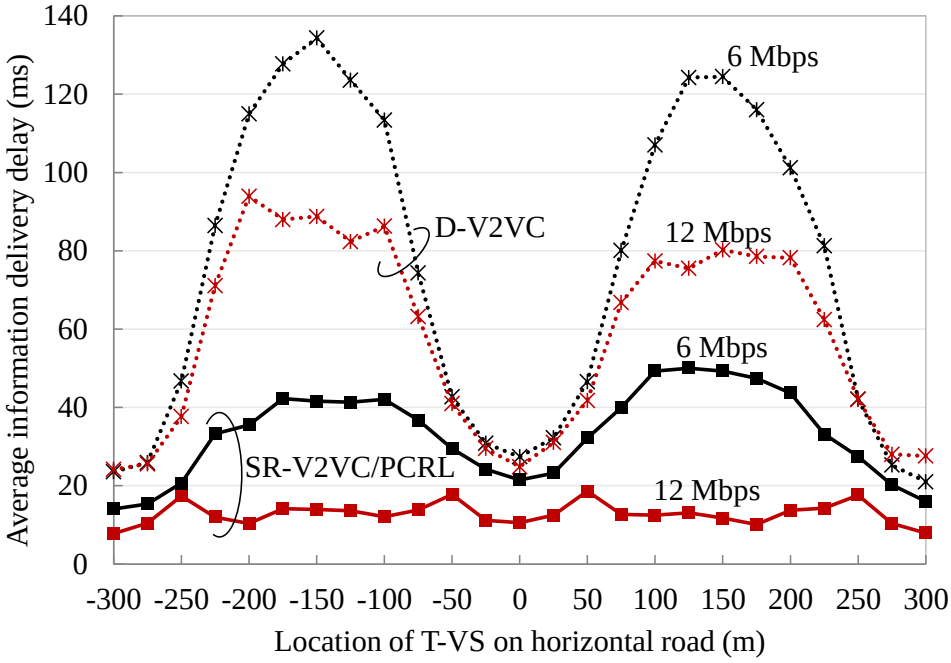

Fig. 5.13: Average delivery delay of V2V communications

(Vehicle density; 160 VSs/km)

of 12 Mbps improves the BPDR, and hence reduce the average delivery delay at the intermediate point to around 80 ms.

The proposed SR-V2VC/PCRL scheme improves BPDR of V2V communications (Fig. 5.12), and then shorten the delivery delay. The average delivery delay for the case of 6 Mbps is reduced to below 50 ms for all locations of T-VS. When 12 Mbps is employed for V2V transmissions, The average delay is even reduced to below 20 ms. This shows the effectiveness of the relay-assisted scheme in reducing the delivery delay.

5.5 Chapter Summary

In this chapter, PDR performance of the proposed SR-V2VC/PCRL scheme is studied considering urban environment with multiple intersections. First, effect of relaying transmissions to V2V communications is analyzed. Next, cooperation among RSs in urban scenario is discussed to obtain the largest RS diversity gain. Then, the utilization of higher data rate than the default 6 Mbps is proposed to mitigate the congestion issue

due to the increased traffic load. Finally, large-scale computer simulations are conducted to confirm the effectiveness of the proposed SR-V2VC/PCRL scheme. Based on the analytical and simulated results, the following observations can be obtained:

1) Effect of HT problem due to relaying transmissions can be remarkably alleviated by the sectorized receiving scheme.

2) By setting the coverage area of sectorized receiving RSs with an appropriate overlapping rate, the RS diversity effect can be obtained that improves the reliability of V2V communications.

3) The use of higher data rates such as 18 Mbps for V2V communications can reduce the overlapping probability and then improve the performance of V2V communications in high traffic conditions. In addition, employing high data rates results in low channel busy ratio that further mitigates the packet congestion issue at RSs. In relay-assisted V2V communications, the disadvantage of high required CINRs can be compensated and then the PDR improves.

4) Considering the maximum vehicle density of 160 VSs/km, more than 90 % of BPDR can be obtained by the proposed SR-V2VC/PCRL scheme regardless of T-VS location. It means that the probability that packets from a T-VS are successfully received at a R-VS in the communication range is higher than 99 % after two times of transmissions.

5) Effectiveness of the proposed scheme is also evaluated in terms of average information delivery delay. It is shown that the average delivery delay is reduced to below 20 ms regardless of T-VS location by SR-V2VC/PCRL scheme.

Chapter 6. Network Coding Based Payload Combining Relay Scheme

In chapter 5, it is shown that the use of high data rates such as 18 Mbps for V2V transmission under high traffic conditions can alleviate the congestion issue at RSs due to the increased air traffic. However, when traffic becomes higher, the congestion still happens at RSs. The utilization of even higher data rates such as 24 Mbps is no longer an effective solution because the higher required CINR cannot be compensated by relay-assist. In this chapter, an NC based PCRL scheme with a payload sorting and selection algorithm is proposed to further improve the congestion issue at RSs. Large-scale computer simulations considering urban intersections scenario with 6 lanes are conducted to evaluate the PDR performance of the scheme. Simulated results show that the proposed scheme can further enhance the improvement brought by relay-assist.

6.1 Introduction

Dealing with congestion issue is an important challenge in vehicular communications. The effect of employing high data rates for V2V and relay transmissions has been proposed as a solution to reduce the collision probability as well as lower the CBR of the channel that, at the same time, further alleviates the congestion issue at RSs due to the increased air traffic. However, as the traffic load becomes higher, the congestion issue may still happen at RSs. The utilization of even higher data rates such as 24 Mbps is no longer an effective solution because the high required CINR of the high-order modulation cannot be compensated by relay-assist. In addition, the effectiveness in reducing collision probability and CBR becomes saturated with the increased data rate

(refer to Fig. 5.4). Other traffic congestion avoidance method is thus needed to further mitigate the congestion issue at RSs.

Using NC is considered as an effective solution to reduce CBR. As one application of NC in vehicular communications, a cooperative content downloading scheme using vehicle-to-infrastructure (V2I) communications has been proposed [76]-[77]. A few works have exploited the benefit of NC to safety related beaconing using V2VC [21]. In [21], a packet loss recovery scheme using NC is proposed, and it is shown to be effective in a highway scenario. For the intersection environments, an NC based scheme that uses the *intersection vehicle* to encode and re-broadcast all its received beacon messages is proposed [78]. It is shown that total retransmission time as well as the number of rebroadcast slots can be reduced by the scheme. However, it is not guaranteed that PDR can be considerably improved, especially in multiple node environment. In [79], the authors have proposed a relay-assisted V2V scheme using NC to compress relaying traffic considering intersection scenario. In the scheme, two native V2V packet payloads are encoded by XOR operation to generate a coded packet, which is rebroadcasted by the RS to all vehicles. At a receiver, the relayed packet can be successfully decoded if one of the two original V2V payloads has been already received by the direct path. In order to improve the successful decoding probability (SDP), the scheme selects the two original packets which the transmitters are from horizontal and vertical streets. Since the receiver locates on the same street with either of the transmitters, the probability that the receiver receives at least one of the two original packets increases. Although the number of relaying packets that RS has to transmit is halved, the improvement brought by the scheme is insufficient.

The proposed PCRL scheme can forward up to a maximum number of K=14 V2V payloads in a transmission chance, and thus effectively mitigate the congestion issue at RS. In this chapter, a NC based PCRL scheme is proposed to compress relaying traffic and further mitigate the congestion issue at RS. In addition, in order to minimize the disadvantage while obtaining the benefit of NC, a payload sorting and selection algorithm is presented considering intersection scenarios. Large-scale computer simulations are conducted to confirm the effectiveness of the proposed scheme. It is shown that the joint use of the NC based PCRL and the sectorized receiving scheme (SR-V2VC/PCRL-NC) can further enhance the improvement brought by relay-assist.

6.2 SR-V2VC/PCRL-NC Scheme

6.2.1 Operational Principle

In the normal PCRL scheme, RS stores the received V2V payloads in a single queue and concatenates payloads to generate a relaying packet as shown in Fig. 6.1(a). The payload concatenation is initiated once the number of payloads in the queue reaches the predetermined number K or the waiting time of one of the payloads reaches the predetermined time $T_{\max}$.

Fig. 6.1(b) shows the operation of RS in the proposed PCRL-NC scheme. RS has G queues and stores each received payload in one of the queues. For example, G can be set as the number of streets at the intersection where RS is located. In this case, the payloads received from T-VSs on the different streets are stored in different queues. Upon the initiation of the payload concatenation process, RS selects G payloads from the queues and creates (G-1) distinct pairs. We will discuss about the payload selection in detail in the Section 6.2.3. Next, each payload pair is encoded by XOR operation to generate a network coded payload. For example, if G=4 and the three selected pairs are (A, B), (B, C) and (C, D), the corresponding network coded payloads are A⊕B, B⊕C and C⊕D, respectively where ⊕ denotes the bitwise XOR operation. Hereafter, let us denote the set of (G-1) network coded payloads by *NC payload block*. Defining $J_{\min}=\min_{1\le i\le G}(|Q_i|)$ with $|Q|$ being the size of queue Q, the pairing and encoding processes are carried out for $G\times J_{\min}$ original payloads to generate $J_{\min}$ NC payload blocks. The number of concatenated payloads k_{NC} for PCRL-NC scheme is given by

$$k_{\mathrm{NC}} = (G-1)\times J_{\min} + \sum_{i=1}^{G}\left(\left\lfloor \mathrm{Q}_i \right\rfloor - J_{\min}\right) \qquad \textbf{(6.1)}$$

The payload concatenation process is initiated once k_{NC} reaches K or $T_{\max}$ counts up. Here, $\lfloor x \rfloor$ is the largest integer less than or equal to x.

The payload of a relaying packet consists of (G-1)×$J_{\min}$ network coded payloads and $\{k_{\mathrm{NC}}-(G-1)\times J_{\min}\}$ normal payloads. The normal payloads are arbitrarily selected from the remaining payloads after selecting the payloads for network coding in the queues. Note that in the scenario of low traffic condition or extremely unbalanced vehicle distribution among streets, $J_{\min}$ may become 0. In that case, the proposed PCRL-NC

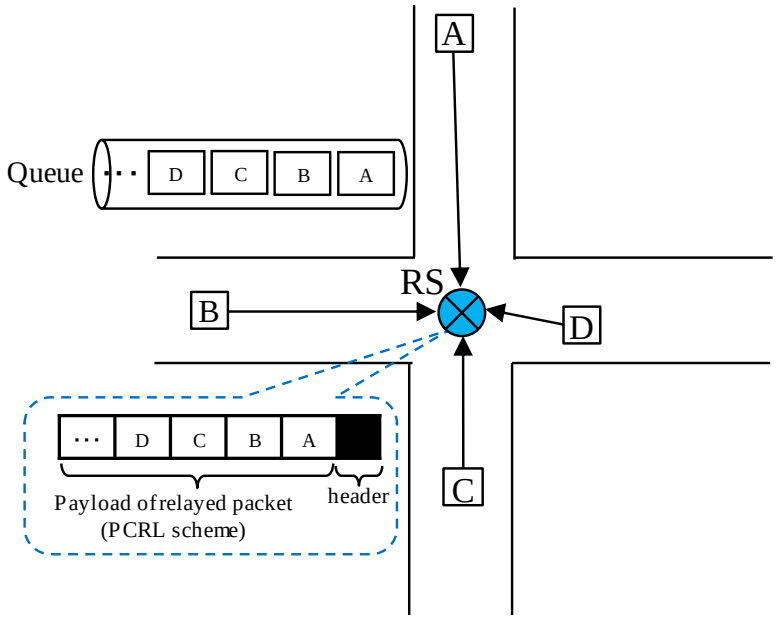

(a) PCRL scheme

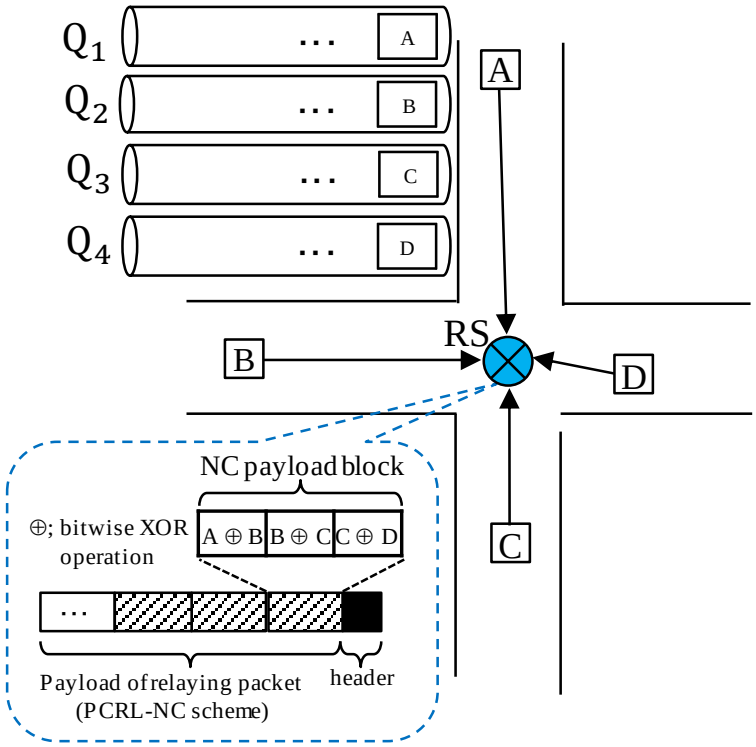

(b) PCRL-NC scheme

Fig. 6.1: PCRL schemes with and without NC

scheme degenerates to the conventional PCRL scheme. The header of the relaying packet needs to contain the values of $J_{\min}$ and G so that R-VSs can determine the number of NC payload blocks in each relaying packet. R-VS first retrieves the values in the header of relaying packet and then decodes $J_{\min}$ NC payload blocks. All of G original payloads in each NC payload block can be successfully decoded if at least one of them has been already received by R-VS via the direct communication.

6.2.2 Effect of PCRL-NC Scheme in Mitigating Congestion Issue and Reducing CBR

The proposed PCRL-NC scheme can forward up to (K+$J_{\min}$) V2V payloads in a transmission opportunity, and thus may improve the transmission rate at RS under high traffic load conditions. While K is determined by the V2V payload size and restriction on IEEE 802.11p frame size, the maximum value of $J_{\min}$ depends on G. For instance, the largest $J_{\min}$ is equal to K for G=2, and a maximum number of 2K payloads can be sent out in a transmission by PCRL-NC scheme. Even in moderate or low traffic conditions, packet collision can be mitigated by the proposed scheme by reducing air traffic. Fig. 6.2 shows the effectiveness of the PCRL-NC scheme in shortening the duration of relaying packets. It can be seen from the figure that the length of relayed packets is remarkably shortened by PCRL-NC. The packet duration is almost halved when G=2. When G=4, the packet length is reduced to 77 %.

6.2.3 Payload Sorting and Selection Algorithm

Let p_g ($1 \le g \le G$) denote the PDR of the original packet payloads at typical R-VS. If none of the original packet payloads within the NC payload block has been successfully received, decoding failure happens. Thus, SDP of the NC payload block at R-VS is defined as

$$\text{SDP} = 1 - \prod_{g=1}^{G} \left(1 - p_g\right) \qquad \textbf{(6.2)}$$

Considering the street-based grouping method, one possible situation that decoding failure happens is when an NC payload block solely is composed of the payloads

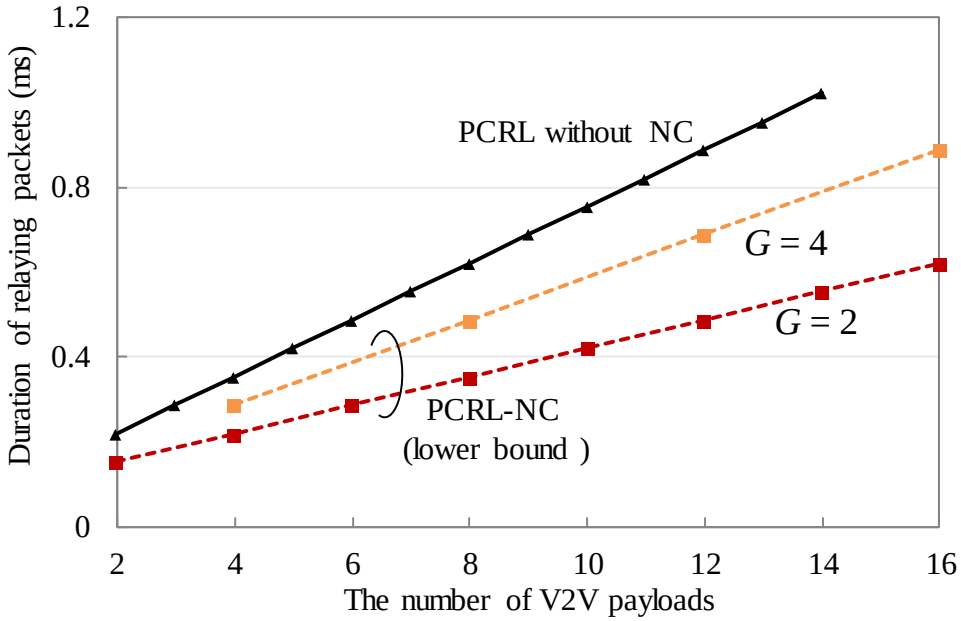

Fig. 6.2: Effectiveness of PCRL-NC scheme in reducing packet length

(Data rate; 12 Mbps, V2V payload size; 100 bytes)

transmitted from T-VSs that are far from the R-VS. In such a situation, the successful reception rate of the direct link is quite low and hence the SDP becomes low. In order to avoid such a situation, we propose a sorting algorithm of payloads in each queue at RS. The sorting can be performed based on the distance between RS and the T-VS of each payload. The sorting order is alternated at certain interval to avoid unbalanced situation. As a result, the probability that all of T-VSs are far from specific R-VS becomes much lower.

6.3 Evaluation by Simulations

6.3.1 Node layout and simulation set up

In this section, the joint use of the proposed PCRL-NC and the sectorized receiving scheme, i.e. SR-V2VC/PCRL-NC, is evaluated using computer simulations. We consider the same an urban environment as shown in Fig. 5.5. There cases of vehicle density of 80 VSs/km, 160 VSs/km and 240 VSs/km are considered. The number of

lanes is set to 2, 4 and 6, respectively. Three V2V schemes of D-V2VC, SR-V2VC/PCRL and SR-V2VC/PCRL-NC are compared in terms of the BPDR. The communication range is set to 250 m, same as the previous chapter.

One RS equipped with four sectorized receiving antenna is installed at the center of each intersection. The configuration of the sector antenna is the same to the previous chapter. The radius of covering area of each RS is set to 225 m. The RS first decides the grouping method and the value of *G*. Then, it creates *G* queue for storing the received packets. In this chapter, the street-based grouping method [52] is considered, and G is equal to 4. The maximum number of payloads in one relaying packet is set to K =14. Thus, the proposed PCRL-NC scheme can forward up to 18 V2V payloads in a single transmission opportunity, which is 28 % higher than the PCRL scheme without NC. Fig. 6.3 shows the block diagram of the RS for a four-corner intersection environment.

The radio transmission parameters and traffic conditions for V2V communications are the same as those in Table 3.1 and 3.2. As an observation from the previous chapter, the data rate of 18 Mbps are employed for both V2V and relay transmission.

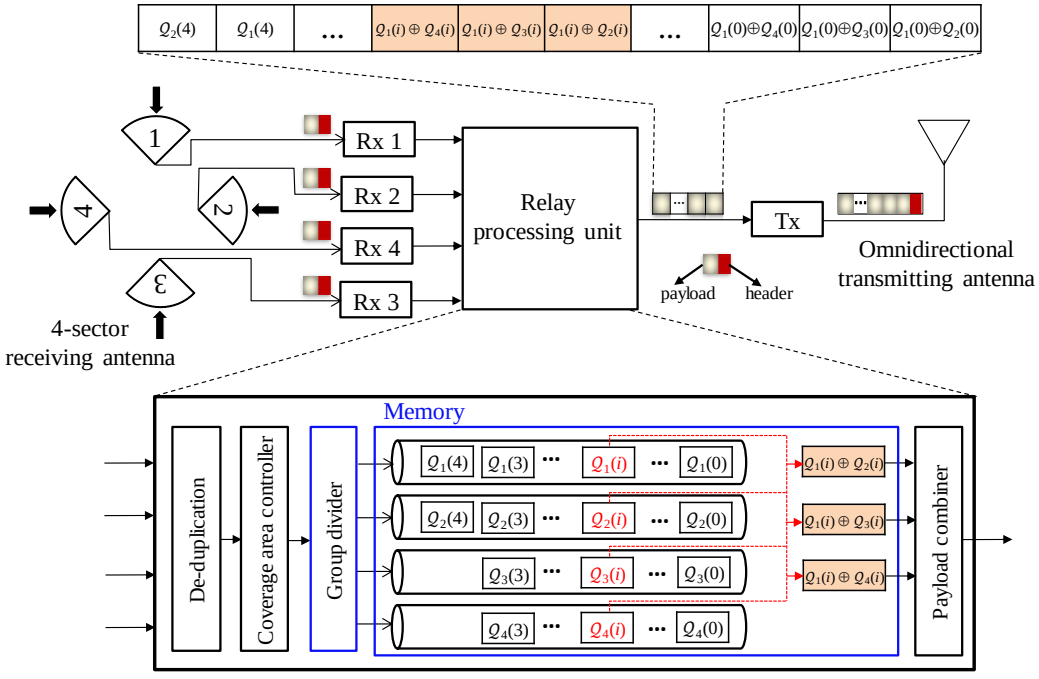

Fig. 6.3: Block diagram of RS for SR-V2VC/PCRL-NC scheme (G=4)

6.3.2 Packet Transmission Rate at RS

Fig. 6.4 shows the packet transmission rate at RS for PCRL schemes with and without NC. From the result obtained in Chapter 5, the data rate for V2V transmission is set to 6 Mbps, 12 Mbps and 18 Mbps for the three cases of vehicle density of 80 VSs/km, 160 VSs/km and 240 VSs/km, respectively. The transmission rate is 100 % for the lowest density of 80 VSs/km, i.e. packet congestion issue at RS can be effectively alleviated by PCRL schemes. As the vehicle density becomes higher, the congestion issue occurs and the transmission rate for PCRL scheme without NC decreases. It is around 92 % when the density is 160 VSs/km, and even drops below 60 % when the density is 240 VSs/km. The packet transmission rate is improved by employing NC. The transmission rate for PCRL-NC scheme is kept as high as 100 % for the vehicle density of 160 VSs/km, and 88 % for the highest density case. This shows the effect of PCRL-NC scheme in mitigating the congestion issue at RS.

From the next subsection, we investigate the effect of the proposed SR-V2VC/PCRL-NS scheme considering the most severe traffic condition of vehicle density of 240 VSs/km.

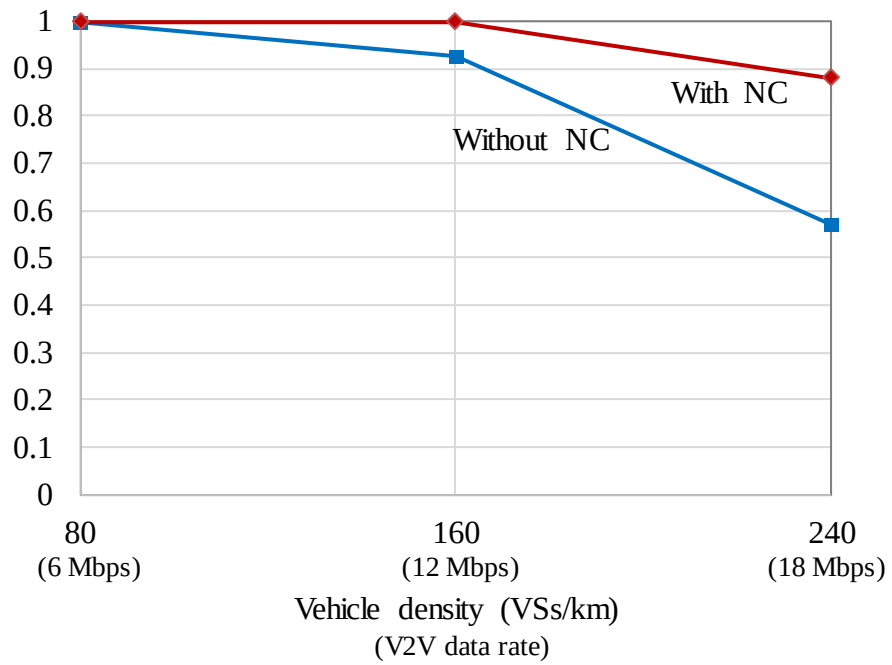

Fig. 6.4: Packet transmission rate at RS for PCRL schemes with and without NC

6.3.3 Average SDP

Fig. 6.5 shows the average SDP of the NC payload blocks transmitted from RS5 when R-VS is on the horizontal street. When R-VS is located near the intersection center (and RS5), the reception rates of original packet payloads at R-VS via direct communications are relatively high. Furthermore, since the R-VS only needs one of the original payloads for decoding an NC block, highly diversity gain can be obtained among the direct links. Thus, the average SDP is kept to be high. However, without the sorting algorithm at RS, decoding failure happens when all the T-VSs of the original payloads are far from R-VS. Hence, the SDP slightly decreases. The bad situation is reduced by the sorting algorithm, and thus the average SDP improves and keeps higher than 99 % for an area of R-VS of ±225 m range.

When R-VS is located far from RS5, the probability that R-VS can directly receive the original payloads from T-VSs on the streets other than the segment street that R-VS locates is quite low due to the large propagation loss. Hence, the average SDP mainly depends on the reception rate of the original payload transmitted from T-VS on the same segment street with R-VS. The diversity effect among the direct links becomes lower, and the average SDP decreases as R-VS moves away from RS5. For instance, if the T-VS locates near RS5, direct transmission from T-VS to R-VS is strongly affected by attenuation loss and HT problem, and thus the reception rate of the original payload from T-VS at R-VS becomes very low. This leads to the degradation in average SDP. However, the decreasing rate is negligible when employing the sorting algorithm. This can be explained as follows. Without loss of generality, we assume that R-VS is located between RS5 and RS6. Packet transmitted from T-VS may be received and relayed by RS6. Since R-VS is near RS6, the SDP for the NC payload block from RS6 is high. By receiving and decoding the relayed packet from RS6, R-VS can obtain the payload data and use it to decode the NC payload block from RS5. The average SDP is then higher than 96 % for the sorting case regardless of R-VS location.

From these results, it is concluded that the disadvantage of NC can be effectively alleviated by the street-based grouping method and the sorting algorithm. This enables us to fully achieve the benefit of NC in reducing air traffic.

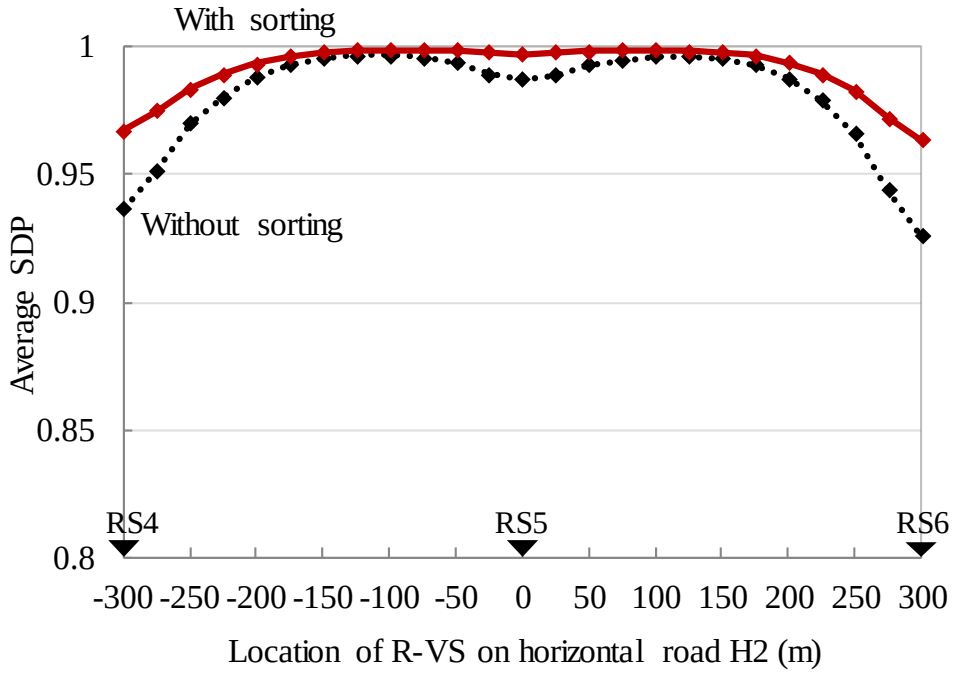

Fig. 6.5: Average SDP

(Vehicle density; 240 VSs/km)

6.3.4 BPDR Performance

Fig. 6.6 shows the BPDRs of the three V2V schemes. BPDR of D-V2VC scheme decreases when traffic becomes higher (refer to Fig. 5.10). It is around 75 % when T-VS locates near the intersection center, and drops to 54 % when T-VS is at the intermediate points, i.e. 150 m from RS5. The reliability of V2V communications is remarkably improved by the SR-V2VC/PCRL scheme, especially around the intermediate points. The BPDR of SR-V2VC/PCRL scheme is around 72 %, which is 18 % higher than that of the non-relay system. This shows the effect of SR-V2VC/PCRL under dense traffic environments. However, even the high data rate of 18 Mbps is employed, the congestion issue till happens at RSs due to the increased traffic load. We obtained from the simulations that the packet transmission rate at RS5 is only 57 %. This indicates that almost half of relaying packets created cannot be transmitted due to congestion.

The proposed SR-V2VC/PCRL-NC scheme exploits the benefit of NC to forward more V2V packets in a transmission chance, and then increases the packet transmission rate at RS5 up to 88 %. As a result, the reliability of V2V communications is further

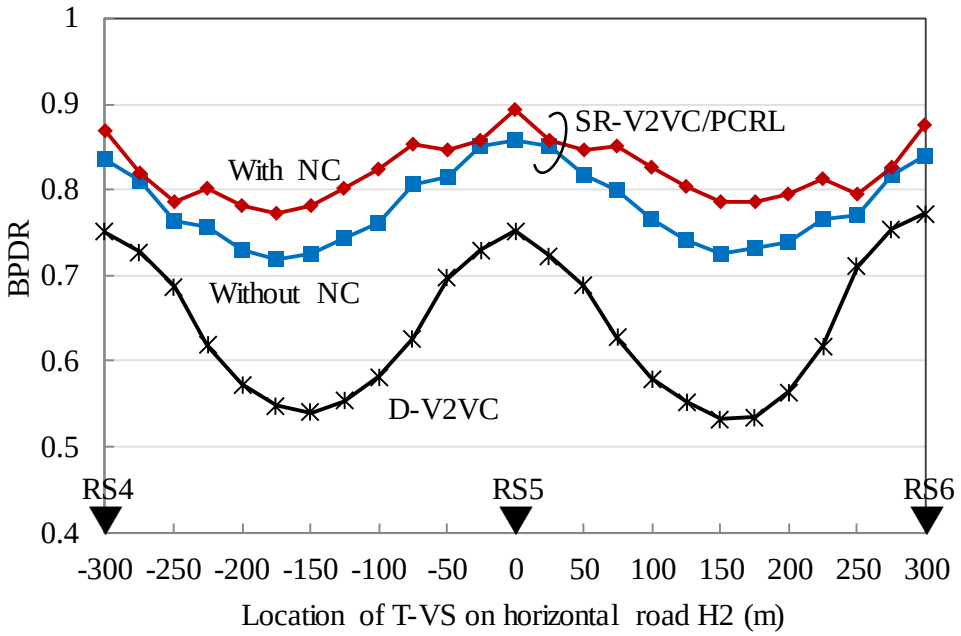

Fig. 6.6: Performance of SR-V2VC/PCRL-NC scheme

(Vehicle density; 240 VSs/km)

improved by the proposed scheme. BPDR of SR-V2VC/PCRL-NC scheme is higher than 78 % for all locations of T-VS. It is means that every R-VS in the evaluation of T-VS can receive packets from T-VS after three times of transmissions with the probability of as high as 99 %. This shows the effectiveness of the proposed scheme in mitigating the congestion issue.

6.4 Chapter Summary

In this chapter, a NC based PCRL scheme is proposed to further mitigate the packet congestion issue at RSs and improve the performance of relay-assist. The proposed PCRL-NC scheme is then introduced to the sectorized receiving scheme, i.e. SR-V2VC/PCRL-NC. Large-scale computer simulations are conducted to evaluate the BPDR performance of the proposed scheme considering urban intersections scenario. From the simulated results, the following conclusions can be obtained:

1) Effect of SR-V2VC/PCRL scheme is still remarkable under very high traffic conditions such as the vehicle density of 240 VSs/km.

2) The proposed PCRL-NC scheme can effectively mitigate the congestion issue at RS by exploiting the benefit of NC in reducing air traffic. The disadvantage of NC can be alleviated by employing an appropriate vehicle grouping method and payload sorting and selection algorithm.

3) When the vehicle density is as dense as 240 VSs/km, more than 78 % of BPDR can be obtained by the proposed SR-V2VC/PCRL-NC scheme. This indicates that the R-VSs in communication rang of a T-VS can receive packets from T-VS after three times of transmissions with the probability of as high as 99 %.

Chapter 7. Conclusions and Future Works

7.1 Conclusions

Highly reliable V2V communications is essential for safety support applications to prevent traffic accidents and for the future automated driving systems. This dissertation has focused on the utilization of roadside relay station (RS) to improve the reliability of V2V communications. Several techniques have been introduced to the relay-assisted scheme in order to achieve dependable V2V communications around intersection environments. The contributions of this dissertation are summarized as follows:

1. Proposed a packet payload combining relay (PCRL) scheme to alleviate the congestion issue at RS:
   - Effectiveness of the proposed PCRL scheme has been theoretically evaluated using an evaluation metric of packet transmission rate at RS. Computer simulations considering a single intersection scenario are also conducted to validate the analytical model as well as confirm the effectiveness of PCRL scheme. From the obtained results, it is shown that the proposed PCRL scheme can effectively remedy the congestion at RS, improve the performance of relay, and hence increase the reliability of V2V communications.

2. Introduced a HT avoidance method of sectorized receiving RS to PCRL scheme, i.e. SR-V2VC/PCRL to further improve the gain of relay-assist:
   - After describing the principle of the proposed SR-V2VC/PCRL scheme, an expression of packet reception rate at sectorized RS under multiple interference sources is derived to theoretically evaluate effectiveness of the sectorized receiving scheme in mitigating HT problem. Then the packet delivery rate

performance of the proposed SR-V2VC/PCRL scheme is studied by using a CSMA/CA collision model.

- Computer simulations considering a single intersection scenario are also conducted to evaluate the effectiveness of the scheme by using a more general metric of broadcast packet delivery rate (BPDR). It is shown that the scheme can effectively alleviate the congestion issue as well as mitigate HT problem at RS, and thus remarkably improve the reliability of V2V communications.

3. Evaluated the performance of SR-V2VC/PCRL scheme in urban environments with multiple intersections:
   - We applied the proposed SR-V2VC/PCRL to the urban scenario considering vehicle density is 160 VSs/km or lower. The obtained results show that the sectorized receiving scheme can perform well under such severe environments. In addition, by setting the coverage area between two adjacent RSs with an appropriate overlapping rate, the largest RS diversity gain can be obtained while drawback such as the congestion issue at RSs is minimized. Furthermore, the SR-V2VC/PCRL scheme even performs better when employing higher data rates than the default 6 Mbps when traffic load is high. The BPDR is higher than 90 % for all locations of transmitting vehicles.

4. Proposed a network coding (NC) based PCRL (PCRL-NC) scheme with a payload selection and sorting algorithm to further mitigate the congestion issue at RSs when traffic becomes higher:
   - The proposed scheme can benefit from network coding in reducing air traffic, and hence further mitigate the congestion issue at RS, while the disadvantage of NC is alleviated by employing a location-based grouping method and the payload selection algorithm. The proposed PCRL-NC scheme is then introduced to the sectorized receiving scheme, i.e. SR-V2VC/PCRL-NC. Simulated results show that the lowest BPDR of 64 % for the non-relay system is improved to higher than 78 % by SR-V2VC/PCRL-NC scheme when the vehicle density is as high as 240 VSs/km.

The results achieved in this dissertation constitute a fundamental contribution to the development of vehicular communications by providing a highly reliable V2V communications system under various traffic conditions. The BPDR of 90 % when the vehicle density is 160 VSs/km or lower is sufficiently high considering safety support applications. It ensures a target probability of 99 % on reliability that a transmitting vehicle can deliver its mobility information to the surrounding vehicles after two times of periodic transmissions. When the vehicle density is as high as 240 VSs/km, the target probability can be achieved after three times of transmissions. Note that the information delivery delay in this case is at most 300 ms, which is three times of the periodic transmission interval. Considering the velocity of 72 km/h, the transmitting vehicle moves only 6 m in 300 ms. This distance is shorter than the current GPS accuracy level of 10 m in urban environment. The proposed schemes in this dissertation provide an effective solution to support safety applications to reduce amount of fatalities due to traffic accidents. Note that the proposed relay-assisted V2V communication schemes require little modifications to the IEEE 802.11p protocol so that they are feasible for the future deployment.

This dissertation also contributes to the development of wireless communications for the future automated driving systems. Future information exchange applications of automated driving systems can be based on the broadcast applications of current safe driving support, and thus can benefit from the proposed relay-assisted V2V communications.

7.2 Future Works

In this dissertation, uniform vehicle distribution was considered to analyze the performance improvement by the proposed schemes. In the real world, however, unbalanced distribution is the most common scenario, especially in streets with traffic signals where vehicles have tendency to gather in front of the red lights. Although the

performance improvement by SR-V2VC/PCRL scheme in such a scenario is supposed to be high, it should be carefully investigated.

Next, the distance between two adjacent RSs is fixed at 300 m in this dissertation. For the future deployment of the proposed relay-assisted schemes, it is necessary to further evaluate the schemes in various urban intersections scenarios. In such cases, the coverage area of RSs should be adaptively controlled regarding the current traffic load. This also remains as a future study.

Considering vehicular communications for the automated driving systems, the exchanged data for automated driving may be larger in size in order to collect environmental information necessary for cooperated vehicle control. In such a case, packet congestion will become the next research topic in the area of vehicular communications. In addition, as the location measurement accuracy becomes better, lower delay and higher reliability will be required for V2V communications. Making use of MIMO (multiple-input and multiple-output) techniques could be considered as a solution to further improve the reliability as well as increase the channel capacity.

References

[1] World Health Organization, “Global status report on road safety 2015,” 2015. Available online: http://www.who.int/violence_injury_prevention/road_safety_status/2015/en/.

[2] Systematics, Cambridge, and M. D. Meyer, “Crashes vs. Congestion - What's the Cost to Society,” A Report prepared for AAA by Cambridge Systematics, 2008.

[3] Japan National Police Agency, “Traffic accidents situation,” 2016. Available online: https://www.npa.go.jp/toukei/koutuu48/toukeie.htm

[4] Ministry of Land, Infrastructure, Transport and Tourism, “Realization of Secure and Safe Traffic Society by Harmonizing Humans and Vehicles,” 2011. Available online: http://www.mlit.go.jp/jidosha/anzen/01asv/resourse/data/asv5pamphlet-e.pdf

[5] U.S. Department of Transportation, “Connected and Automated Vehicle Research in the United States,” 2014. Available online: https://www.unece.org/fileadmin/DAM/trans/events/2014/Joint_BELGIUM-UNECE_ITS/02_ITS_Nov2014_Kevin_Gay__US_DOT.pdf

[6] E. Uhlemann, “Introducing connected vehicles,” *IEEE Vehicular Technology Magazine*, vol. 10, no. 1, pp. 23-31, Feb. 2015.

[7] Federal Communications Commission, “Amendment of the commission’s rules regarding dedicated short-range communication services in the 5.850-5.925 GHz Band (5.9 GHz Band),” FCC 06-110, Tech. Rep., 2006.

[8] IEEE 802.11p, “IEEE Standard for Information Technology – Telecommunications and Information Exchange Between Systems – Local and Metropolitan Area Networks Specific requirements – Part 11: Wireless LAN Medium Access Control (MAC) and Physical Layer (PHY) Specifications-Amendment 6: Wireless Access in Vehicular Environments,” IEEE Std. IEEE 802.11p, version 2010, 2010.

[9] IEEE 1609.1, “Trial-Use Standard for Wireless Access in Vehicular Environments (WAVE) - Resource Manager,” IEEE Std. IEEE 1609.1, version 2006, 2006.

[10] IEEE 1609.2, “Trial-Use Standard for Wireless Access in Vehicular Environments (WAVE) Security Services for Applications and Management Messages,” IEEE Std. IEEE 1609.2, version 2006, 2006.

[11] IEEE 1609.3, “IEEE Trial-Use Standard for Wireless Access in Vehicular Environments (WAVE)-Networking Services,” IEEE Std. IEEE 1609.3, version 2007, 2007.

[12] IEEE 1609.4, “Trial-Use Standard for Wireless Access in Vehicular Environments (WAVE) Multi-Channel Operation,” IEEE Std. IEEE 1609.4, version 2006, 2006.

[13] ARIB Technical report TR-T20 Version 1.1, “700 MHz Band Intelligent Transport Systems Test Items and Conditions for Mobile Station Compatibility Confirmation,” Association of Radio Industries and Businesses (ARIB) Std. 2012, Japanese Standard (English translation).

[14] ARIB, “700 MHz Band Intelligent Transport Systems,” English, ARIB, STD T109-v1.2, Dec. 2013.

[15] *Study on LTE Support for Vehicle to Everything (V2X) Services*, document TR 22.885 V14.0.0, TSG SA, 3GPP, 2015.

[16] E. Uhlemann, “The United States and Europe Advances Vehicle-to-Vehicle Deployment,” *IEEE Vehicular Technology Magazine*, vol. 12, no. 2, pp. 18-22, Jun. 2017.

[17] H. Cheng and Y. Yamao, “Performance Analysis of ITS V2V Broadcast Communication Using CSMA/CA and a Roadside Relay Station at Intersections,” *J. of Inform. Process.*, vol. 21, no. 1, pp. 90-98, Jan. 2013.

[18] F. A. Tobagi and L. Kleinrock, “Packet switching in radio channels: Part II the hidden terminal problem in carrier sense multiple-access and the busy-tone solution,” *IEEE Trans. Commun.*, vol. 23, no. 12, pp. 1417-1433, Dec. 1975.

[19] J. Dai and Y. Yamao, “CSMA/CA Unicast Communication Performance under Fading Environment with Two-Dimensional Distribution of Hidden Terminal,” *IEICE Trans. Commun.*, vol. E95-B, no. 9, pp. 2708-2717, Sep. 2012.

[20] M. I. Hassan, H. L. Vu, and T. Sakurai, “Performance Analysis of the IEEE 802.11 MAC Protocol for DSRC Safety Applications,” *IEEE Trans. Veh. Tech.*, pp. 3882–3896, 2011.

[21] Z. Wang, M. Hassan, T. Moors, "Efficient Loss Recovery using Network Coding in Vehicular Safety Communication", *Proc. IEEE WCNC*, Sydney, Australia, Apr. 2010.

[22] L. Le, R. Baldessari, P. Salvador, A. Festag, and W. Zhang, “Performance Evaluation of Beacon Congestion Control Algorithms for VANETs,” *Proc. IEEE Global Telecommunications Conference*, Kathmandu, Nepal, Dec. 2011.

[23] M. Torrent-Monero, “Inter-Vehicle Communications: Achieving Safety in a Distributed Wireless Environment,” Doctoral dissertation, University Karlsruhe, Jul. 2007.

[24] R. Stanica, E. Chaput and A.-L Beylot, “Physical Carrier Sense in Vehicular Ad-Hoc Networks,” *Proc. IEEE MASS*, Valencia, Spain, 17-22 Oct. 2011.

[25] C. Sommer, D. Eckhoff, and F. Dressler, “I-VS in Cities: Signal Attenuation by Buildings and How Parked Cars Can Improve the Situation,” *IEEE Trans. Mobile. Comp.*, vol. 13, no. 8, pp. 1733–1745, 2014.

[26] S. O. Omar, et al., "'UVAR: An intersection UAV-assisted VANET routing protocol," *Proc. IEEE WCNC*, Doha, Qatar, 2016.

[27] ETSI EN 302 637-2 V1.3.2, *Intelligent Transport Systems (ITS); Vehicular Communications; Basic Set of Applications; Part 2: Specification of Cooperative Awareness Basic Service*, Nov. 2014.

[28] ETSI EN 302 637-3 V1.2.2, *Intelligent Transport Systems (ITS); Vehicular Communications; Basic Set of Applications; Part 3: Specification of Decentralized Environmental Notification Basic Service*, Nov. 2014.

[29] G. Karagiannis, et. al, "Vehicular Networking: A Survey and Tutorial on Requirements, Architectures, Challenges, Standards and Solutions," *IEEE Communications Surveys & Tutorials*, vol.13, no.4, pp.584-616, Fourth Quarter 2011.

[30] Ministry of Internal Affairs and Communications, "Report of Technical Committee on the Enhancement of ITS Radio Communication System," Jun. 2009.

[31] Qing Xu, T. Mak, Jeff Ko and R. Sengupta, "Vehicle-to-vehicle Safety Messaging in DSRC," *Proc. the 1st ACM international workshop on Vehicular ad hoc networks*, pp. 19-28, 2004.

[32] U.S. Department of Transportation, *Vehicle Safety Communications Project Task 3 Final Report: Identify Intelligent Vehicle Safety Applications Enabled by DSRC*, Mar. 2005.

[33] Z. Zhao, H. Zhang, W. Sun, Z. Bai, "Performance evaluation of IEEE 802.11p vehicle to infrastructure communication using off-the-shelf IEEE 802.11a hardware," *Proc. IEEE ITSC*, QuingDao, China, Oct. 2014.

[34] L. Cheng, et. al, "Multi-Path Propagation Measurements for Vehicular Networks at 5.9 GHz," *Proc. IEEE WCNC*, Las Vegas, US, Apr. 2008.

[35] P. Alexander, D. Haley, A. Grant, "Outdoor Mobile Broadband Access with 802.11," *IEEE Commun. Mag.*, Vol. 45, No. 11, pp. 108-114, 2007.

[36] IEEE 802.11, "IEEE Standard for Information Technology – Telecommunications and Information Exchange Between Systems – Local and Metropolitan Area Networks Specific requirements – Part 11: Wireless LAN Medium Access Control (MAC) and Physical Layer (PHY) Specifications," IEEE Std. IEEE 802.11, version 2012, 2012.

[37] F. A. Tobagi, and L. Kleinrock, "Packet Switching in Radio Channels: Part II the Hidden Terminal Problem in Carrier Sense Multiple-Access and the Busy-Tone Solution," *IEEE Trans. Commun.*, Vol. 23, No. 12, pp. 1417-1433, 1975.

[38] J. Dai, and Y. Yamao, "CSMA/CA Unicast Communication Performance under Fading Environment with Two-Dimensional Distribution of Hidden Terminal," *IEICE Trans. Commun.*, Vol. E95-B, No. 9, pp. 2708-2717, 2012.

[39] C. Thorpe and L. Murphy, "A Survey of Adaptive Carrier Sensing Mechanisms for IEEE 802.11 Wireless Networks," *IEEE Communications Surveys & Tutorials*, Vol. 16, Mar., 2014.

[40] D. Jiang, Q. Chen, L. Delgrossi, "Optimal data rate selection for vehicle safety communications," *Proc. ACM international workshop on vehicular inter-networking*, San Francisco, USA, pp. 30-38, Sep. 2008.

[41] M. Sepulcre, J. Gozalvez, B. Coll-Perales, "Why 6Mbps is not (always) the Optimum Data Rate for Beaconing in Vehicular Networks," IEEE Trans. Mobil. Compt., DOI: 10.1109/TMC.2017.2696533.

[42] Recommendation ITU-R M.1453-2, "Intelligent transport systems – dedicated short range communications at 5.8 GHz," International Telecommunication Union, 2005. S. Oyama, "Activities on ITS Radio communications Standards in ITUR and in Japan," Proc. of ETSI TC-ITS Workshop, Sophia Antipolis, France, Feb. 2009.

[43] Thomas Weilacher, "Intelligent Transport Systems (ITS) 5.9 GHz in Europe and worldwide," *Proc. of ETSI TC ITS Workshop*, Doha, Qatar, Feb. 2012.

[44] ARIB Technical report TR-T20 Version 1.1, "700 MHz Band Intelligent Transport Systems Test Items and Conditions for Mobile Station Compatibility Confirmation," Association of Radio Industries and Businesses (ARIB) Std. 2012, Japanese Standard.

[45] Recommendation ITU-R P.1411-6: Propagation data and prediction methods for the planning of short-range outdoor radio communication systems and radio local area networks in the frequency range 300 MHz to 100 GHz, 2012. International Telecommunication Union.

[46] S. R. Saunders and A. Aragon-Zavala, "Antennas and Propagation for Wireless Communication Systems," Wiley John & Sons, Inc., Second Edition, 2007.

[47] Y. Yamao, K. Minato, "Vehicle-roadside-vehicle relay communication network employing multiple frequencies and routing function," *Proc. 6th International Symposium on Wireless Communication Systems*, Tuscany, Italy, Oct. 2009.

[48] G. Bianchi, L. Fsatta and M. Oliveri, "Performance Evaluation and Enhancement of the CSMA/CA MAC Protocol for 802.11 Wireless LANs," *Proc. IEEE PIMRC*, Taipei, Taiwan, Oct. 1996.

[49] H. Ma, X. Li, H. Li, P. Zhang, S. Luo and C. Yuan, "Dynamic Optimization of IEEE 802.11 CSMA/CA based on the Number of Competing Stations," *Proc. IEEE ICC*, Paris, France, Jun. 2004.

[50] R. Ahlswede, N. Cai, S.-Y. R. Li, and R. W. Yeung, "Network Information Flow," *IEEE Trans. Inf. Theory*, Vol. 46, No. 4, pp. 1204–1216, 2000.

[51] S. Katti, H. Rahul, W. Hu, D. Katabi, M. Médard and J. Crowcroft, "XORs in the Air: Practical Wireless Network Coding," *IEEE Trans. Networking*, Vol. 16, No. 3, pp.497-510, 2008.

[52] T. Cover and A. El Gamal, "Capacity theorems for the relay channel," *IEEE Trans. Inf. Theory*, Vol. 25, No. 5, pp. 572–584, Sep. 1979.

[53] H. Sugawara, H. Cheng and Y. Yamao, "Reduction of V2V Packet Collision due to Traffic Concentration in Integrated V2V/I2V ITS Communication System," *Proc. 19th ITS World Congress 2012*, AP-00066, Wien, Austria, Oct. 2012.

[54] H. Zhai, Y. Kwon and Y. Fang, "Performance analysis of IEEE 802.11 MAC protocols in wireless LANs," *Trans. Wirel. Commun. Mob. Comput*, Vol. 4, pp. 917-931, 2004.

[55] W. Feller, "On the normal approximation to the binomial distribution," *The Annals of Mathematical Statistics*, Vol. 16, No. 4, pp. 319-329, 1945.

[56] Scenargie, http://www.spacetime-eng.com/.

[57] G. Bianchi, "Performance Analysis of IEEE 802.11 Distributed Coordination Function", *IEEE J. Select. Areas Commun.*, Vol. 18, No. 3, pp. 535–547, Mar. 2000.

[58] S. V. Bana and P. Varaiya, "Space Division Multiple Access (SDMA) for Robust Ad hoc Vehicle Communication Networks," *Proc. IEEE Intelligent Transportation Syst. Conf.*, pp. 962-967, Oakland, CA, 2001.

[59] A. P. Subramanian, V. Navda, P. Deshpande, and S. R. Das, "A measurement study of inter-vehicular communication using steerable beam directional antenna," *Proc. the 5th ACM Int. Workshop on Veh. Inter-Networking*, San Francisco, USA, 2008.

[60] P-C. Yeh, W.E. Stark, S. A. Zummo, "Performance Analysis of Wireless Networks With Directional Antennas," *IEEE Trans. on Veh. Technol.*, Vol. 57, No. 5, pp. 3187-3199, Sep. 2008.

[61] H. Cheng and Y. Yamao, "Reliable Inter-Vehicle Broadcast Communication with Sectorized Roadside Relay Station," *Proc. IEEE Veh. Technol. Conf. (VTC)' 13-Spring*, pp. 1-5, Dresden, Germany, Jun. 2013.

[62] M. Xiaomin, C. Xianbo, and H.H. Refai, "On the Broadcast Packet Reception Rates in One-Dimensional MANETs," *Proc. IEEE GLOBECOM*, pp. 1-8, New Orleans, USA, Nov. 2008.

[63] Z. Hadzi-Velkov and B. Spasenovski, "On the Capacity of IEEE 802.11 DCF with Capture in Multipath-faded Channels", *Int. Journal of Wireless Inform. Networks*, Vol. 9, No. 3, pp. 191-199, July 2002, Kluwer Academic.

[64] Z. Hadzi-Velkov and B. Spasenovski, "Capture Effect with Diversity in IEEE 802.11 DCF," *Proc. IEEE Symp. on Comput. And Commun. (ISCC)'03*, pp. 699-704, Antalya, Turkey, Jun. 2003.

[65] R. Khalaf, I. Rubin, and J. Hsu, “Throughput and Delay Analysis of Multihop IEEE 802.11 Networks with Capture,” *Proc. IEEE ICC*, pp. 3787-3792, Glasgow, Scotland, Jun. 2007.

[66] H.S. Chhaya and S. Gupta, “Performance modeling of asynchronous data transfer methods of IEEE 802.11 MAC protocol”, *Wireless Networks*, Vol. 3, pp. 217-234, 1997.

[67] H. Tchouankem, T. Zinchenko, H. Schumacher, “Impact of Buildings on Vehicle-to-Vehicle Communication at Urban Intersections,” Proc. IEEE CCNC, Las Vegas, US, Jan. 2015.

[68] N. F. Abdullah, A. Doufexi, R. J. Piechocki, “Multi-rate Vehicular Communications with Systematic Raptor Codes in Urban Scenarios,” *Proc. IEEE ICC*, Ottawa, Canada, Jun. 2012.

[69] T. Mangel, F. Schweizer, T. Kosch, and H. Hartenstein, “Vehicular Safety Communication at Intersections: Buildings, Non-Line-Of-Sight and Representative Scenarios,” *Proc. 8th International Conference on Wireless On-Demand Network Systems and Services (WONS)*, pp. 35–41, 2011.

[70] N. V. Tien, et al., “A Performance Analysis of CSMA Based Broadcast Protocol in VANETs,” *Proc. IEEE INFOCOM*, Turin, Italy, Apr. 2013.

[71] K. Minato, J. Dai, Y. Yamao, “Theoretical Analysis of Broadcast Packet Delivery Rate in ITS V2V Communication with CSMA/CA,” *Proc. IEEE VTC2011-Fall*, San Francisco, USA, Sep. 2011.

[72] Gaurav Bansal, John B. Kenney, “Controlling Congestion in Safety-Message Transmissions: A Philosophy for Vehicular DSRC Systems,” *IEEE Vehicular Technology Magazine*, Vol. 8, pp. 20-26, 2013.

[73] T. Tielert, D. Jiang, Q. Chen, L. Delgrossi, H. Hartenstein, “Design Methodology and Evaluation of Rate Adaptation Based Congestion Control for Vehicle Safety Communications”, *Proc. IEEE VNC*, Amsterdam, Netherlands, pp. 116-123, Nov. 2011.

[74] M. Sepulcre, J. Gozalvez, Onur Altintas and Haris Kremo, “Integration of congestion and awareness control in vehicular networks”, *Ad Hoc Networks*, Vol. 37, Part 1, pp. 29–43, Feb. 2016.

[75] R. Reinders, M. v. Eenennaam, G. Karagiannis and G. Heijenk, “Contention Window Analysis for Beaconing in VANETs,” *Proc. IEEE IWCMC*, Istanbul, Turkey, Aug. 2011.

[76] M. Li, Z. Yang and W. Lou, “CodeOn: Cooperative Popular Content Distribution for Vehicular Networks using Symbol Level Network Coding,” *IEEE Trans. J. Sel. Areas Commun.*, Vol. 29, No. 1, pp. 223-235, Jan. 2011.

[77] M. H. Firooz and S. Roy, “Collaborative downloading in VANET using Network Coding,” *Proc. IEEE ICC*, Ottawa, Canada, Nov. 2012.

[78] Y. Gao, G. G. M. N. Ali, P. H. J. Chong and Y. L. Guan, “Network Coding based BSM Broadcasting at Road Intersection in V2V Communication,” *Proc. IEEE VTC2016-Fall*, Montreal, Canada, Sep. 2016.

[79] L. T. Trien, Y. Yamao, “An investigation of network coding relay in ITS V2V communication at intersections,” *Proc. IEEE IC-NIDC*, Beijing, China, Sept. 2014.

Publications

Journal Papers

1. L. T. Trien, K. Adachi, Y. Yamao, "Efficient CSMA/CA Packet Relay-Assisted Scheme with Payload Combining for ITS V2V Communication," *Journal of Information Processing*, Vol. 26, No. 1, pp. 11-19, Jan. 2018. (Related to Chapter 3)
2. L. T. Trien, K. Adachi, Y. Yamao, "Packet relay-assisted V2V communication with sectorised relay station employing payload combining scheme," *IET Communications*, Vol. 12, No. 4, pp. 458-465, Mar. 2018 .(Related to Chapter 4).
3. L. T. Trien, K. Adachi, Y. Yamao, "Network Coding Based Payload Concatenation for Relay-Assisted V2V Communication," *IEICE Commun. Express*., 2018, DOI: 10.1587/comex.2018XBL0006. (Related to Chapter 6).

International Conference Papers

1. L. T. Trien, Y. Yamao, "Packet Relay-Assisted V2V Communication with Cooperative Relay Stations in Urban Environment," *Proc. ITS European Congress*, Strasbourg, France, Jun. 2017. (Related to Chapter 5)
2. L. T. Trien, Y. Yamao, "Measured Separation of Sectorized Reception for ITS V2V Relay-Assisted Communication in Urban Environment," *Proc. ISAP2016,* Okinawa, Japan, Oct. 2016.
3. Y. Yamao, L. T. Trien, T. Fujii, K. Ishibashi, "Delay Reduction by Relay-Assisted Broadcast Transmission for Dependable V2V communications," *Proc. ITS World Congress*, Melbourne, Australia, Oct. 2016.
4. L. T. Trien, Y. Yamao, "Packet Relay Assisted V2V Communication with Multiple Sectorized Relay Stations," *Proc. IEEE VTC2016-Spring*, Nanjing, China, May. 2016.
5. L. T. Trien, Y. Yamao, "Performance Analysis of CSMA/CA Packet Relay Assisted V2V Communication with Sectorized Relay Station," *Proc. IEEE VNC*, Kyoto, Japan, Dec. 2015. (Related to Chapter 4)
6. L. T. Trien, Y. Yamao, "Packet Combining Relay Scheme with Sectorized Relay Station for Reliable ITS V2V Communication," *Proc. IEEE VTC2015-Spring*, Glasgow, UK, May. 2015. (Related to Chapter 4)
7. L. T. Trien, Y. Yamao, "An investigation of network coding relay in ITS V2V communication at intersections," *Proc. IEEE IC-NIDC*, Beijing, China, Sep. 2014. (Related to Chapter 6)

8. L. T. Trien, Y. Yamao, “Improving Performance of Packet Combining Relay for ITS V2V Communication,” *Proc. IEEE VTC2014-Fall*, Vancouver, Canada, Sep. 2014. (Related to Chapter 3)
9. L. T. Trien, H. Sugawara, H. Cheng, Y. Yamao, Y. Hirayama and M. Sawada, “Efficient Packet Relay Scheme with Payload Combining for ITS V2V Communications,” *Proc. IEEE WiVEC2013*, Dresden, Germany, Jun. 2013. (Related to Chapter 3)

Domestic Workshop Papers

1. レ ティエン チエン, 山尾泰, “市街地環境における棲分け型協調中継アシスト車車間通信システム, ” 信学技報 RCS2017-19, 2017 年 4 月.
2. 山尾泰, レ ティエン チエン, 藤井威生, 石橋功至, “中継アシストブロードキャスト車車間通信における配信遅延の低減効果, ”信学技報 RCS2016-221, 2016 年 12 月.
3. レ ティエン チエン, 山尾泰, ” 複数路側中継器による棲分け型協調中継アシスト車車間通信システム, ” 信学技報 RCS2016-119, 2016 年 7 月.
4. レ ティエン チエン, 山尾泰, ” セクタ化受信中継器を用いた CSMA/CA 中継アシスト車車間通信の性能解析, ” 信学技報 ITS2016-56, 2016 年 2 月.
5. レ ティエン チエン, 山尾泰, ” セクタ化受信中継局を用いたパケット合成中継法による車車間通信の品質改善効果, ” 信学技報 RCS2014-222, 2014 年 12 月.
6. レ ティエン チエン, 山尾泰, ” ITS 車車間ブロードキャスト通信における合成中継通信の改善, ” 電子情報通信学会ソサイエティ大会, AS-2-1, 2014 年 9 月.
7. レ ティエン チエン, 山尾泰, ” ITS 車車間ブロードキャスト通信でのエアタイム占有率に関する検討, ” 信学技報 RCS2013-226, 2013 年 12 月.
8. レ ティエン チエン, 菅原英紀, CHENG Huiting, 山尾泰, 平山泰弘, 澤田学, “ITS 車車間ブロードキャスト通信のパケットペイロード合成中継法, ” 信学技報 RCS2012-214, 2012 年 12 月.